SWZ Clausthal – Göttingen
Simulation Science Center

Clausthal-Göttingen
International Workshop on

Simulation Science

27–28 April 2017,
Göttingen, Germany

TU Clausthal

GEORG-AUGUST-UNIVERSITÄT
GÖTTINGEN

SWZ Clausthal – Göttingen
Simulation Science Center

ITG INFORMATION TECHNOLOGY SOCIETY
IN THE VDE

Welcome!

Due to the fast development of information technology, the understanding of phenomena in natural, engineering, economic and social sciences increasingly relies on computer simulations. Simulation-based analysis and engineering techniques are traditionally a research focus of Clausthal University of Technology and University of Göttingen, which is especially reflected in their common interdisciplinary research cluster "Simulation Science Center Clausthal-Göttingen". In this context, the first "Clausthal-Göttingen International Workshop on Simulation Science" brings together researchers and practitioners from both industry and academia to report on the latest advances in simulation science.

The workshop takes place in the "Convention Centre by the Observatory" in Göttingen, which is an outbuilding of the Historical Observatory – the former residence and place of work of Göttingen's famous academic Carl Friedrich Gauss.

The welcome address of the workshop is given by Prof. Dr. Norbert Lossau (Vice-President of the University of Göttingen) and Prof. Dr. Thomas Hanschke (President of the TU Clausthal).

In 39 presentations, the workshop considers the broad area of modeling & simulation with a focus on

- simulation and optimization in networks,
- simulation of materials, and
- distributed simulations.

The state of the art in simulation science and an outlook to potential future developments are discussed in three plenary talks given by

- Achim Streit (Karlsruhe Institute of Technology),
- Samuel Forest (MINES Paristech), and
- Kai Nagel (TU Berlin).

The social program consists of a guided city tour through Göttingen's historical old town and a workshop dinner that is held in the Bullerjahn – the "Ratskeller" of Göttingen.

We are grateful to everyone who supported us while organizing the workshop. We would like to thank the Technical Program Committee, the Local Arrangements Chairs Annette Kadziora and Fabian Sigges, and the Finance Chair Alexander Herzog. The registration and payments were managed by VDE conference services. Furthermore, we are in the lucky position to be co-sponsored by the Gesellschaft für Operations Research e.V (GOR) and the Arbeitsgemeinschaft Simulation (ASIM).

We hope that the first "Clausthal-Göttingen International Workshop on Simulation Science" gives you as much pleasure as we had when organizing it for you.

General Chairs,

Marcus Baum
Gunther Brenner
Jens Grabowski
Thomas Hanschke
Stefan Hartmann
Anita Schöbel

2

Organization

3

General Co-Chairs

Marcus Baum, University of Göttingen
Gunther Brenner, TU Clausthal
Jens Grabowski, University of Göttingen
Thomas Hanschke, TU Clausthal
Stefan Hartmann, TU Clausthal
Anita Schöbel, University of Göttingen

Program Committee

Valentina Cacchiani, University of Bologna
Stefan Diebels, Saarland University
Jürgen Dix, TU Clausthal
Umut Durak, DLR Braunschweig
Felix Fritzen, University of Stuttgart
Igor Gilitschenski, ETH Zürich
Marc Goerigk, Lancester University
Marco Huber, USU AG, Karlsruhe
Tobias Kretz, PTV Group
Allan Larsen, Technical University of Denmark
Ming Li, Nanjing University
Laura De Lorenzis, TU Braunschweig
Kai Nagel, TU Berlin
Helmut Neukirchen, University of Iceland
Bernhard Neumair, Karlsruhe
Institute of Technology
Natalia Rezanova, Danske Statsbaner
(Danish State Railways)
Ulrich Rieder, Ulm University
Rüdiger Schwarze, TU Freiberg
Marie Schmidt, Erasmus University Rotterdam
Thomas Spengler, TU Braunschweig
Ulrich Tallarek, Philipps-Universität Marburg
Pieter Vansteenwegen, KU Leuven
Sigrid Wenzel, University of Kassel
Peter Wriggers, University of Hanover
Ramin Yahyapour, GWDG
Martin Zsifkovits, UniBw München

Finance Chair

Alexander Herzog, TU Clausthal

Local Arrangements Co-Chairs

Annette Kadziora, University of Göttingen
Fabian Sigges, University of Göttingen

4 Technical Schedule

Thursday

	Großer Seminarraum	Seminarraum 2
8:30 am	**Welcome Note** 8:30 am – 9:00 am	
9:00 am	**Invited Talk: Samuel Forest, MINES ParisTech** 9:00 am – 10:00 am	
9:30 am		
10:00 am	Break 10:00 am – 10:30 am	Break 10:00 am – 10:30 am
10:30 am		
11:00 am	**Simulation of Materials 1** 10:30 am – 12:10 pm	**Simulation and Optimization in Networks 1** 10:30 am – 12:10 pm
11:30 am		
12:00 pm		
12:30 pm	Lunch 12:10 pm – 1:30 pm	Lunch 12:10 pm – 1:30 pm
1:00 pm		
1:30 pm	**Inivited Talk: Achim Streit, KIT** 1:30 pm – 2:30 pm	
2:00 pm		
2:30 pm	Break 2:30 pm – 3:00 pm	Break 2:30 pm – 3:00 pm
3:00 pm		
3:30 pm	**Distributed Simulations 1** 3:00 pm – 4:40 pm	**Simulation of Materials 2** 3:00 pm – 4:40 pm
4:00 pm		
4:30 pm		

Friday

	Großer Seminarraum	Seminarraum 2
8:30 am	**Invited Talk: Kai Nagel, TU Berlin** 8:30 am – 9:30 am	
9:00 am		
9:30 am	Break 9:30 am – 10:00 am	Break 9:30 am – 10:00 am
10:00 am		
10:30 am	**Simulation and Optimization in Networks 2** 10:00 am – 11:40 am	**Distributed Simulations 2** 10:00 am – 11:40 am
11:00 am		
11:30 am		
12:00 pm	Lunch 11:40 am – 1:00 pm	Lunch 11:40 am – 1:00 pm
12:30 pm		
1:00 pm		
1:30 pm	**Simulation and Optimization in Networks 3** 1:00 pm – 2:40 pm	**Distributed Simulations 3** 1:00 pm – 2:40 pm
2:00 pm		
2:30 pm	Break 2:40 pm – 3:10 pm	Break 2:40 pm – 3:10 pm
3:00 pm		
3:30 pm	**Simulation of Materials 3** 3:10 pm – 4:50 pm	**Poster Session** 3:10 pm – 4:10 pm
4:00 pm		
4:30 pm	**Closing Note** 4:50 pm – 5:00 pm	

6 Plenary Talks

Samuel Forest, Mines ParisTech CNRS, France

Crystal plasticity of polycrystalline aggregates under cyclic loading: 3D experiments and computations, size effects and fatigue cracking

BIO: Samuel Forest, 48 year old, is CNRS Research Director at Centre des Materiaux Mines ParisTech and continuum mechanics professor at Mines ParisTech. He is working on mechanics of materials focusing on crystal plasticity modelling and mechanics of generalized continua. He has beforesten the PhD advisor of 35 PhD students on these scientific topics, each of them corresponding to a contract with industrial partners (SAFRAN, RENAULT, EDF, Arcelor-Mittal, Michelin, CEA, EDF, etc.) or with the state and EU. He got the Bronze and Siver medals of CNRS INSIS and the Plumey prize of the Academie des Sciences. He published more than 120 papers in peer-reviewed international journals. He is associate editor of 5 international journals including Int. J. Solids Structures and Phil. Mag. He is leading the CNRS Federation of Mechanics labs in the Paris Region, promoting cooperation between 14 mechanics labs in the Paris region.

ABSTRACT: The mustiscale approach to the plasticity and fracture of crystalline metals and alloys is based nowadays on large scale simulations of representative volume elements of polycrystalline aggregates. The deformation modes inside the individual grains are described by continuum crystal plasticity models involving dislocation densities and suitable interface conditions at grain boundaries [1]. Recent 3D experiments performed under synchrotron radiation at ESRF reveal the plastic events in the grains like slip banding and development of crystal lattice curvature [2]. These results are compared to finite element simulations involving millions of degrees of freedom for a detailed description of intragranular mechanical fields. The cyclic loading of such samples leads to the initiation and propagation of fatigue cracks going through the grains and stopping at or overcoming grain boundaries. This damage process can also be observed by 3D images and simulated by corresponding finite element simulations [3].

The constitutive laws for crystal plasticity and damage incorporate gradient plasticity and gradient damage contributions in order to account for size effects in the material behaviour [3,4,5]. These effects include the size-dependent piling-up of dislocations during cyclic loading and the description of finite width localization bands and cracks. The provided examples deal with cubic aluminum, titanium and nickel-based alloys.

Achim Streit, Karlsruhe Institute of Technology (KIT), Germany

Enabling Data-Intensive Science in the Helmholtz Association

BIO: Prof. Dr. Achim Streit is the director of the Steinbuch Centre for Computing (SCC) and professor for computer science at Karlsruhe Institute of Technology (KIT) since mid-2010. He is responsible for the HPC and Big Data activities at SCC – both systems as well as R&D activities. He is topic speaker “Data-Intensive Science and Federated Computing” in the Helmholtz Programme “Supercomputing & Big Data” (of which he is also the deputy speaker). He is the coordinator of the Large Scale Data Management

and Analysis (LSDMA) initiative in Helmholtz, which is about fostering data-intensive science in Germany through Data Life Cycle Labs and generic methods research. He is the coordinator of the Helmholtz Data Federation (HDF), a 5-year multi-million Euro investment project to establish an open federated research data infrastructure in Germany. He and his institute are involved in major European e-Infrastructure projects such as EUDAT2020, EOSCpilot, INDIGO-Datacloud, AARC as well as the FET flagship Human Brain project. Prior to KIT, he was at the Jülich Supercomputing Centre (JSC) of Forschungszentrum Jülich, Germany, where he was responsible for the Grid activities and active in several EU e-infrastructure projects such as DEISA, PRACE, OMII-Europe, EGI-InSPIRE and helped to initiate the EMI and EUDAT projects.

ABSTRACT: The Helmholtz Association of German research centres pursues long-term research with large-scale scientific projects and research facilities ranging from life sciences, climate and environment up to matter and the universe. One of its long-term programs is dedicated to research on "Supercomputing & Big Data" (SBD) which is of major importance and provides enabling technologies to all Helmholtz research fields.
In data-intensive science collaboration is a key factor. On the national level we lead the multi-disciplinary initiative LSDMA across the Helmholtz research fields to foster the exchange of knowledge, expertise and technologies. Data experts from the program collaborate closely with domain researchers from other Helmholtz programs and German universities within so-called "Data Life Cycle Labs" (DLCL). These aim at optimizing data life cycles and developing community-specific tools and services in joint R&D with the scientific communities. In addition, new generic data methods and technologies for data life cycle management are designed and developed, large scale data facilities and federated data infrastructures are enhanced and operated, and national/international collaborations such as HDF, EUDAT, INDIGO-DataCloud, EU-T0 and WLCG are advanced.

Kai Nagel, TU Berlin, Germany

Addressing negative effects of transport systems with large scale behavioral transportation simulations

BIO: Kai Nagel is full professor for "Transport systems planning and transport telematics" at the Berlin Institute of Technology (TU Berlin), Germany. He was trained in physics and climate research, and holds a Ph.D. in informatics from University of Cologne, Germany. He worked at Los Alamos National Laboratory, USA, from 1995 to 1999, at ETH Zürich from 1999 to 2004, and holds his current post since 2004. His research interests include large-scale transportation simulations, modeling and simulation of socio-economic systems, and large-scale computing. He leads a group of eight Ph.D. students, six of them funded from competetive sources including the German National Science Foundation and the EU. He has authored more than 100 publications. He is area editor of the journal "Networks and Spatial Economics", member of TRB committee ADB10 "travel behavior and values", and a frequent reviewer for a large number of scientific journals, scientific conferences, research proposals, and scholarships. Also see www.vsp.tu-berlin.de/menue/ueber_uns/team/prof_dr_kai_nagel/

ABSTRACT: The presentation will have three parts. In the first part, I will explain how our own MATSim software (= Multi Agent Transport Simulation, see www.matsim.org) for transport systems simulation works. It is, in short, a system that tracks its entities, in particular persons and vehicles, individuall, and lets them learn from one synthetic day to the next. In the second part, I will show use cases of what one can do with such a system. The use cases will center around externalities, i.e. congestion, noise, and particulate emissions, and what can be done to reduce them. The third part of my presentation will deal with computational methods, i.e. methods and tools from computer science & engineering that we have put to good use vs. methods that have not worked so well.

8 List of Abstracts

Simulation and optimization in networks I

Simulation and optimization in networks II

Simulation and optimization in networks III

9

Simulation of materials I

Simulation of materials II

Simulation of materials III

10

Distributed simulations I

Distributed simulations II

Distributed simulations III

Poster Session

12

Solving Robust Optimization Problems by an Iterative Simulation-Based Approach

Julius Pätzold and Anita Schöbel

Institut für Numerische und Angewandte Mathematik
Georg-August-Universität Göttingen

1 A Simulation-Based Approach for Robust Optimization

Solving robust versions of opimization problems in general is known to be an intrinsically hard task. For many robust optimization problems, however, there exist algorithms for finding an optimal solution under some fixed scenarios chosen from the uncertainty set. On the other hand, the task of evaluating a solution under different scenarios can often also be achieved in reasonable time. These two facts lead to the idea of tackling robust optimization problems by iterating between the two stages of finding a solution under fixed scenarios and retrieving a worst-case scenario by evaluating a solution via simulation.

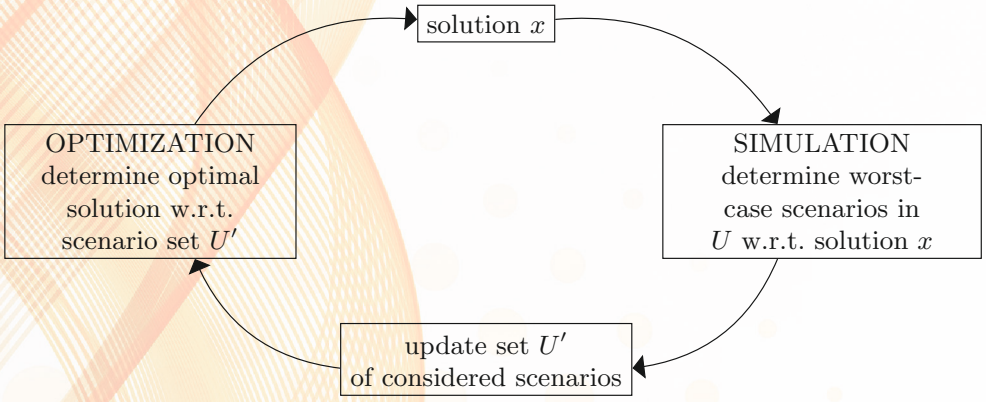

Fig. 1. Basic Scheme

Within this general scheme we show results for the special case of an increasing uncertainty set. The procedure is as follows: Starting with only the nominal scenario, an optimal solution is calculated with respect to this uncertainty set. Then the worst case for this solution is determined and added to the uncertainty set, now consisting of two scenarios. Again an optimal solution is calculated, but this time with respect to the increased uncertainty set. This procedure is repeated until some stopping criterion is met.

2 Literature

A general overview of related literature on solving robust optimization problems via this approach, often called cutting plane algorithms or outer approximation algorithms, is given in [3]. A large drawback that is already mentioned there is the lack of unification of solution approaches for these problems. There exist many papers considering different classes of robust optimization problems and that present similar ideas on how to solve them. Hence they are closely related to the simulation-optimization approach stated above. In [1] a relaxation-based procedure for strictly robust and regret-robust combinatorial optimization with interval uncertainty is presented. Here the uncertainty lies only in the objective function of the optimization problem. By contrast, in [4] strictly robust convex optimization problems with uncertainty in the constraints and the objective function are considered. A convergence proof for their proposed algorithm is given that makes general assumptions on the solvability of the problem. However, the algorithm does not work efficiently if the uncertainty lies exclusively in the objective function of the problem. In [2] an algorithm for regret-robust mixed-integer linear optimization problems is given, but only for the case of a finite uncertainty set.

3 Contribution

Our contribution is two-fold. First, to resolve the problem of missing unification, we propose a formulation that brings all these different approaches together. Our convergence proof makes only general assumptions with respect to the solvability of the nominal problem, requiring that both the robust optimization problem with a finite scenario set as well as the retrievement of a worst-case scenario in the uncertainty set for a given solution need to be solvable. Thus it contains all proofs to the solution algorithms proposed in the previously introduced literature as special cases. Second, the general solution scheme goes beyond the mere applicability to the aforementioned problem classes, which enables us to extend or improve the proposed solvability of each class. In particular, the relaxation-based procedure in [1] can be extended to solve robust combinatorial optimization problems with arbitrary uncertainty sets – provided that a worst-case scenario for a solution can be found efficiently. For [4] one can overcome the lack of efficiency which arises when only the objective is uncertain, and the proposed approach in [2] can be extended to solve problems with more general uncertainty sets.

4 Computational Results

We present computational experiments that underline the general use of the proposed algorithm class. On the one hand, it is shown that the proposed algorithm yields good results for the class of strictly robust combinatorial optimization with polyhedral uncertainty sets. To this end we present results for the Spanning Tree

and Travelling Salesman problem under polyhedral uncertainty in the edge costs. On the other hand, mixed-integer bilevel optimization problems are considered as in [5]. These problems can be transformed to strictly robust mixed-integer optimization problems; thus the proposed solution algorithm can be applied. The computational results show that the simulation-optimization procedure clearly outperforms any of the proposed algorithm presented in [5].

5 Outlook

We will sketch ideas on how further research can be carried out. This can be done on different levels. On the theoretical level the framework can be extended to have approximation results included, meaning that convergence results are extended to the case that either solving the problem with fixed scenarios or evaluating a given solution can only be done approximately. On the algorithm level it can be investigated how to exploit the fact that in each iteration a very similar optimization problem has to be solved. For example, in robust mixed-integer problems, the simulation-optimization procedure can be embedded in a branch-and-bound framework, resulting in a branch-and-cut procedure. A promising research direction on the application level is to use the proposed algorithm for finding robust timetables in public transportation planning. It would be interesting to investigate how the complexity of the two tasks – finding a periodic timetable and evaluating an existing timetable with respect to its delay-resistance – behaves when they are combined within the simulation-optimization framework.

References

1. Aissi, H., Bazgan, C., Vanderpooten, D.: Min–max and min–max regret versions of combinatorial optimization problems: A survey. European journal of operational research 197(2), 427–438 (2009)
2. Assavapokee, T., Realff, M.J., Ammons, J.C., Hong, I.H.: Scenario relaxation algorithm for finite scenario-based min–max regret and min–max relative regret robust optimization. Computers & Operations Research 35(6), 2093–2102 (2008)
3. Goerigk, M., Schöbel, A.: Algorithm engineering in robust optimization. arXiv preprint arXiv:1505.04901 (2015)
4. Mutapcic, A., Boyd, S.: Cutting-set methods for robust convex optimization with pessimizing oracles. Optimization Methods & Software 24(3), 381–406 (2009)
5. Tang, Y., Richard, J.P.P., Smith, J.C.: A class of algorithms for mixed-integer bilevel min–max optimization. Journal of Global Optimization pp. 1–38 (2015)

Heuristics and Simulation for Water Tank Optimization

Corinna Hallmann[1], Sascha Burmeister[1], Michaela Beckschaefer[1], and Leena Suhl[1]

Decision Support & Operations Research Lab, Paderborn University, Germany
{hallmann,burmeister,beckschaefer,suhl}@dsor.de

1 Introduction

In recent years, German municipal utilities responsible for the local water supplies are facing an increasing cost pressure. One of the main reasons is the decreasing water consumption in Germany in the last two decades. When building water distribution systems, the planners forecasted an increasing demand of water in the future and planned the size of the components accordingly. Due to decreasing water consumption there are now many components that work inefficiently. In this paper, the focus is on optimizing water tanks, which means deciding their optimal locations and dimensions. The utilities require an accurate solution in reasonable time for this problem.

Optimizing water tanks is a highly complex task due to their great influence on the hydraulics in the whole water distribution system. When modeling the hydraulics it is necessary to use non-convex and nonlinear equations, which make the corresponding optimization models hard to solve. There are a few approaches to tackle this problem in the literature. Farmani et. al. ([3]) propose a model which optimizes not only the locations and dimensions of tanks but also pump operation schedules. They combine an Elitist Nondominated Sorting Genetic Algorithm method (NSGAII) with an extended time period simulation to compute the hydraulic properties. Vamvakeridou-Lyroudia ([6]) also uses such a simulation to handle the problem of optimizing water tanks. The simulation is used to determine the inflow and outflow of water tanks. This information is combined with a genetic algorithm that chooses new level for the tanks. The optimization of size and location of water tanks is also considered in the work of Kurek and Ostfeld ([5]) who present two optimization models that additionally minimize the energy costs of pumps and optimize the water quality in the system. The multi-objective optimization models are solved via a combination of Strength Pareto Evolutionary Algorithm II (SPEA2) and a simulation. Inspired by those ideas, we tackle our developed optimization model, see [4], with a combination of heuristics and hydraulic simulation. In the following, we will present the optimization model and the application of three different heuristics, namely a Simulated Annealing algorithm, a Shuffled Complex Evolution algorithm and a Shuffled Frog-Leaping Algorithm. After introducing these algorithms we show some computational results.

2 Solving an Optimization Model for Water Tanks

This section describes shortly the optimization model. The complete version of the model can be found in [4]. We consider a water distribution system that can be completely new or an existing system. The optimization task is to minimize the costs of all water tanks in the system. Depending on the costs, the model can decide where to build new tanks, replace or scale up or down existing tanks. In addition, the dimensions

and the material properties of a tank can be determined. This task is restricted by several constraints. There has to be a minimal amount of water in the system to satisfy the demand of each client at any time and provide the necessary amount of water for firefighting or any other kind of incident that can occur. Furthermore, the hydraulics in a water distribution system have to be considered, such as the volumetric flow through each pipe and the hydraulic head on each node. To model the hydraulics accurately, we add a nonlinear head loss equation to the model. Due to discrete decisions and this equation, the proposed optimization model becomes a NP-hard non-convex Mixed Integer Quadratically Constrained Program (MIQCP).

The first algorithm applied to this model is a Simulated Annealing (SA) algorithm. Details of this algorithm can for example be read in the work of Barakat et. al. ([1]).In our work the algorithm is used to find feasible values for the volume of stored water in a tank and the decision, if a tank should be built or change its size. To find a solution in the neighborhood we choose one tank. For this tank we define a new configuration of parameters. The cost function is the objective function of the MIQCP.

The second technique is a Shuffled Complex Evolution (SCE) algorithm. This technique is also described in [1]. In our implementation a population is a configuration for all possible tank locations. Besides the volume of each tank, this configuration defines, if a tank should be built, replaced by a new one or change its properties. After creating the populations, the SCE sorts these populations according to their objective function value and divides them into complexes. Each of the complexes evolves by changing the assigned volumes during reflection, correction and contraction steps. After checking the feasibility of the new populations with the simulation and evaluating the objective function, the populations are ranked and divided into complexes again.

As a third technique we use a Shuffled Frog-Leaping Algorithm (SFLA), see for example [2]. Similar to the SCE, we start by defining some populations representing different tank configurations. These populations are ranked and divided into memeplexes. The SFLA now tries to improve the worst population by changing the properties of the tanks. Therefore, positive and negative reflection steps are performed as well as negative and positive construction steps. After that, the memeplexes are shuffled and the whole process is carried out until some stopping criterion is satisfied.

As all three algorithms presented need an evaluation of the solutions, we use a hydraulic simulation for evaluation. The simulation calculates the hydraulic properties in a water distribution system such as flows and hydraulic heads during all time periods and takes into account all components that may appear in a water distribution system such as pipes, pumps, valves, reservoirs and tanks. With this simulation we are able to gather information about the different solutions.

3 Computational Results

For the computational results we use 24 different network models. These models have a size of 8 nodes and 10 links up to a size of 1913 nodes and 2487 links. Most of those networks are realistic networks based on German cities, while others are fictitious.

Figure 1 shows some computational results. To compare the computational times we use SCIP as a reference. For smaller networks (indicated with *S*) it is not efficient to use one of the three heuristics but to use SCIP instead. Comparing the three heuristics applied to the small networks, it can be seen that SFLA yields the best results related to

the computational time. Furthermore, the SA performs better than the SCE. For middle sized (*M*) and large (*L*) networks it is very efficient to use the SFLA. The SA and SCE perform also very well and find solutions in reasonable time. We also analyzed how well the heuristics performed regarding the gap to the optimal solution. We found that at smaller and middle sized networks all heuristics performed well and found solutions close to the optimal one. When considering larger networks the SCE and SFLA are superior to the SA.

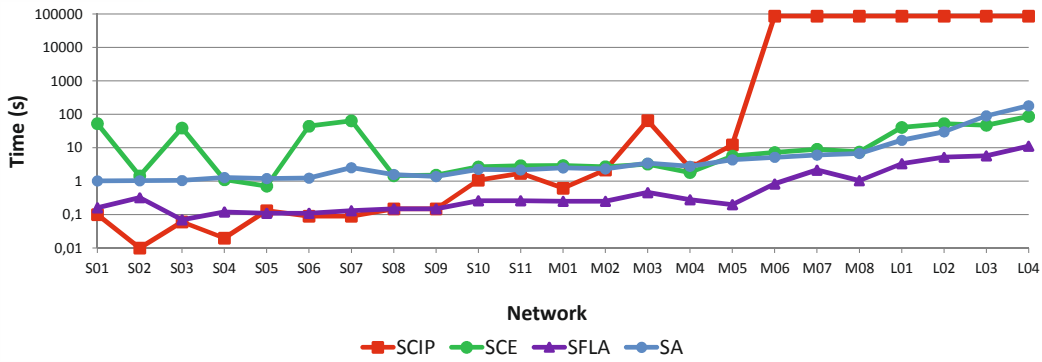

Fig. 1. Comparison of the computational times of the algorithms

4 Conclusion and Future Work

In this work we presented an optimization model to determine optimal locations and dimensions of water tanks in a water distribution system. As the model is a non-convex MIQCP and therefore hard to solve, we implemented three different heuristic solution methods, namely a Simulated Annealing, a Shuffled Complex Evolution and a Shuffled Frog-Leaping Algorithm and combined them with a hydraulic simulation. In the computational results we showed that all heuristics found solutions with a high quality in a short amount of time. The most efficient heuristic regarding the solution time and the quality of the solution is the SFLA. In future work we would like to find better parameter settings for the implemented heuristics to achieve even more efficient results.

References

1. Barakat, S.A., Altoubat, S.: Application of evolutionary global optimization techniques in the design of RC water tanks. Eng Struct 31(2), 332–344 (2009)
2. Eusuff, M., Lansey, K., Pasha, F.: Shuffled frog-leaping algorithm: a memetic meta-heuristic for discrete optimization. Eng Opt 38:2, 129–154 (2006)
3. Farmani, R., Walters, G.A., Savic, D.A.: Trade-off between total cost and reliability for Anytown water distribution network. J Water Resour Plan Manag 131(3), 161–171 (2005)
4. Hallmann, C., Suhl, L.: Optimizing water tanks in water distribution systems by combining network reduction, mathematical optimization and hydraulic simulation. OR Spectrum 38 No. 3, 577–595 (2015)
5. Kurek, W., Ostfeld, A.: Multi-objective optimization of water quality, pumps operation, and storage sizing of water distribution systems. J Environ Manag 115, 189–197 (2013)
6. Vamvakeridou-Lyroudia, L.: Tank simulation for the optimization of water distribution networks. J Hydraul Eng 133 No. 6, 625–636 (2007)

18

Simulation and Optimization with a Bayesian Selection of Alternatives

Björn Görder and Michael Kolonko

Institute of Applied Stochastics and OR, Clausthal University of Technology
kolonko@math.tu-clausthal.de

1 Introduction

Optimization of complex systems often requires to find the optimum with respect to a target function that depends on some random influence, like market or weather conditions or random delays e.g. in traffic systems. In most cases, the aim is to select a solution or *alternative* $i^* \in \mathcal{L}$ that shows maximal expected performance $\mu_{i^*} := \mathbf{E}\, r(i^*, Z)$ among all solutions from a set $\mathcal{L} = \{1, , \ldots, L\}$. Here, r is some reward function and Z describes the random scenarios.

To determine μ_i analytically is possible only in very simple cases. Often, μ_i has to be estimated from a sample $r(i, z_1), \ldots, r(i, z_n)$ of simulated performances with different scenarios $z_1, \ldots, z_n$. As the estimated value includes an error, the selection of i^* as best alternative may also be wrong with a certain error probability.

Generally, this error probability will decrease with the number n of samples used. However, if selection of the best alternative has to be done repeatedly, as e.g. in an heuristic optimization procedure like ant algorithms, the necessary sample size n should be small.

In classical statistics, this problem is known as 'ranking and selection' (R&S), see e.g. [KN1]. Here, random observations from different alternatives are made and the one with the largest mean value has to be selected. Procedures are given to find the minimal sample size needed to guarantee a selection error probability of less than a given bound α.

Most such procedures assume that the observations of different alternatives are *independent*. However, it is well known that for the comparison of different alternatives that have positively correlated performance, it is more efficient to use the *same* random scenarios or *common random numbers* (CRN) for all alternatives which results in *dependent* observations.

We present here a new ranking and selection procedure BayesRS that works well for dependent observations and requires, different from other approaches, no additional prior knowledge about the distribution of the observations apart from being normal.

2 The Bayesian Model

We assume that a joint observation of *all* alternatives with the same scenario or random seed results in an L-dimensional normally distributed random variable with *unknown* mean $\mu = (\mu_1, \ldots, \mu_L)$ and *unknown* covariance matrix Σ. We take a Bayesian point of view and and assume that mean μ and covariance matrix Σ are random variables with the so-called non-informative prior distribution.

Our procedure is organized in stages or rounds of observations. In the first stage, it simulates all alternatives with the first n_0 random seeds, where n_0 is a given parameter. In each of the subsequent stages, we have a fixed *budget* $b \in \mathbb{N}$ of trials that we may allocate freely to alternatives to generate the next round of observations.

After each round of observations, we update the posterior distributions based on the available observations $\boldsymbol{x}$. We can approximate the posterior distribution of the mean by an L-dimensional Student distribution with mean $(\hat{\mu}_1(\boldsymbol{x}), \ldots, \hat{\mu}_L(\boldsymbol{x}))$.

3 Allocation of Trials to Alternatives

The *allocation* of the simulation budget in each round is based on the latest posterior distribution. We allocate more trials to those alternatives, for which the posterior distribution does not allow a clear ranking of the (estimated) means and that have a relatively large variance. To determine this allocation, we just have to evaluate quantiles of the posterior Student distribution.

Moreover, these values are reused to give a Bonferroni bound to the error probability for the present stage. As soon as this is below the given bound α, the procedure stops and selects the alternative i^* with the present maximal posterior mean: $\hat{\mu}_{i^*}(\boldsymbol{x}) = \max_i \hat{\mu}_i(\boldsymbol{x})$.

Free allocation of trials may result in incomplete data: not all alternatives have been simulated with all seeds used so far. We have to apply a particular sampling scheme to guarantee a so-called monotone pattern of missing data that is needed for the posterior estimation of the means.

Our procedure is very flexible, it may be used for any selection target that is based on pairwise comparison of alternatives. This includes e.g. selection of the m best solutions or a complete ranking of all solutions in $\mathcal{L}$.

4 Empirical results

We have tested our procedure with observations generated with the true mean $\mu := (\delta, 0, 0, \ldots, 0)$ and $\delta > 0$. Thus the true best alternative was $i = 1$, but its mean performance is only slightly better than from all the other alternatives, making it difficult to detect the difference. Of course, the true mean (and covariance matrix) were not known to the procedure.

The tests showed, that our simple allocation strategy was as least as good as a greedy allocation suggested in the literature which needs more complex calculations.

Also, we compared our procedure to well-known R&S-strategies, namely PLUCK from [Qu1] and KN++ from [KN2]. Both procedures require more information and/or restrictions for the underlying distributions and both needed (much) more simulation trials to meet the given error bound on the average.

Literatur

[KN1] S.-H. Kim and B.L. Nelson. Selecting the best system. In *Simulation Handbooks in Operations Research and Management Science*, chapter 17, pages 501–532. North-Holland, Elsevier, 2006.

[KN2] Seong-Hee Kim and Barry L Nelson. On the asymptotic validity of fully sequential selection procedures for steady-state simulation. *Operations Research*, 54(3):475–488, 2006.

[Qu1] Huashuai Qu, Ilya O Ryzhov, and Michael C Fu. Ranking and selection with unknown correlation structures. In *Proceedings of the Winter Simulation Conference*, page 12. Winter Simulation Conference, 2012.

20

LP Decoding: When Channel Coding meets Optimization

Florian Gensheimer[1], Stefan Ruzika[1], Norbert Wehn[2], and Kira Kraft[2]

[1] Mathematical Institute
University of Koblenz-Landau, 56070 Koblenz, Germany
[2] Microelectronic Systems Design Research Group
University of Kaiserslautern, 67663 Kaiserslautern, Germany

1 Introduction

We present a rather new application of discrete optimization, which is called LP decoding. It was first established by Feldman et al. [1]. LP decoding combines the two fields channel coding and mathematical optimization. More precisely, LP decoding uses methods from integer and linear programming to correct transmission errors that occur in digital communication systems.

Transmission errors can be observed in almost every communication system, as e. g. in smartphones, satellites, TV broadcasting and storage systems. Reasons for these errors can be a bad reception quality, e. g. due to bad weather, the interference with other signals, as it can be observed in smartphones, or physical damage in storage systems.

The goal of channel coding is to correct such transmission errors via a two-stage system: an encoder on the sender device and a decoder on the receiver device. This system is illustrated in Figure 1. The encoder gets an information word $x \in \{0,1\}^k$, i. e. the original message, as input and outputs a codeword $y \in \{0,1\}^n$, which is obtained by adding $n-k$ redundant bits. In our research, we consider the important class of linear codes. Here, the set C of codewords forms a linear subspace in $\{0,1\}^n$ over the field $\mathbb{F}_2$. Such codes can be represented as

$$C = \{y \in \{0,1\}^n : Hy \equiv 0 \mod 2\}, \tag{1}$$

where $H \in \{0,1\}^{(n-k)\times n}$ is the so-called parity-check matrix of C. After the encoding process, the codeword y is sent through a noisy channel, e. g. a wire or air. This adds disturbance to the codeword such that the receiver only obtains an erroneous codeword $\widetilde{y}$. Hence, the task of the decoder is to reconstruct the sent codeword y out of $\widetilde{y}$. If the decoder accomplished this task, the computation of x out of y is straightforward.

The quality of a decoder in terms of its error correction rate can be evaluated in large Monte-Carlo simulations. For this purpose, the noise of the channel is modeled via a random variable for every bit, as e. g. in the binary symmetric channel, that flips a bit with a certain probability, or by using the additive white Gaussian noise (AWGN) channel, that is based on the Gaussian distribution. The error correction rate can then be estimated by generating a high number

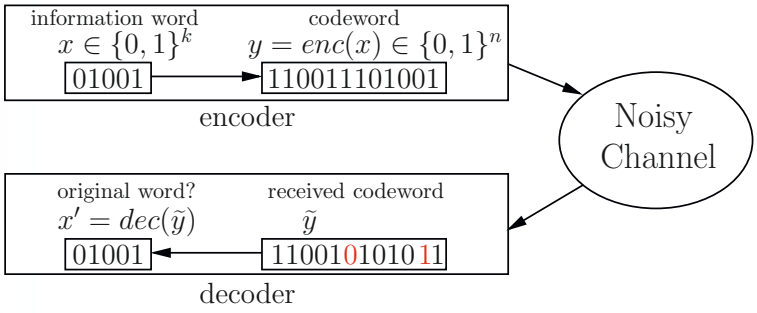

Fig. 1. The two stages of a channel coding system

of disturbed codewords and counting the number of times when the decoder can reconstruct the original codeword. This is usually done for different signal strengths (signal-to-noise ratios).

The decoder with the best possible error rate is the so-called maximum likelihood decoder, a maximum likelihood estimator that outputs that codeword which was most likely sent, provided that $\tilde{y}$ was received. Compared to current decoders in practice, which are implemented in hardware, the ML decoder has a far better error correction rate, i. e. there is a huge potential in the development of ML decoders.

2 LP Decoding

An efficient approach, that made ML decoding for the first time accessible for many small codes, is the usage of mathematical optimization [1]. Here, the ML decoding problem is formulated as an integer program (IP)

$$\begin{aligned} \min \quad & \lambda^\top y && \text{(2a)} \\ \text{s. t.} \quad & Ay = b && \text{(2b)} \\ & 0 \le y \le 1 && \text{(2c)} \\ & y \in \mathbb{Z}^n, && \text{(2d)} \end{aligned}$$

where $A \in \mathbb{R}^{m \times n}$ and $b \in \mathbb{R}^n$ depend on the parity-check matrix H and information about the probability model of the noise is incorporated in $\lambda \in \mathbb{R}^n$. With this model, the large theory of mathematical optimization can be applied to the ML decoding problem. This integer program can be solved by a cutting-plane approach [2] or a branch-and-bound algorithm [3]. On our ML simulation homepage [4], we used this integer programming approach to compute error rates of the ML decoder for many linear codes.

The main effort of these IP-based ML decoders consists of the repeated solving of the so-called LP decoding problem, i. e. the linear program obtained by (2a)-(2c). Hence, the essential part of an efficient ML decoder is the implementation of an efficient LP decoder. In the literature, there are many LP decoding

algorithms. They are based, e. g., on an adaptive approach [5] or the alternating direction method of multipliers (ADMM) of convex optimization [6].

3 Hardware Efficiency

However, an important unsolved question in this context is the hardware efficiency of LP decoders. In practice, this question is important, because for many communication devices, as e. g. smartphones, the decoding algorithms are implemented in hardware. Additionally, the hardware efficiency of an algorithm can be quite different compared to its efficiency in software on a PC. For example, the hardware complexity (power consumption, chip area, etc.) of a division is much higher than the one of an addition. Furthermore, the usage of a fixed-point number representation with a low number of bits is preferred to the more complex floating-point number representation as it is used on a PC.

In this workshop, we investigate the hardware efficiency of current LP decoders for different code classes. For this purpose we compare these algorithms regarding their needed different arithmetic operations and their required number of bits in a fixed-point number representation that are necessary to ensure the numerical stability of the decoder. The comparisons are done by extensive Monte-Carlo simulations. These measures play an important role in the design of a future hardware implementation. In the bigger picture, this can be seen as a first step to an efficient ML decoder in hardware.

References

1. Feldman, J., Wainwright, M.J., Karger, D.R.: Using linear programming to Decode Binary linear codes. IEEE Transactions on Information Theory **51** (2005) 954–972
2. Tanatmis, A., Ruzika, S., Hamacher, H.W., Punekar, M., Kienle, F., Wehn, N.: A Separation Algorithm for Improved LP-Decoding of Linear Block Codes. IEEE Transactions on Information Theory **56**(7) (2010) 3277–3289
3. Helmling, M., Rosnes, E., Ruzika, S., Scholl, S.: Efficient maximum-likelihood decoding of linear block codes on binary memoryless channels. In: Proc. IEEE Int. Symp. Inform. Theory, Honolulu, HI, USA (June/July 2014) 2589–2593
4. Helmling, M., Scholl, S.: Database of channel codes and ML simulation results. Web Page (2016)
5. Zhang, X., Siegel, P.H.: Adaptive cut generation algorithm for improved linear programming decoding of binary linear codes. IEEE Trans. Inf. Theory **58**(10) (October 2012) 6581–6594
6. Zhang, X., Siegel, P.H.: Efficient iterative LP decoding of LDPC codes with alternating direction method of multipliers. In: Proc. IEEE Int. Symp. Inform. Theory. (2013) 1501–1505

Modelling Vehicle Sharing with Driverless Cars

Prof. Dr.-Ing. Markus Friedrich

University of Stuttgart,
Department for Transport Planning and Traffic Engineering,
Pfaffenwaldring 7, D-70569 Stuttgart, Phone +49-711-68582480,
markus.friedrich@isv.uni-stuttgart.de

Maximilian Hartl, M.Sc.

University of Stuttgart,
Department for Transport Planning and Traffic Engineering,
Pfaffenwaldring 7, D-70569 Stuttgart, Phone +49-711-68584414,
maximilian.hartl@isv.uni-stuttgart.de

Dipl.-Ing. Christoph Magg

University of Stuttgart,
Department for Transport Planning and Traffic Engineering,
Pfaffenwaldring 7, D-70569 Stuttgart, Phone +49-711-68582483,
christoph.magg@isv.uni-stuttgart.de

Abstract.
Autonomous vehicles (= AV) permitting driverless car transport will change mobility and transport dramatically. To estimate potential impacts of AV on traffic in an urban area nine scenarios are examined, varying the rate of carsharing, ridesharing and the availability of rail services. The number of required vehicles, vehicle-kilometres and the necessary number or parking spaces quantify each scenario.
The study builds on an existing travel demand model of the Stuttgart Region. This model is extended by an algorithm for bundling person trips in ridesharing systems and by an algorithm for vehicle blocking. The results show that the size of the car fleet can be reduced considerably. The vehicle-kilometres travelled in the network, however, can only be reduced in cases where most travellers use ridesharing instead of carsharing or privately owned cars.

Keywords: autonomous vehicle, automated driving, self-driving car, carsharing, ridesharing, public transport

Motivation.

Autonomous vehicles (= AV) permitting driverless car transport will change mobility and transport dramatically. At the moment, it seems impossible to forecast the point in time, when driverless cars will be ready to operate in the entire road network. The probability, however, that this time will come is high. Therefore, transport planning should address the topic.

AV will affect the transport supply and thus change travel demand. AV permit comfortable car journeys for all travellers including persons without driving licence. A better transport supply can increase the distance travelled and influence the mode choice in favour of the car. At the same time, AV enable more efficient vehicle sharing schemes, as the vehicles can be relocated without driver. Several studies and position papers [3-6] describe the spectrum of possible scenarios ranging from „Driverless Nightmare" to „Driverless Utopia“ ([4] page 9ff) and from “death of the public transport” to “integrated part of public transport”.

The research project MEGAFON [1] examined the impacts of AV on traffic in the Stuttgart Region in nine scenarios, varying the rate of carsharing, ridesharing and the availability of rail services. The number of required vehicles, vehicle-kilometres and the necessary number or parking spaces quantify each scenario. This paper presents the method and the algorithms applied in the project.

Study Area and Assumptions.

The study builds on demand and supply data from the macro- and microscopic travel demand model of the Stuttgart Region. The travel demand is taken from the microscopic model, which covers the travel demand of 2.7 million inhabitants and distinguishes the five modes walk, bike, public transport, car-driver and car-passenger. Every trip is described by origin, destination, mode, day of week, departure and arrival. The approx. 1,000 traffic zones of the model serve as origins and destinations.

The study assumes that AV will replace buses completely. Bus lines with fixed line routes and schedules will no longer exist in their present form. Rail transport, however, will continue to exist in most scenarios. AV can transport travellers on a direct route to their destination or take them to, respectively pick them up from, a railway station. AV then cover trip legs formerly served by buses. Transfers between AV and rail are assigned to railway stations offering the shortest travel time. Thus, the transfer station may differ from the railway station used before the implementation of AV.

It is further assumed that the overall travel demand will not change with the introduction of AV. This means that the number of person trips and the trip destinations remain unchanged. Mode choice is not influenced by prices. Instead, all travellers will select the mode with the shortest travel time.

Modelling Travel Demand.

Trips, which today use motorised modes (public transport, car-driver and car-passenger), are distributed to the following modes:

- Private AV (AV-NS): Privately owned vehicles only used by members of one family (NS = NoSharing).
- Public AV for private use (AV-CS): Publicly owned vehicles used by several travellers consecutively as part of a carsharing system.
- Public AV for public use (AV-RS): Publicly owned vehicles used by several travellers simultaneously as part of a ridesharing system.
- Rail: Public rail services.
- Rail + CS: Combination of rail and carsharing as feeder.
- Rail + RS: Combination of rail and ridesharing as feeder.

Empty public AV can be relocated to serve the next passenger.

Carsharing and Ridesharing.

Specific methods are applied to derive a set of vehicle trips for carsharing and ridesharing from the set of person trips of travellers using AV sharing. An average occupancy rate of 1.3 is assumed for carsharing. For ridesharing several person trips are bundled to one vehicle trip. For the bundling of the person trips the algorithm described in [2] is applied. This algorithm can handle both integer and non-integer demand volumes and is thus suitable for macroscopic and microscopic travel demand models. The algorithm considers the temporal distribution of travel demand and determines the route of vehicle trips collecting travellers within a buffer along the route. A shortest path algorithm determines one suitable route for every origin-destination pair. The buffer of a particular route is defined by the set of traversed network objects, for instance traffic zones or specific stop locations. In the next step, the description of a route is reduced from a longer and spatially more precise sequence of road links to a much shorter and spatially broader sequence of network objects. To identify matches in the set of person trips the sequences of network objects of all trips are compared with each other, starting with the first trip. If there is a match, the trips are bundled as long as a given vehicle capacity is not exceeded. Obviously, the procedure falls in the class of Greedy Algorithms not guaranteeing an optimal solution for the matching problem.

The demand has to be available in sufficiently small time intervals (ideally 15 minutes) and in traffic zones of an appropriate size (interzonal travel time much smaller than average trip travel time).

Vehicle Blocking.

The vehicle trips with sharing vehicles are concatenated to blocks in such a way that the number of required vehicles is minimal. This results in empty vehicle trips. The scenarios require the handling of up to 3 million vehicle trips. For this reason, a simple Nearest Neighbour Algorithm is applied for the vehicle blocking. The algorithm selects as successor either the vehicle trip requiring the shortest empty vehicle trip or the shortest waiting time. The conditions for concatenating two vehicle trips are relaxed in four steps. Two vehicle trips are concatenated, if the following conditions hold for the predecessor and the successor trip:

- They are located in the same traffic zone and the waiting time lies below 60 minutes.
- They are located in the same area (urban district, part of an administrative district) and the waiting time lies below 60 minutes.
- They are located in the same area (urban district, part of an administrative district) without restrictions with respect to time.
- They are located in the area without restrictions with respect to time.

Results.

With a level of motorization of approximately 590 vehicles per 1,000 residents, the households in the Stuttgart Region own about 1.6 million cars (status: 2010). On a normal workday only 1.0 million of these cars are in use. During peak hours, less than 12% of the 1.0 million cars run simultaneously. These cars are in use 60 minutes per day. Considering all 1.6 million cars the operating time falls to 40 minutes per day. In a scenario with 100% ridesharing combined with rail transport, the number of required vehicles decreases to only 7% of today's fleet size. On average, the vehicles will then be in use around 8.6 hours. 1.4 hours of this time is required for empty vehicle trips and buffer times. However, vehicle-kilometres travelled in the network can only be reduced in scenarios with decent shares of ridesharing. Carsharing does not lead to a relief in traffic. The share of empty kilometres referred to the kilometres travelled by all vehicles (including NoSharing) lies between 1% and 6%. Referred to the distance travelled with sharing vehicles 4% to 9% of the kilometres are empty vehicle trips.

The full version of the paper will describe the algorithms in more detail and will discuss the results including assignment results showing the impact in the road network. The potential of ridesharing is analysed by looking at the spatial and temporal distributions of occupancy rates.

Literature.

1. Friedrich, M., Hartl, M. (2016): MEGAFON – Modellergebnisse geteilter autonomer Fahrzeugflotten des öffentlichen Nahverkehrs, Schlussbericht, gefördert von: Ministerium für Verkehr Baden-Württemberg, Verband Deutscher Verkehrsunternehmen e. V., Stuttgarter Straßenbahnen AG, Verkehrs- und Tarifverbund Stuttgart GmbH.
2. Hartl, M., Magg, C., Friedrich, M. (2017): Ridesharing – Ein Modellierungsansatz für das Matching von Fahrtwünschen in makroskopischen Verkehrsnachfragemodellen. Tagungsbericht Heureka 17, FGSV Verlag, Köln.
3. Hazan, J., Lang, Ulrich, P., Chua, J., Doubara, X., Steffens, T. (2016): Will Autonomous Vehicles Derail Trains? The Boston Consulting Group Online available at https://www.bcgperspectives.com/content/articles/transportation-travel-tourism-automotive-will-autonomous-vehicles-derail-trains/, accessed on 06.01.2017.
4. Isaac, L. (2015): Driving Towards Driverless – A guide for government agencies. WSP Parsons Brinckerhoff
5. OECD, International Transport Forum (2015): Urban Mobility System Upgrade. How shared self-driving cars could change city traffic.
6. VDV (2015): Zukunftsszenarien autonomer Fahrzeuge - Chancen und Risiken für Verkehrsunternehmen, Positionspapier.

Detecting Structures in Network Models of Integrated Traffic Planning

Marco Lübbecke[1], Christian Puchert[1], Philine Schiewe[2], and Anita Schöbel[2]

[1] Chair of Operations Research
RWTH Aachen University
[2] Institute for Numerical and Applied Mathematics
University of Göttingen

1 Introduction

When planning a public transportation system, many steps are followed sequentially: Given a transportation network with its stations and direct connections, one first determines a line plan which shows the lines to be operated. The next step is to find a *timetable*, i.e., to fix the arrival and departure times of all lines at all stations. If the timetable is known, the *vehicle schedules* are planned. In the easiest case, each vehicle stays on the same line and goes forth and back the whole day. However, it has been shown that costs can be decreased dramatically if vehicles can switch between lines.

In our work we deal with the two steps of *timetabling* and *vehicle routing*. It is common to treat these two steps sequentially one after the other, i.e., first the timetable is fixed and then the vehicle schedules are optimized for the fixed timetable. It would lead to better solutions if timetabling and vehicle scheduling could be solved as one integrated optimization problem [7]. In this work we formulate such an integrated model. Its structure still reflects that it originates from two single problems which have been integrated. Using decomposition approaches from integer optimization this structure can be exploited numerically. We further investigate if we can find other hidden structures in the integrated formulation other than the structure which comes from the two single problems. We also investigate runtimes of decomposition approaches based on the special decompositions used.

2 Integrating Timetabling and Vehicle Scheduling

We first describe the main characteristics of timetabling and vehicle scheduling:

Timetabling is usually modeled as so-called periodic event scheduling problem (PESP), which is an intrinsically hard problem. It is periodic (because the timetable is repeated every hour). The goal is to minimize the traveling time for the passengers, see, e.g. [6]

Vehicle scheduling in its basic form can be modeled and solved as flow problem which is in its simplest form even possible in polynomial time. The problem is aperiodic, because the vehicle schedules need not be repeated from

hour to hour. The goal here is to minimize the costs for the public transport company, see [2] for an overview.

For integrating periodic timetabling and vehicle scheduling, we hence add a flow formulation for vehicle scheduling to the standard PESP formulation of timetabling. Still, there remain challenges: As we want to find a timetable which is passenger friendly and a vehicle schedule which is cost efficient we get a bicriteria problem with two conflicting objective functions. We solve it by a weighted sum approach. Additionally, we have to overcome the differences between the periodic timetabling model and the aperiodic vehicle scheduling part. This is done by introducing new variables which contain the actual start time of the p-th operation of a line to make sure that only trips which are compatible timewise can be done directly after one another. These time restrictions between trips are the coupling constraints between the timetabling part and the vehicle scheduling part.

Structure of the Integrated Model

We may model integrated timetabling and vehicle scheduling as integer program (IP). Its structure can be seen here. We have variables needed for describing the timetable and we have variables for describing the vehicle schedules. Both types of variables appear in the coupling constraints and also in the objective function.

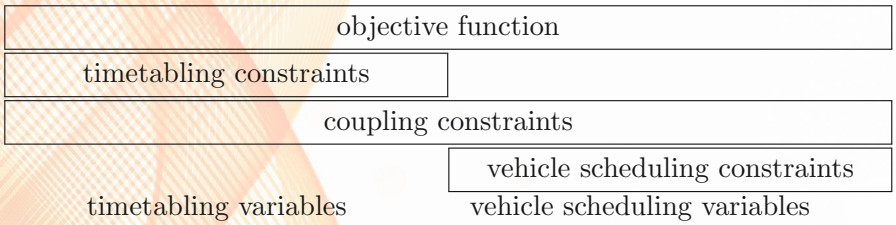

Reformulation

The structure of the given model can be exploited using the *Dantzig-Wolfe decomposition*: The model is reformulated as a *master problem*, containing variables for each feasible timetable as well as for each vehicle schedule. The problem consists then in selecting a timetable and for each line and period exactly one vehicle schedule. Since the number of variables in this model is exponentially high, it is solved using *branch-and-price*: To this end, the linear programming relaxations are solved by *column generation*, i.e. the problem is solved with only a subset of the variables (initially none), and improving variables are added dynamically by solving auxiliary *pricing problems*, one for each of the two components timetabling and vehicle scheduling. In other words, timetables and vehicle schedules are calculated separately, while their compatibility is ensured by the master problem.

This approach can theoretically be applied on any structure which subdivides the constraint matrix into blocks, possibly linked by coupling constraints. In the

above case, we have two such blocks, the timetabling and the vehicle scheduling constraints, respectively. Apart from the above "obvious" structure known by the modeler, the model might contain one or more different "hidden" structures such that the resulting reformulation might yield better results regarding e.g. the running time of the algorithm or the bounds yielded by the relaxation. Such structures can e.g. be found by representing the matrix as a hypergraph and applying partitioning algorithms [1].

3 Experiments

We tested the branch-and-price approach with the above reformulation on two datasets: *Lowersaxony* is derived from the regional train network in Lower Saxony, Germany. It contains 36 stations and 26 lines. The instance *Grid* was created by [3] as realistic demonstrator. It is a grid-network with 25 stations and 80 lines. The vehicle schedule has been calculated for four periods for all instances.

To solve the reformulated model, we use the generic branch-and-price solver GCG [5] based on the SCIP framework [4]. Given an integer programming (IP) model e.g. in `.lp` or `.mps` format together with appropriate structure information, GCG applies a Dantzig-Wolfe decomposition and then runs a fully generic branch-and-price algorithm on the reformulated problem.

The model structure can be manually passed directly by the user, as we have done with the above structure. Additionally, GCG comes with various structure detectors which we employed to search for other, different structures.

We performed tests with GCG using the structure from above as well as one structure detected by the solver.

	Manual			Solver Structure		
Dataset	Dual Bd.	Primal Bd.	Gap(%)	Dual Bd.	Primal Bd.	Gap(%)
Lowersaxony	3255528	3297544	1.3	-20965300	∞	–
Grid	-48374	81863	–	$-\infty$	∞	–

The results show the best dual and primal bounds and the gap for the manual approach as well as for a reformulation based on a structure found by the solver. The manual approach already yields reasonably good feasible solutions on small instances. On dataset *Lowersaxony*, the algorithm was even able to reach a gap of only 1.3%. The manual decomposition currently outperforms any structure found by the solver—where no feasible solutions at all could be found. However, the structure detection is currently undergoing a re-design, so that further investigation will be done in the near future.

The branch-and-price approach itself still has potential for further improvement. Currently, much of the solving is used for the pricing problems, which are solved as generic IPs. It is planned to replace this by a problem specific algorithm. Furthermore, pricing problems do not need to be solved exactly; solving can be stopped as soon as an improving column has been found.

References

1. Bergner, M., Caprara, A., Ceselli, A., Furini, F., Lübbecke, M.E., Malaguti, E., Traversi, E.: Automatic Dantzig–Wolfe reformulation of mixed integer programs. Mathematical Programming 149(1), 391–424 (2015)
2. S. Bunte and N. Kliewer: An overview on Vehicle Scheduling models. Public Transport 4:1, 299-317 (2009)
3. M. Friedrich, M. Hartl, A. Schiewe, A. Schöbel: Angebotsplanung im öffentlichen Verkehr: Planerische und algorithmische Lösungen. HEUREKA'17
4. Gamrath, G., Fischer, T., Gally, T., Gleixner, A.M., Hendel, G., Koch, T., Maher, S.J., Miltenberger, M., Müller, B., Pfetsch, M.E., Puchert, C., Rehfeldt, D., Schenker, S., Schwarz, R., Serrano, F., Shinano, Y., Vigerske, S., Weninger, D., Winkler, M., Witt, J.T., Witzig, J.: The SCIP Optimization Suite 3.2. Tech. Rep. 15–60, ZIB, Takustr. 7, 14195 Berlin (2016)
5. Gamrath, G., Lübbecke, M.E.: Experiments with a Generic Dantzig-Wolfe Decomposition for Integer Programs. In: Festa, P. (ed.) Experimental Algorithms, Lecture Notes in Computer Science, vol. 6049, pp. 239–252. Springer Berlin / Heidelberg (2010)
6. C. Liebchen: Periodic Timetable Optimization in Public Transport. Dissertationsschrift TU Berlin (2006)
7. A. Schöbel: An Eigenmodel for Iterative Line Planning, Timetabling and Vehicle Scheduling in Public Transportation. Transportation Research C 74, 348–365 (2017)

A Complementary Optimization-Simulation Framework for the Evacuation of Large Urban Areas

Stefan Ruzika and David Willems*

Mathematisches Institut
Universität Koblenz-Landau
Universitätsstraße 1
56070 Koblenz, Germany

1 Introduction

The International Federation of Red Cross and Red Crescent Societies defines a disaster or a catastrophe as "a sudden, calamitous event that seriously disrupts the functioning of a community or society and causes human, material, and economic or environmental losses that exceed the community's or society's ability to cope using its own resources" [1].

In most cases, such catastrophes occur unexpectedly to the residents and give reason to immediately evacuate all affected people from the danger zone. Recent examples for well-known catastrophes are the tsunami and nuclear plant disaster in Fukushima or the volcanic eruption in Indonesia.

However, a large-scale evacuation is not only mandatory in response to a disaster, but also due to precaution measures to prevent damage and injuries, e.g. in case of a bomb disposal. Particularly in Germany, several unexploded Second World War bombs are found every year such that thousands of people have to be evacuated from the danger zone before special forces defuse the bombs. Examples from the last years include bomb finds in Koblenz, Mainz and Augsburg.

In order to ensure a fluent large-scale evacuation, one option is to define and analyze possible scenarios and develop different solution strategies. In such situations, decision makers have to act quickly and, often, they lack experience or expertise. Mathematical models help in such situations and support the decision making process.

2 Methodology

Modeling evacuation processes with mathematical methods offers the possibility to learn about the practical admissibility and feasibility of such a recommendation. Moreover, a mathematical model can provide further valuable insights into the evacuation process.

* The research of David Willems was partially funded by BMBF project *MultikOSi*, grant nr. 13N12825.

From a mathematical point of view, there are several concepts to model an evacuation process, ranging from microscopic models as in [2] over mesoscopic models as in [3] to macroscopic models as in [4].

2.1 The network flow model

Within this paper we model a general evacuation process as a quickest flow problem as in [5] and give an overview on how to construct the model: streets are identified as edges, intersections as vertices of a graph and people moving in the streets are mapped as flow units onto the network.

The methods we propose are not scenario-specific and can easily be transferred to other scenarios. The model is a macroscopic approach, using discrete time steps, for which we make several optimistic assumptions such as uniform speed independent of flow density or no individual route selections. Those assumptions simplify the model in such a way that it can be solved to optimality, and that the real evacuation time is guaranteed to be larger than the model result. Hence, we obtain a provable lower bound on the real evacuation time.

Additionally, we discuss how the introduction of a parameter set extends the model to a scenario-based approach. We also include time-dependent departure times, which are not part of the standard quickest flow problem.

Since it is desirable for the optimization model and the simulation model to "operate" on the same data set, we use a time-expanded network to compute the quickest flow using the *triple optimization result* shown in [6] and adapt the sources such that they are similar to the ones in the simulation model.

2.2 The simulation model

The aforementioned model is complemented by a discrete-event macroscopic approach: the evacuees are modeled as agents that travel from the sources of the flow-based model through the network to the zones that are assumed to be safe. Both models share the same parameter set, but in contrast to the flow-based model, we can relax several assumptions like the absence of individual route selection and allow stochastic parameters like varying travel times in the simulation model.

At the beginning of the simulation, each agent is assigned to the sink that he can reach on the "cheapest" way from his source. Here, the cheapest way can be interpreted either as the shortest path concerning the actual distance, the fastest way regarding the travel time from source to sink or arbitrary generalizations like quickest paths.

This approach allows interaction between the agents in a simple way. At each time step every agent has a certain state: the agent is either traveling along an edge in the underlying network or has to wait because the street has reached its capacity limit. If the agent has waited several time steps, he might choose another path to the sink or even a completely different sink at all.

3 Conclusion

In [7], the authors propose a hybrid and multiscale approach based on coupling macroscopic network flows with mesoscopic pedestrian flow. In their setting, the macroscopic part is represented by a shuttle bus system transporting festival visitors from parking areas to the festival site. After leaving the buses the visitors are transformed into objects on a cellular automaton grid populating the event.

The sandwich-method proposed in [8] follows a similar idea, but again focusses on the movement of pedestrians on a different spatial resolution and thus uses a different simulation approach. The considered area is roughly in the magnitude of $1\,\mathrm{km}^2$, whereas the area of a city like Koblenz is about $100\,\mathrm{km}^2$. To cope with this large area, a network-based flow model and a discrete event simulation have been implemented.

For the flow model, several parameters allow us to use the same network to consider different evacuation scenarios of the same area, obtaining provable lower bounds on the evacuation time. This includes different traffic volumes, different travel speeds, and delayed departure times, but can be easily extended by additional parameters.

This hybrid approach combines the "best of both worlds" in the sense that we get a provable lower bound on the evacuation time from the network flow problem. On the other hand, optimization alone would not give the full picture, as the dynamic aspects, such as varying travel speed, captured in the simulation push the model's behavior to a more realistic behavior and thus gives a somewhat more realistic estimate on the evacuation time.

References

1. International Federation of Red Cross and Red Crescent Societies: What is a disaster? `http://www.ifrc.org/en/what-we-do/disaster-management/about-disasters/what-is-a-disaster/` (2017)
2. Kneidl, A., Borrmann, A., Hartmann, D.: Generation and use of sparse navigation graphs for microscopic pedestrian simulation models. Advanced Engineering Informatics **26**(4) (2012) 669–680
3. Dietrich, F., Köster, G., Seitz, M., von Sivers, I.: Bridging the gap: From cellular automata to differential equation models for pedestrian dynamics. Journal of Computational Science **5**(5) (2014) 841–846
4. Hamacher, H.W., Tjandra, S.A.: Mathematical modelling of evacuation problems: A state of art. Fraunhofer-Institut für Techno-und Wirtschaftsmathematik (2001)
5. Burkard, R.E., Dlaska, K., Klinz, B.: The quickest flow problem. Zeitschrift für Operations Research **37**(1) (1993) 31–58
6. Jarvis, J.J., Ratliff, H.D.: Some equivalent objectives for dynamic network flow problems. Management Science **28**(1) (1982) 106–109
7. Biedermann, D.H., Torchiani, C., Kielar, P.M., Willems, D., Handel, O., Ruzika, S., Borrmann, A.: A hybrid and multiscale approach to model and simulate mobility in the context of public events. In: International Scientific Conference on Mobility and Transport Transforming Urban Mobility. (2016)
8. Hamacher, H.W., Heller, S., Klein, W., Köster, G., Ruzika, S.: A sandwich approach for evacuation time bounds. In: Pedestrian and Evacuation Dynamics. Springer (2011) 503–513

Agent-based Simulation of Passengers in Rail Networks

Sebastian Albert[1], Philipp Kraus[2], Jörg Müller[2], and Anita Schöbel[1]

[1] Georg-August-Universität Göttingen
[2] Technische Universität Clausthal

1 Delay management in public rail transportation

Delay management in rail transportation decides how to react to delays of trains. In case of delays, different trains may compete for the occupancy of a particular piece of a track at overlapping time windows, hence *priority decisions* have to be made: Which train is allowed to go first, and should a train take a different route? Extended simulation tools exist to predict the effects by routing trains along the track system taking all safety constraints into account [5]. From a passenger-oriented point of view, the *wait-depart decision* is more important: Which of the connecting trains should wait for a delayed feeder train, and which of them should depart on time? Such decisions are usually made at railway traffic control centres.

Apart from fixed waiting time rules, which are usually applied in practice, further models and decision strategies exist for the delay management problem, see [7]. Yet, most of them use historical, static traffic loads, which are merely a mediocre approximation to the real streams of passengers affected by these decisions in a particular instance. For instance, it is mostly neglected that the route a passenger would take depends in turn on the delays and on the delay management decisions. In many cases, waiting an entire cycle time for the next train of the same service after missing a connection is inefficient for travellers, because a different combination of train services may result in an earlier arrival at their respective destinations. Only very few approaches take this into account [3,6]. Moreover, the delay of a train may even result in new opportunities for connections that do not exist at all in regular, undisturbed operations.

Another completely neglected aspect is related to the behaviour of passengers at the stations: What do they do if a transfer is likely to be missed? People running from one platform to another in a hurry can interfere with others, heavy luggage may slow down passengers and increase the time they need for changing trains, and crowds in the station also slow down traffic. In some situations, particular patterns of passenger flow can cause additional train delays when, for instance, a steady trickle of people stepping in prevents the doors from closing.

Since the microscopic modelling of individual passengers and their reactions to the decisions that are to be optimised renders classic optimisation models intractably large, we pursue a simulation-based approach; our goal is to investigate

and evaluate by agent-based simulation if, how and to what extent passenger behaviour affects delays, and whether and how delay management decisions can be adapted accordingly. This includes the choice of routes as well as their behaviour in the station, both of which also depend on the passengers' individual levels of information. Hence, not only do we study the influence of delays on passengers but also the influence of passengers on delays.

In this work-in-progress paper, we describe the current status of our research including the agent-based simulation model and platform, first insights gained in terms of design decisions e.g. related to scalability; we sketch the unified data model which establishes the nucleus of our integrated simulation model, and describe an example scenario and the specification of a test instance of the simulation derived from this example. Finally, we discuss opportunities of future work.

2 Agent-based simulation model and platform

Agent-based modelling and simulation (ABMS) [2] is a computational paradigm in which the concepts of agents and multiagent systems form the metaphor underlying the simulation model. While ABMS is often associated with microscopic modelling, in our work we use the agent paradigm as a basis for creating an integrated simulation including macroscopic modelling of trains moving through the railway network, and a microscopic view of train stations, with a detailed simulation of passenger behaviour, such as movements within the train station and on platforms. Agents in our approach are not only the passengers, but all behaviour-bearing system entities such as trains, stations, information devices, and dispatchers. We use the agent framework LightJason [1] (http://lightjason.org/), which supports an extension of the logical language AgentSpeak(+) to implement Belief, Desire, Intention (BDI) models. LightJason combines a declarative, script-based agent programming language with a concurrent and scalable runtime architecture. It supports high-level scripting of agent behaviour with its detailed analysis (also at runtime) for all agents in the simulation.

At the microscopic level, passengers move through the train station and try to catch their trains on the appropriate platform. If the train is delayed, passengers will consider changing their routes based on their goals and preferences. While moving through the station, a passenger will be attracted or repelled by other simulation elements such as shops and other passengers, where the resulting behaviour also depends on the passenger's preference structure. Towards this end, we use a combination of a graph routing algorithm with a modification of a Social Force model [4] in order to combine explicit goal-driven behaviour with realistic behaviour in crowds.

Passengers can be simulated with different degrees of access to information and information services. In detail passengers are generated with individual preferences and behavioural predispositions, based on average distributions of these values over the population where known; the values of certain properties (e.g., stress level, tiredness, hunger) change over time and parameterise the travellers'

opportunistic behaviour. The agent perceives its environment, such that changes (like announced platform changes, obstacles in the station hallway, or modified departure times) will also cause changes in the agent's goals, decisions, and actions, e.g., deciding to enter a shop, walking faster, or consulting a mobile device to access information.

The first main outcome of passenger simulation will be information about minimal, average, or maximal transfer times for passengers changing trains. This information is expected to be used to refine dispatching (and ultimately: timetabling) models, enabling dispatchers to select and optimise strategies to determine waiting decisions and departure times, and to analyse vice versa how different dispatching strategies influence train delays and passenger satisfaction.

3 Integrated data model

We defined an integrated data model, which provides the basis for the overall simulation system; in particular, it combines the macroscopic with the microscopic view of the simulation environment.

The microscopic part (see Fig. 1, left) defines the initial knowledge (beliefs) of each agent and the information about property distributions and origin-destination structures. These structural models are complemented by behavioural models of the agents (passengers, trains, stations), which are represented by LightJason scripts that contain agents' initial and potential goals, as well as plans for achieving them.

The macroscopic model (see Fig. 1, right) represents the static environment including the railroad network, aspects of the physical layout of train stations and trains, demand models, and passenger generators, as well as an initial train timetable. The entire model is defined as an XML Schema (XSD) structure. To ensure interoperability with industrial modelling standards, the macroscopic model is based on RailML (http://www.railml.org/).

4 Test instances and further work

We will present initial results on a small instance with a railway network consisting of eight stations and a simplified station architecture. This instance is meant as a proof of concept to show functional correctness of the integrated simulation, including trains running through the railway network, passengers travelling between their origins and destinations and moving through the station, and a simulated traffic control centre that can use different strategies to react to delays.

We currently collect data for applying the simulation with an extended station layout resembling the station of Göttingen and the railway network of Lower Saxony including 34 stations, which will then also enable us to evaluate the effects of passengers' behaviour on delays and on delay management strategies in a realistic scenario. We furthermore aim at developing an integrated hybrid simulation *and* optimisation model which can assist decision makers in finding good delay management decisions online.

References

1. Aschermann, M., Kraus, P., Müller, J.P.: LightJason: A BDI Framework inspired by Jason. In: 14th Europen Conference on Multiagent Systems (EUMAS 2016). Valencia, Spain (2016), `https://www.in.tu-clausthal.de/fileadmin/homes/techreports/ifi1604aschermann.pdf`, to appear, extended version available as Technical Report TR IfI-16-04, TU Clausthal, Nov. 2016
2. Bazzan, A.L.C., Klügl, F.: Agent-based Modeling and Simulation. AI Magazine 33(3), 29–40 (2013)
3. Dollevoet, T., Huisman, D., Schmidt, M., Schöbel, A.: Delay management with rerouting of passengers. Transportation Science 46(1), 74–89 (2012)
4. Helbing, D., Molnár, P.: Social force model for pedestrian dynamics. Physical Review E 51, 4282–4286 (1995)
5. Pachl, J.: Railway Operations and Control. VTD Rail Publishing, Mountlake Terrace, USA, 2 edn. (2014)
6. Rückert, R., Lemnian, M., Blendinger, C., Rechner, S., Müller-Hannemann, M.: Panda: a software tool for improved train dispatching with focus on passenger flows. Public Transport (2017), to appear
7. Schachtebeck, M., Schöbel, A.: IP-based techniques for delay management with priority decisions. In: Fischetti, M., Widmayer, P. (eds.) ATMOS 2008 - 8th Workshop on Algorithmic Approaches for Transportation Modeling, Optimization, and Systems. Dagstuhl Seminar proceedings (2008)

A Appendix

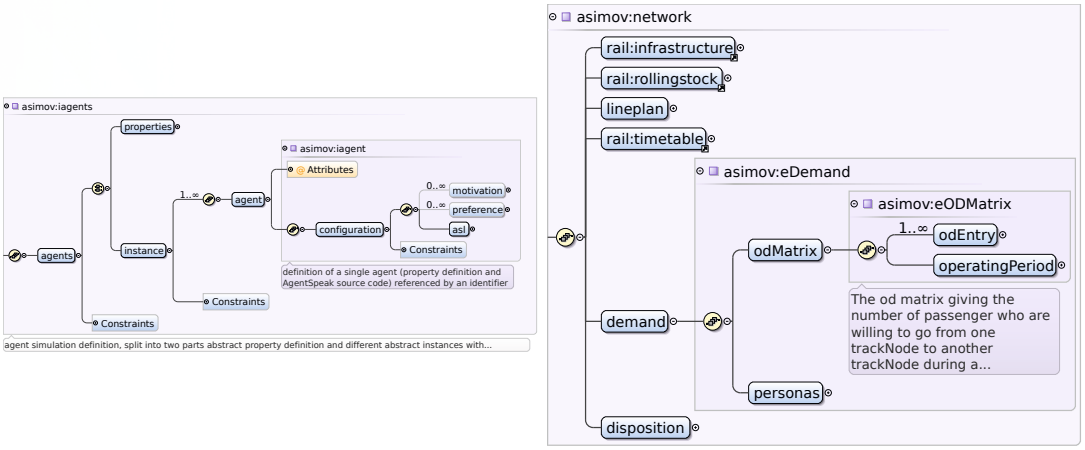

Fig. 1. Asimov data model

38

Combining Simulation and Optimization for Extended Double Row Facility Layout Problems in Factory Planning*

Uwe Bracht[1], Mirko Dahlbeck[2], Anja Fischer[2], and Thomas Krüger[1]

[1] Clausthal University of Technology, Inst. of Plant Engineering and Fatigue Analysis
[2] University of Göttingen, Institute for Numerical and Applied Mathematics

Globalization, the growing dynamics of the markets, the increase in customized products, decreasing product life cycles and technological innovations are only some of the challenges today's manufacturing enterprises have to cope with. As a result, manufacturing enterprises are forced to implement a cost efficient production in order to remain competitive. The layout of the production areas and operating materials (assets and machines) is one of the main influencing factors and provides a basis to uphold the long-term productivity and competitiveness [6].

In this work we present a combined optimization-simulation approach for determining a good start solution for the layout of the departments (or operational areas) along several paths that is then the basis for the following steps of the factory planners on a much finer level of detail. In order to handle many of the requirements posed on the layout in real-world production, the existing mathematical optimization models have to be extended.

From a mathematical point of view, this leads to facility layout problems, where one tries to determine the position of departments and machines inside a (restricted) area of a factory in order to minimize the weighted pairwise distances between them. These are widely studied [3]. Several methods have been developed in this area ranging from graphical methods, heuristics, which allow deriving solutions rather fast but without some knowledge of the quality of the solutions, and exact optimization methods. Unfortunately, even small instances are rather challenging. So the exact solution or even deriving good solution with appropriate solution guarantees for small to medium-sized instances is often rather time-consuming. For this reason, one often concentrates on special cases where one restricts the structure of the layout and the paths. In the so called *Single Row Facility Layout Problem (SRFLP)*, that is well understood from a mathematical point of view, one arranges departments along one side of a path, see, e. g. the recent survey [5]. We consider in this work the *Double Row Facility Layout Problem (DRFLP)*, an extension of the $\mathcal{NP}$-hard SRFLP, originally introduced in [2]. In the basic model one is given a set N of n departments with length $l_i, i \in N$, as well as pairwise transport weights $c_{i,j} = c_{j,i}, i, j \in N, i \neq j$, between the departments. The task is to arrange the departments right and left to one path, i. e., in two rows along a central corridor, such that the weighted sum of the center-to-center distances is minimized. So for the DRFLP we look for a vector $p \in \mathbb{R}^n$ of positions and a vector $r \in \{1, 2\}^n$ of the assignment of the

* This work is supported by the Simulation Science Center Clausthal/Göttingen.

departments to rows such that

$$\min_{p,r} \sum_{i,j \in N, i \neq j} c_{i,j}|p_i - p_j|$$

$$\text{subject to } |p_i - p_j| \geq \tfrac{l_i + l_j}{2}, \qquad \text{for } i, j \in N, i \neq j, \text{ if } r_i = r_j.$$

The best known approach for solving these problems is presented in [4]. One is able to solve instances with up to 16 departments in reasonable time, i. e., 12 hours. There one combines a strong model for the DRFLP with fixed row assignments, where the row of each department is known in advance, with a branching scheme enumerating over all possible row assignments (some of these are excluded due to further investigations).

In comparison to factory layout problems in practice several simplifications were done. So several adjustments and extensions are necessary in order to create a valuable tool for real-world factory planning. In the literature the solution approaches are usually compared for some specifically generated instances, see, e. g., [4]. Real-world instances might have some specific structures that can and have to be exploited in the mathematical models. In job shop production there are often several machines of the same type and the total workload is distributed between these, hopefully rather equally. Assuming an equal distribution between these, all specifications, i. e., the size and the transport weights, are the same for machines of the same type. In order to speed up the solution process, we consider these symmetries during the solution process adapting the approach in [4]. We use two different ways to break the symmetries. First, we can reduce the number of row assignments that have to be considered by just testing different numbers of machines of that type in the rows. Second, we can use a specific order of the departments in a common row and enforce these by several constraints. The detailed optimization model of [4] as well as our extensions will be given in the talk and in the full version of the paper. Using our symmetry-breaking allows us to solve realistic instances with up to 21 departments in reasonable time, extending the solvability of such instances by several departments.

A next aim of our work is to overcome several simplifications that are usually done in the mathematical DRFLP models. So we show how to include interrow-distances as well as minimal distances between departments in the same row and in general that might, for instance, be motivated by safety restrictions. It might be necessary as well to limit the distance between certain departments, for instance, in order to reduce the walking distances of certain workers or simplify the connection to certain supply lines. Furthermore, we show how to take the total area used for the layout into account.

In order to implement common structural layout concepts for improving the transparency of the directed material flow, we extend the DRFLP such that given two specific departments (e. g. the stores of the incoming goods or primary products and the final products (in the shipping department)) are on both ends of the path and all other departments are arranged along the path, see the illustration below. It is worth to compare solutions of these problems with classical DRFLP solutions.

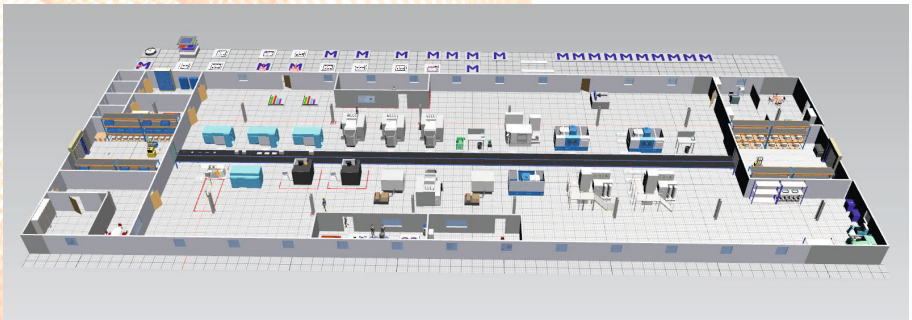

Unfortunately, only the transportation weights and so the weighted transport load are taken into account in the DRFLP models. But there are several indicators that are important for guaranteeing a smooth production, e. g., the throughput of the factory, the cycle times of the products or the used storage and buffer capacities. For this reason we combine our mathematical models with a simulation of the production. This allows detecting potential problems or conflicts. These are then our starting point for extending the mathematical models. This process is repeated as long as the solution satisfies all desired criteria. Our tests show that considering the portion of time used for transports of the total cycle time of single product groups in job shop production can vary drastically depending on the targeted output. This can be prevented by bounding the transportation distances associated to single products. A second way is to set up a desired distance (or time) for the transportation processes and to penalize the difference to this value with piecewise linear functions. One big advantage of our iterative layout creation is that afterwards we can nicely compare the found solutions. So the decision-maker sees the direct consequences of including certain restrictions.

To verify the quality of the extended DRFLP model we use discrete event simulation. As a software tool Tecnomatix Plant simulation was chosen. An DRFLP solution is transferred in a simulation model to generate dynamic and realistic information about the transport processes. Apart from these information, additional input variables and key performance indicators can also be analyzed with the simulation. These are the basis for adapting the mathematical optimization models. A second benefit of the simulation is the visualization of processes to increase the understanding of complex relations [1], only partially visible in the available indicators provided by Tecnomatix Plant simulation. So, if the simulation results show the need for improvements of the current layout, the DRFLP models are customized as described above and the interplay between optimization and simulation continues. We test our approach on realistic instances. Visualizations of the optimized layouts and their transformed variants will be provided in the talk and in the full version of the paper.

Our work can be extended in several directions. One could combine our current optimization-simulation framework with respect to the DRFLP with more general path structures and try to include robustness aspects. Furthermore, we combine the simulation with 3D models since a 3D visualization might simplify the analysis of the results and improve the integration of the workers.

References

1. U. Bracht, D. Geckler, and S. Wenzel. *Digitale Fabrik*. 2011.
2. Jaewoo Chung and J.M.A. Tanchoco. The double row layout problem. *International Journal of Production Research*, 48(3):709–727, 2010.
3. Amine Drira, Henri Pierreval, and Sonia Hajri-Gabouj. Facility layout problems: A survey. *Annual Reviews in Control*, 31(2):255–267, 2007.
4. A. Fischer, F. Fischer, and P. Hungerländer. New exact approaches to row layout problems, 2015. NAM Preprint 2015-11.
5. Birgit Keller and Udo Buscher. Single row layout models. *European Journal of Operational Research*, 245(3):629–644, 2015.
6. T. Rooks. Rechnergestützte Simulationsmodellgenerierung zur dynamischen Absicherung der Montagelogistikplanung bei der Fahrzeugneutypplanung im Rahmen der Digitalen Fabrik. Number 20 in Innovationen der Fabrikplaung und -organisation. Shaker Verlag, 2009. Dissertation.

Solving multiobjective optimization problems with parameter uncertainty: an interactive approach

Yue Zhou-Kangas[1], Anita Schöbel[2], Kaisa Miettinen[1], and Karthik Sindhya[1]

[1] University of Jyvaskyla, Faculty of Information Technology,
FI-40014 University of Jyvaskyla, Finland,
yue.y.zhou-kangas@jyu.fi,
[2] University of Göttingen, Institute for Numerical and Applied Mathematics,
Lotzestraße 16-18, 37083 Göttingen,Germany

1 Multiobjective optimization

For multiobjective optimization problems, there does not exist a single best solution. Instead, there is a set of mathematically equally good solutions called Pareto optimal solutions. The Pareto optimal solutions are not comparable without additional information. Usually, the preferences of a decision maker are utilized to compare the Pareto optimal solutions and find the most preferred one for the needs of the decision maker. Multiobjective optimization methods can be classified according to the role of the decision maker in the solution process. The class of interactive methods [8] can best support the decision maker to find the most preferred solution by allowing her/him to progressively specify her/his preferences and learn about attainable solutions as well as the feasibility of one's preferences until the most preferred solution is found.

2 Robustness in multiobjective optimization

Even though conventional interactive methods consider only deterministic multiobjective optimization problem, many practical problems involve uncertainties which can originate from various sources. The uncertainties can render the computed solution to unexpected and undesired degradations on their quality (i.e., the objective function values). Thus, sufficient immunity to the uncertainties (i.e., robustness) of the solutions should be considered and presented to the decision maker at the same time as their quality during the interactive solution process. As a final result, the decision maker should find a most preferred solution with a satisfactory balance on the quality and the robustness. Not much attention has been paid in the literature to supporting the decision maker in terms of solving uncertain multiobjective optimization problems. In [4], a most preferred worst case solution is found for the decision maker. In [6] and [10], multiple realizations of the uncertain parameters are considered simultaneously.

Research on multiobjective robust optimization has only been started in recent years. A survey [5] provides a comprehensive summary on the robustness concepts in multiobjective optimization. Among them, the concept of minmax robust Pareto optimality [3] is an extension from single-objective robust optimization (e.g., [1]) for problems with uncertain parameters in objective functions. Together with the definition of minmax robust Pareto optimality, the robust variants of the weighted-sum method and the ϵ-constrained method were presented in [3]. This concept was also studied in [2] where general scalarization functions were discussed and in [7], the situation where an uncertain parameter is involved in one of the objectives in bi-objective problems was analyzed.

In this talk, as in [2], [3], and [7], we generate solutions and simulate their outcomes with the help of the concept of minmax robust Pareto optimality for multiobjective optimization problems with uncertain parameters in the objective functions. We assume that the uncertain parameters stem from some finite set. A realization of the uncertain parameters is called a *scenario*, among which the normal case is referred to as the *nominal scenario*. But on the contrary to the earlier research, we concentrate on supporting the decision maker to find a most preferred solution with a satisfactory balance on the quality and the robustness. We design an interactive solution process utilizing and extending elements of the synchronous NIMBUS method [9] to simulate the outcomes of the solutions in different scenarios.

3 Challenges in designing interactive methods

When solving uncertain multiobjective optimization problems with an interactive method, there are at least three major challenges. First, the approach to quantify robustness in an understandable way to the decision maker is not trivial. The existence of a robust solution which at the same time has a high quality is usually unlikely. So the decision maker has to sacrifice some of the quality to obtain a more robust solution. However, it is challenging to provide information on how 'much more' robust a solution can be when a certain amount of quality is sacrificed. Second, during the interactive solution process, only a limited amount of information can be provided to the decision maker without exposing her/him to too heavy cognitive load. But the information presented should still be sufficiently adequate for the decision maker to understand and consider simultaneously both the quality and the robustness of the solution. Third, when a solution is presented, a proper visualization of both types of information of the solution is important to help the decision maker.

4 Extending NIMBUS to simulate and evaluate robustness of solutions

With the recognition of the three major challenges, we develop a variant of the synchronous NIMBUS method by utilizing elements of it. Outcomes in different scenarios are simulated. Based on the concept of minmax robust Pareto optimality, we present the robust counterpart of the synchronous NIMBUS scalarization function, with which we simulate the outcomes in the worst case scenario. By simulating the outcomes in the worst case and the nominal scenario, two types of solutions are available. During the solution process, it would be challenging for the decision maker to consider these solutions in the two scenarios simultaneously.

Instead of providing both solutions to the decision maker, we add an additional preprocessing step to ask the decision maker to select a scenario. By selecting a scenario, the decision maker chooses whether (s)he emphases on a most preferred Pareto optimal solution in the nominal scenario or a best possible solution when the worst case scenario is realized, i.e., a minmax robust Pareto optimal solution, whose objective function values in the nominal scenario are most satisfying.

Based on the answer, we simulate the outcomes by solving the corresponding problem. If the decision maker would like to have a most preferred Pareto optimal solution in the nominal scenario, we solve the problem with the synchronous NIMBUS method as solving a deterministic problem. If the decision maker would like to have a minmax robust

Pareto optimal solution, we first compute/approximate the set of minmax robust optimal solutions and then find the one which satisfies the decision maker's preferences best based on their objective function values in the nominal scenario. As in the original synchronous NIMBUS method, the decision maker is expected to classify the objective functions to indicate how their current values should be changed to get a more preferred solution.

At the end of the solution process, i.e., when the decision maker has found a satisfactory solution in the selected scenario, we present the objective function values of the solution in the other scenario. If the decision maker desires, (s)he can specify new preferences and obtain a new solution. The solution process continues until the decision maker finds a satisfactory solution. To help the decision maker to make an informed choice of the solution, we visualize the quality and the robustness of a solution during the interactive solution process. As with all interactive methods, the visualization of the information exchanged plays an important role. The need is even more obvious here when the decision maker must understand different types of information. We demonstrate this robust variant of synchronous NIMBUS with an example problem.

References

1. Ben-Tal, A., El Ghaoui, L., Nemirovski, A.: Robust Optimization. Princeton Series in Applied Mathematics, Princeton University Press (2009)
2. Bokrantz, R., Fredriksson, A.: Necessary and sufficient conditions for Pareto efficiency in robust multiobjective optimization. arXiv preprint (2014)
3. Ehrgott, M., Ide, J., Schöbel, A.: Minmax robustness for multi-objective optimization problems. European Journal of Operational Research 239(1), 17 – 31 (2014)
4. Hassanzadeh, F., Nemati, H., Sun, M.: Robust optimization for multiobjective programming problems with imprecise information. Procedia Computer Science 17, 357 – 364 (2013), first International Conference on Information Technology and Quantitative Management
5. Ide, J., Schöbel, A.: Robustness for uncertain multi-objective optimization: a survey and analysis of different concepts. OR Spectrum 38(1), 235–271 (2016)
6. Klein, G., Moskowitz, H., Ravindran, A.: Interactive multiobjective optimization under uncertainty. Management Science 36(1), 58–75 (1990)
7. Kuroiwa, D., Lee, G.M.: On robust multiobjective optimization. Vietnam Journal of Mathematics 40(2,3), 305–317 (2012)
8. Miettinen, K.: Nonlinear Multiobjective Optimization. Kluwer Academic Publishers, Boston (1999)
9. Miettinen, K., Mäkelä, M.M.: Synchronous approach in interactive multiobjective optimization. European Journal of Operational Research 170(3), 909 – 922 (2006)
10. Miettinen, K., Mustajoki, J., Stewart, T.J.: Interactive multiobjective optimization with NIMBUS for decision making under uncertainty. OR Spectrum 36(1), 39–56 (2014)

Decomposition of multi class open queueing networks with batch service

Wiebke Klünder

Clausthal University of Technology – Simulation Science Center Clausthal-Göttingen

1 Introduction

The importance of analysis of non-product form networks by apllying approximations has increased steadily in recent years. The most important strategy approach is given by the decomposition method. The decomposition method enables an isolated treatment of the nodes within the network. The method is particularly applied in planning and optimization of production systems by calculating characteristics of each node. In this article a decomposition method will be presented serving primarily as a pre-evaluation tool. If the calculated characteristics move in acceptable ranges Monte-Carlo simulation can be performed. Until now the decomposition method for open queueing networks with batch service in the single class case was developed [1] by using the approach of Pujolle/Ai [2]. The aim is the generalization of the method to the multi class case of open networks with batch service.

For the modeling of production processes non-product form networks are usually used. However these networks have a number of properties which prevent an exact analytical calculation of measures such as the average queue length on a machine. One possibility analyzing non-product form networks is the Monte-Carlo simulation which can be computationally expensive depending on the size of the modeled production system and does not provide any functional relationships between the parameters and the measures. An important analytical solution strategy is the decomposition method. The method uses approximations to determine the measures of the model and also provides functional relationships between parameters and measures which are helpful for a general model understanding.

2 Decomposition

The decomposition method allows the disaggregation of non-product form networks into single components and connected those adequately by traffic equations. Each component represents a queueing system consisting of machines and a waiting area. The machines can optionally process batches which have a size greater than 1 (batch service). In case of multi class it is assumed that batches consists of one product class and the machines can process all product classes.

The service and interarrival times of the batches are modeled by stochastic processes which differ between the components. The decomposition method involves the construction and solving two linear systems of equations. The solutions provide values for the approximately calculations of the measures by using the modified approximation formula of Allen and Cunneen [3],[4],[5]. The first linear system of equations treats the streams between the components and the equations are formed by the modified traffic equation

$$\tau_i^{(k)} = p_{0i}^{(k)} \frac{b_0^{(k)}}{b_i^{(k)}} + \sum_{j=1}^{N} \tau_j^{(k)} p_{ji}^{(k)} \frac{b_j^{(k)}}{b_i^{(k)}} \qquad \tau_0^{(k)} := 1. \tag{1}$$

The solutions of (1) are integrated into the second linear system of equations which describes the streams to and inside a component. To describe these streams the approximations of Pujolle/Ai [2] is used:

$$SCV[I_i^{(k)}] = \left(\sum_{j=0}^{N} \tau_j^{(k)} p_{ji}^{(k)} \right)^{-1} \left(\sum_{j=0}^{N} \tau_j^{(k)} p_{ji}^{(k)} \left(1 + p_{ji}^{(k)} \left(\rho_j^{\circ 2} SCV[S_j^{\circ}] + (1-\rho_j^{\circ}) \cdot \left[\sum_{k=1}^{K} \frac{\lambda_j^{*(k)}}{\lambda_j^{\circ}} \frac{E[X_j^{(k)}]}{b_j^{(k)}} (SCV[X_j^{(k)}] + SCV[I_j^{(k)}]) \right] + (1-\rho_j^{\circ})\rho_j^{\circ} \right) - 1 \right) \right).$$

3 Numerical results

The realized simulation study includes two reference models. The first represents a six-stage series with three product classes and the second a network with two product classes. The simulation models constructing of the reference models can be divided into six different model classes. The first three model classes describe models which components have the same batch size for each product classes. But the batch size between the components are different. The service times of the product classes differ between the components. In case of the last three model classes the batch sizes of the product classes on a component are also various. The model classes 1 and 4 have the property that the batch sizes increase from component to component and reach their maximum at the exit point of the network. Model classes 2 and 3 respectively 5 and 6 include models with fluctuating batch sizes. A comparison method is used to investigate the additional value of the generalization of the decomposition (multi class case). The comparison method is the decomposition (single class case) describing in [1]. The established method uses average input values and the streams to and inside the components were approximate by Pujolle/Ai. The resulting measures were converted to the product classes afterwards.

The figure shows that the generalization of the established decomposition in the first four model classes is superior by its product class observation and provides good approximations for a pre-evaluation of a model. The fluctuations of batch sizes within the network lead to errors (model classes 5 and 6). The reason is the violation of the assumption that the streams form renewal processes. The comparison method is superior to the generalization in model classes 5 and

6 since a product class observation is made after the method and the error is caused only once. Decomposition with product class view causes the error several times within the method whereby the error can be built up more strongly in such situations.

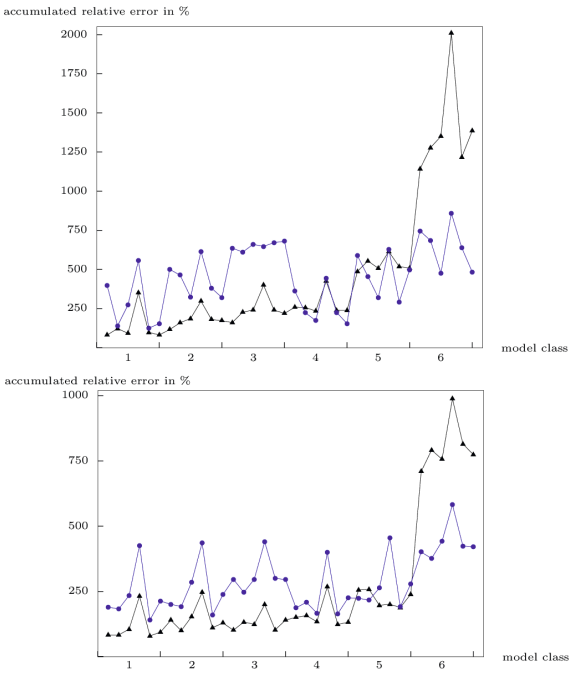

Fig. 1. accumulated relative errors of the generalization (black) and the comparison method (blue), top: series, buttom: network

4 References

[1]Th. Hanschke and H. Zisgen, Queueing networks with batch service, European Journal of Industrial Engineering, 5(3):313-326, 2011
[2]G. Pujolle and W. Ai, A solution for multiserver and multicall open queueing networks, INFOR, 24(3):221-230, 1986
[3]Th. Hanschke, Approximations for the mean queue length of the $GI^X GI^{(b,b)}/c$ queue, Operations Research Letters, 34(2): 205-213, 2006
[4]T. Gröger, Warteschlangensysteme mit Gruppenanknften, Gruppenbedienung und heterogenen Kunden, Diplomarbeit, TU Clausthal, 2007
[5]W. Krämer and M. Langenbach-Belz, Approximate formulae for the delay in the queueing system GI/G/1, 8th International Teletraffic Congress, 1976

48

Confidence Intervals for Coagulation–Advection Simulations

Robert I. A. Patterson

Weierstrass Institute, Berlin

Abstract. An Ornstein-Uhlenbeck model for the rescaled fluctuations of a direct simulation Monte Carlo method around the solution of a coagulation–advection equation is presented and used to derive confidence intervals for time averaged quantities. The approach is numerically validated for simulations of a previously studied test case.

1 Introduction

Direct Simulation Monte Carlo is a well established tool for systems of particles that interact (react) with each other on collision (or close approach). Classical examples are the Bird algorithm for the Boltzmann equation [2, 3] and the Gillespie algorithm for chemical reactions [6]. In this work the focus is on a related method for coagulating particles in a laminar flow field.

The physical problem is expected to exhibit a steady state, although individual particles keep moving with the flow and do not reach any kind of equilibrium. In order to sample the steady state of the system one starts a simulation from an initial condition, runs it until the initial transients dissipate (burn in) and then samples the simulation at multiple times. Successive samples are statistically correlated, but the correlation structures are generally not known and so it is difficult to estimate the variance of the samples and generate confidence intervals.

In some particular situations, such as Markov chains whose generators have a suitable spectral gap, processes on a domain without boundary [7] or with an equilibrium measure [11] it can be shown that the rescaled fluctuations of a simulation converge in distribution to an Ornstein-Uhlenbeck (O-U) process. This implies an exponential in time decay of the correlation between samples and gives a simple formula for confidence intervals.

In this work it is shown numerically that the O-U model provides an excellent description of the rescaled statistical fluctuations arising in the simulation of a coagulation–advection problem motivated by applications in chemical engineering. The O-U fluctuation model can be seen to be plausible on mathematical grounds, beginning with a Martingale Central Limit Theorem, but we do not explore this aspect here. Instead the O-U model for the rescaled fluctuations is formulated and its consequences developed, including explicit confidence intervals. Statistical properties predicted by the O-U model are also successfully compared to simulation data.

2 Coagulation–Advection Problem

In a wide range of physical systems the coagulation of particles plays a significant role. Modelling coagulation leads to an evolution problem with a quadratic non-linearity that is also non-local in particle size (and other properties). If $c(t,x,y)$ is the concentration of particles of size (or more generally type) y at position x and time t moving in a velocity field $u(t,x)$ and if particles are created at rate I_{int} then assuming that the set of possible particle sizes (or types) is countable so that the summations make sense one arrives at the following population balance equation:

$$\begin{aligned}&\frac{\mathrm{d}}{\mathrm{d}t}c(t,x,y)+\nabla\cdot(u(t,x)c(t,x,y))=I_{\text{int}}(t,x,y)\\&+\frac{1}{2}\sum_{y_1+y_2=y}K(y_1,y_2)c(t,x,y_1)c(t,x,y_2)-c(t,x,y)\sum_{y_2}K(y,y_2)c(t,x,y_2).\end{aligned}\tag{1}$$

This equation neglects diffusive transport effects, which is reasonable for non-molecular particles in a flow; mathematical well posedness results are given in [9]. This problem structure is characteristic of soot formation in laminar premixed flames [1] as well as inorganic nano-particle synthesis [12] and some crystallisation problems [4], see also the review article [8].

Direct Simulation Monte Carlo methods define a family of computational particles which behave, apart from some rescaling, in the same way as the real world particles they represent. For each $V>0$ (which can be though of as the volume of a microscopic model system) this random particle system $\left(X_i^V(t),Y_i^V(t)\right)_{i=1}^{N^V(t)}$ undergoes advection according to u, particle creation according to VI_{int} and pairs coagulate at a rate proportional to $K\left(Y_i^V(t),Y_j^V(t)\right)/V$ after adjusting for spatial proximity.

In many situations [5, 7, 10] one can show that for a large class of functions f

$$\lim_{V\to\infty}\frac{1}{V}\sum_{i=1}^{N^V(t)}f\left(X_i^V(t),Y_i^V(t)\right)=\int_x\sum_y f(x,y)c(t,x,y)\mathrm{d}x\tag{2}$$

where c is the solution of (a variant of) (1). Simulations are only possible for finite V so the present work considers the properties of

$$F_t^V:=\sqrt{V}\left(\frac{1}{V}\sum_{i=1}^{N^V(t)}f\left(X_i^V(t),Y_i^V(t)\right)-\int_x\sum_y f(x,y)c(t,x,y)\mathrm{d}x\right).\tag{3}$$

As mentioned in the introduction in some cases it is known that in the limit $V\to\infty$, F_t^V converges in distribution to an Ornstein-Uhlenbeck process F satisfying the SDE

$$\mathrm{d}F_t=\theta\left(m-F_t\right)\mathrm{d}t+\sigma^f(t)\mathrm{d}W_t\tag{4}$$

where W is a standard Brownian motion. Although the present setting is not covered by these rigorous results it will be shown numerically that (4) is a good model for F_t^V even for the values of V accessible by simulation.

The equation (4) has an explicit solution for $t_{i+1} = t_i + \Delta t$:

$$F_{t_{i+1}} = F_{t_i} e^{-\theta \Delta t} + m\left(1 - e^{-\theta \Delta t}\right) + \sigma^f \sqrt{\frac{1 - e^{-2\theta \Delta t}}{2\theta}} Z_i \tag{5}$$

where the Z_i are independent standard normal random variables. For finite V one can therefore perform linear regression of the $F^V_{t_{i+1}}$ on the $F^V_{t_i}$ to recover $e^{-\theta \Delta t}$ as the slope, $m\left(1 - e^{-\theta \Delta t}\right)$ as the intercept and $\sigma^f \sqrt{\frac{1-e^{-2\theta \Delta t}}{2\theta}}$ as the standard deviation of the residuals. The correlation structure can thus be extracted from the data and used to generate confidence intervals. It will also be shown that natural a priori estimates of θ and σ^f are of reasonable accuracy.

Bibliography

[1] M. Balthasar and M. Kraft. A stochastic approach to solve the particle size distribution function of soot particles in laminar premixed flames. *Combust. Flame*, 133:289–298, 2003.

[2] G. A. Bird. Approach to translational equilibrium in a rigid sphere gas. *Phys. Fluids*, 6(10):1518–1519, 1963.

[3] G. A. Bird, M. A. Gallis, J. R. Torczynski, and D. J. Rader. Accuracy and efficiency of the sophisticated direct simulation Monte Carlo algorithm for simulating noncontinuum gas flows. *Phys. Fluids*, 21:017103, 2009.

[4] R. J. P. Eder, S. Radl, E. Schmitt, S. Innerhofer, M. Maier, H. Gruber-Woelfer, and J. G. Khinast. Continuously seeded, continuously operated tubular crystallizer for the production of active pharmaceutical ingredients. *Crystal Growth & Design*, 10:2247–2257, 2010.

[5] A. Eibeck and W. Wagner. Stochastic interacting particle systems and nonlinear kinetic equations. *Ann. Appl. Probab.*, 13:845–889, 2003.

[6] D. T. Gillespie. Approximate accelerated stochastic simulation of chemically reacting systems. *J. Chem. Phys.*, 114(4):1716–1733, 2001.

[7] V. N. Kolokoltsov. *Nonlinear Markov Processes and Kinetic Equations*. Cambridge University Press, Cambridge, UK, 2010. ISBN 9780521111843.

[8] M. Kraft. Modelling of particulate processes. *KONA, Powder and Particle*, (23):18–35, 2005.

[9] R. I. A. Patterson. Properties of the solutions of delocalised coagulation and inception problems with outflow boundaries. *J. Evol. Eqn.*, 16:261–291, 2016.

[10] R. I. A. Patterson and W. Wagner. Cell size error in stochastic particle methods for coagulation equations with advection. *SIAM J. Numer. Anal.*, 52(1):424–442, 2014. ISSN 0036-1429.

[11] M. Ranjbar and F. Rezakhanlou. Equilibrium fluctuations for a model of coagulating-fragmenting planar Brownian particles. *Commun. Math. Phys.*, 296:769–826, 2010.

[12] M. Sander, R. H. West, M. S. Celnik, and M. Kraft. A detailed model for the sintering of polydispersed nanoparticle agglomerates. *Aerosol Sci. Tech.*, 43:978–989, 2009.

Numerical investigation of mass transfer in bulk, random packings of core–shell particles

Dzmitry Hlushkou, Anton Daneyko, Vasili Baranau, Ulrich Tallarek

Department of Chemistry, Philipps-Universität Marburg, Hans-Meerwein-Strasse 4, 35032 Marburg, Germany

E-mail addresses: hlushkou@staff.uni-marburg.de (D.H.), tallarek@staff.uni-marburg.de (U.T.)

A prominent class of porous media, hierarchically structured materials, typically consist of spatial domains with different morphology and physical characteristics of the pore space. This results in specific transport properties for the different domains, e.g., in domination of diffusion in small pores, in contrast to composite advective–diffusive mass transport in large pores. An example of such hierarchically structured porous media are packings of core–shell particles, used as fixed-beds (stationary phase) for highly efficient, fast chromatographic analysis at comparatively low operating pressure. Core-shell particles consist of a nonporous fused-silica core surrounded by a porous layer having essentially the properties of fully porous particles. The hierarchical structure of the void space in core–shell packings is characterized by two scales in pore size. Interconnected macropores form a continuous, highly permeable network of flow-through channels in the interparticle void space. These flow-through pores are responsible for advection-dominated transport through the bed and towards the mesopore networks inside the shells of particles. In contrast to the macropore domain, diffusion-limited transport prevails in the mesopores, where the tailored surface chemistry and the required surface area are critical to specific molecule–surface interactions.

Though in recent years columns packed with core-shell particles have been widely used for efficient and fast chromatographic separations, the influence of the porous shell properties on the mass transfer kinetics in core-shell packings is still not fully understood. A comprehensive approach to the analysis of the chromatographic bed efficiency must account for and distinguish between all the individual contributions to the broadening of analyte bands during their migration along the column, arising from different mass transfer mechanisms. They basically include (i) longitudinal diffusion of analyte molecules, (ii) hydrodynamic (eddy) dispersion due to sample transport and diffusion-controlled exchange between the anastomosed flow paths in a packed bed, (iii) mass transfer resistance across a stagnant fluid film formed at the fluid-solid interface, (iv) adsorption-desorption of analyte molecules at the surface of the stationary phase, (v) mass transfer resistance across the stationary phase including pore and surface diffusion, and (vi) the friction–expansion of the mobile phase (solvent).

The theoretical determination of the individual contributions to the band broadening is generally an outstanding problem as it requires resolvable and accurate mathematical models for all mass transfer phenomena occurring in chromatographic columns. A greatest challenge results from the random and heterogeneous nature of packed particulate beds. In this regards, computer simulations provide the exceptional possibility to evaluate the mass transfer characteristics in packed beds and analyze systematically the dependence of separation efficiency on individual parameters of the chromatographic column.

Here, we report on results of a numerical investigation of advective–diffusive mass transfer in bulk random packings of spherical core-shell particles. We analyze the impact of the effective diffusivity of analyte molecules in the porous shell as well as the shell thickness on the reduced plate height h, one of the basic characteristics of the chromatographic separation efficiency. The computer simulations of mass transport in this study involved three successive steps. First, we computer-generated ten different isotropic and macroscopically homogeneous random packings (to account for statistical variations in different packing realizations) of monosized spherical particles with the interparticle porosity or void volume fraction of 0.4, using a collective-rearrangement algorithm based on the Jodrey-Tory method. Each packing contained about 16000 particles with packing dimensions of $10d_p \times 10d_p \times 140d_p$, where d_p is the particle diameter. The morphology of the particles was characterized by the core-to-particle diameter ratio, ρ. In this study, we analyzed packings composed of core–shell particles with nine values of ρ, covering the range from fully porous particles ($\rho = 0.0$) to nonporous particles ($\rho = 1.0$). Second, the three-dimensional fluid flow velocity fields in the interparticle void space was computed using the lattice-Boltzmann method – a kinetic mesoscopic approach with discrete space and time, based on resolving the microscopic Boltzmann equation instead of the macroscopic Navier-Stokes equation. We assumed that the fluid flow velocity in mesopores of the particles is zero because of the much higher hydraulic resistance compared to that of macropores in the interparticle void space. Third, mass transport in the interparticle void space of the packings and in the porous shells of the particles was modeled with a random-walking particle-tracking (RWPT) method. The idea of the RWPT approach is to distribute a large number of tracers (associated with analyte molecules) in the volume of interest and let them move at small time-iteration steps according to the local flow velocity and local diffusion properties. Pure diffusive transport of tracers in the porous shells of the particles was simulated for two values of $\Omega = 0.2$ and 0.9, the ratio between the effective diffusion coefficient of tracers in the shells, D_{shell}, and their molecular diffusion coefficient in bulk solution, D_m. Advective–diffusive transport in the interparticle void space of the packings was modeled for the values of the reduced flow velocity $\nu = u_{av}d_p/D_m$ (where u_{av} is the average fluid flow velocity in the interparticle void space) varied from 0.5 up to 1000. All the three above numerical approaches were realized as parallel codes in C language using the Message Passing Interface library and implemented on a supercomputer (IBM BlueGene/Q, Rechenzentrum Garching, Germany).

The developed simulation framework was employed to determine the reduced plate height as a function of the reduced flow velocity ν in the random bulk packings of

core-shell particles for different values of ρ and Ω and analyze the contributions associated with individual mass transfer mechanisms to the total reduced plate height depending on porous shell characteristics [1]. Simulated h–ν curves were fitted by the reduced plate height equation, involving three independent terms due to longitudinal diffusion (h_{long}), eddy dispersion (h_{eddy}), and trans-particle mass transfer resistance (h_{shell}). To perform the fitting procedure, the h_{long} term was obtained by independent simulations of purely diffusive transport in the interparticle void space and porous shells. The h_{shell} term was assumed to depend linearly on the reduced velocity, in line with the model of Kaczmarski and Guiochon [2], which accounts for analyte retention in the porous shell of a single particle. We showed that the reduced plate height equation involving the h_{eddy} term from the original Giddings theory of coupled eddy dispersion [3] does not describe adequately the h–ν curves for core–shell particles. By contrast, the reduced plate height equation involving the proposed extension of the original Giddings theory to core–shell particles fits the simulated h–ν curved very well. In addition, our analysis indicates that the model of trans-particle mass transfer resistance for a single core–shell particle is applicable as well to particle-packings but requires the introduction of a scaling factor, the value of which depends on Ω. The carried out numerical simulations confirmed that the enhanced chromatographic efficiency of columns packed with core–shell particles compared to fully porous particles comes from a reduced contribution of h_{eddy} in the plate height equation.

The proposed simulation approach can be extended to investigate individual contributions to the total plate height in real chromatographic columns (particulate packings, silica and polymer monoliths), using information on the actual bed morphology or even on particle and monolith mesopore space characteristics, obtained from three-dimensional physical reconstruction.

1. A. Daneyko, D. Hlushkou, V. Baranau, S. Khirevich, A. Seidel-Morgenstern, U. Tallarek. J. Chromatogr. A 1407 (2015) 139–156.
2. K. Kaczmarski, G. Guiochon. Anal. Chem. 79 (2007) 4648–4656.
3. J.C. Giddings. Dynamics of Chromatography. Part 1: Principles and Theory, Marcel Dekker, New York, NY, 1965.

Multiscale simulation of anisotropic surface stress and bulk stresses in transition metal oxide nanoparticles

Peter Stein[1], Ashkan Moradabadi[2], Manuel Diehm[2], Bai-Xiang Xu[1], and Karsten Albe[2]

[1] Mechanics of Functional Materials Division, Technische Universität Darmstadt, Jovanka-Bontschits-Str. 2, 64287 Darmstadt, Germany
[2] Materials Modeling Division, Technische Universität Darmstadt, Jovanka-Bontschits-Str. 2, 64287 Darmstadt, Germany

Keywords: Surface stress, Nanoparticle, Stress analysis

Nanostructured materials exhibit properties different from their bulk macroscopic counterparts. In particular the thermodynamic properties show a great deviation due to the violation of the thermodynamic limit assumption. As a consequence, intensive quantities start to show a size-dependent behavior, which is typically described by excess energies. According to the Shuttleworth equation, surface or interface stresses also have to be taken into account in solid materials.

In this study we analyze the impact of surface stress on the stress and strain distributions within a nanoparticle. As model system we consider nanoparticulate $LiCoO_2$, a material that is widely applied in cathodes of Li-ion secondary batteries. Based on the work described in Ref. [1], we incorporate anisotropic surface stress into linear-elastic continuum models. Parameters for bulk elasticity and and facet-dependent surface stress are determined through ab-initio simulations of $LiCoO_2$ single crystals. The model is implemented via the Finite Element Method and provides a basis for the computation of energy barriers for intercalation and the transport kinetics within the particle.

References

1. Gross, D., Müller, R., Müller, M., Xu, B.X., Albe, K.: On the origin of inhomogeneous stress and strain distributions in single-crystalline metallic nanoparticles. Int. J. Mater. Res. 102(6), 743–747 (2011)

Validation of a synthetic 3D mesoscale model of hot mix asphalt

Johannes Neumann, Jaan-Willem Simon, and Stefanie Reese

Institute of Applied Mechanics, RWTH Aachen University, Mies-van-der-Rohe-Str. 1, 52074 Aachen, Germany
jneumann@ifam.rwth-aachen.de,
homepage: www.ifam.rwth-aachen.de

Abstract. Hot mix asphalt is studied as a composite material consisting of a linear elastic mineral aggregate phase and a linear viscoelastic bituminous mortar phase using finite elements. A first order homogenisation scheme is used to derive effective properties of the heterogeneous microstructure. In the present contribution, the significance of the model is critically assessed in an twofold manner. First, the synthetic aggregate morphology is compared to CT-scanned real aggregates. Second, the effective response is compared to experimental mix data in a frequency regime of approximately 8 decades.

Keywords: hot mix asphalt, computational homogenisation, micromechanics

1 Introduction

Hot mix asphalt is a composite material consisting of bituminous binders, mineral aggregates, and voids. A detailed analysis of its intricate mechanical behaviour makes it worthwhile to have a mechanical toolbox at hand which resolves the involved phases seperately. Several 2D approaches exist, but it has been shown that the reduction to two dimensions is not valid [3, 5].

A method to obtain 3D synthetic models of asphalt concrete recently proposed by [10] has been extended to capture the particle size distributions within typical hot mix asphalts. The geometric modelling is based on Voronoi tesselations. Hence, the mineral aggregates are idealised to be strictly convex irregular polyhedra.

It is hypothesised, that aggregate shape and roughness play an important role in the intricate reinforcement of (hot mix) asphalt. Here we try to explore the governing effects through a parameter study.

2 Methodology

Real and synthetic aggregates are compared by the degree of true sphericity [8]

$$\Psi = \frac{\pi}{A_p} \left(\frac{6V_p}{\pi} \right)^{\frac{2}{3}} , \tag{1}$$

where A_p and V_p are the surface area and the volume of a given particle p. However, a fundamental problem arises from the fractal nature of rough bodies, such as broken rock. Our "real" aggregates stem from a triangulated surface representation of CT-scanned aggregates. Therefore, the micro-roughness is already lost and the surface area is underestimated. Please see Figure 1(a) for a depiction of such a representation for six aggregates.

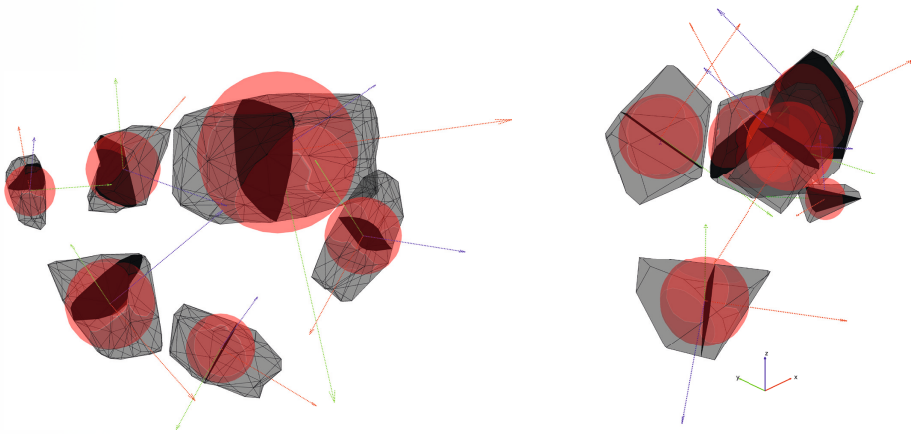

(a) Six CT-scanned aggregates of SMA 13 S (b) Six synthetic aggregates

Fig. 1. Surface representations of six CT-scanned (a), and synthetic (b), aggregates. The arrows represent the principal axes (linear dimension) and the red spheres represent the volumes (cubic dimension).

By nesting the Voronoi tesselation, the particle size distribution prescribed by typical standards is met. Geometry and mesh are constructed in a periodic fashion in order to apply displacement based periodic boundary conditions. By using a strain driven first-order computational homogenisation scheme, effective properties are derived from representative volume elements.

3 Results & Discussion

The mean value of true sphericity, $\bar{\Psi}$, for the CT-scanned aggregates shown in Figure 1(a) is 0.7982, and $\bar{\Psi} = 0.7669$ for the aggregates shown in Figure 1(b). Both values are higher than the values reported in [9]. There, $\bar{\Psi} \approx 0.56$, indicating that the surface has been measured with higher resolution. The surface area of the reinforcing phase is of particular importance for the bulk behaviour of composites. It is commonly believed, that — given a fixed volume fraction — smaller particles raise the stiffness, see e.g. [1]. The problem seems to be twofold, neither can the surface area be measured accurately, nor can it be represented in a discrete fashion with surmountable complexity. The assessment of methods to

estimate the surface area from easily determinable linear and cubic dimensions of the aggregate [2] are currently under investigation.

We find that our approach currently underestimates typical mix response. The mortar design neglects that the aggregates adsorb a fraction of the bitumen which results in an interphase between aggregates and mortar that is believed to be a few µm thick [6, 7]. Thus, bitumen is overdosed in the mortar tested so far. [4] have tested mortar specimens in a similar setup to the one described here and determined a stiffer response. We calibrate the generalised Maxwell-model using their data and match the PSD. Investigation of the effective response using the reported data is currently under investigation.

References

[1] Ahmed, S., Jones, F.R.: A review of particulate reinforcement theories for polymer composites. Journal of Materials Science 25(12), 4933–4942 (1990)

[2] Erdogan, S.T.: Simple estimation of the surface area of irregular 3d particles. Journal of Materials in Civil Engineering 28 (2016)

[3] Fakhari Tehrani, F., Absi, J., Allou, F., Petit, C.: Investigation into the impact of the use of 2d/3d digital models on the numerical calculation of the bituminous composites' complex modulus. Computational Materials Science 79, 377–389 (2013)

[4] Karki, P., Kim, Y.R., Little, D.N.: Dynamic modulus prediction of asphalt concrete mixtures through computational micromechanics. Transportation Research Record: Journal of the Transportation Research Board 2507, 1–9 (2015)

[5] Ozer, H., Ghauch, Z.G., Dhasmana, H., Al-Qadi, I.L.: Computational micromechanical analysis of the representative volume element of bituminous composite materials. Mechanics of Time-Dependent Materials (2016)

[6] Radovskiy, B.: Analytical formulas for film thickness in compacted asphalt mixture. Transportation Research Record: Journal of the Transportation Research Board 1829, 26–32 (2003)

[7] Underwood, B.S., Kim, Y.R.: A four phase micro-mechanical model for asphalt mastic modulus. Mechanics of Materials 75, 13–33 (2014)

[8] Wadell, H.: Volume, shape, and roundness of quartz particles. The Journal of Geology 43(3), 250–280 (1935)

[9] Wang, H., Bu, Y., Wang, D., Oeser, M.: Dreidimensionale charakterisierung der kornform und scharfkantigkeit von gesteinskörnungen mittels röntgencomputertomographie. Bauingenieur 90, 1–8 (2015)

[10] Wimmer, J., Stier, B., Simon, J.W., Reese, S.: Computational homogenisation from a 3d finite element model of asphalt concrete — linear elastic computations. Finite Elements in Analysis and Design 110, 43–57 (2016)

Mechanical Simulation of 3D-Microstructures in Dual-Phase Steel

Frederik Scherff[1], Sebastian Scholl[2], and Stefan Diebels[1]

[1] Universität des Saarlandes, Lehrstuhl für Technische Mechanik, Campus A4 2, D-66123 Saarbrücken, Germany
[2] AG der Dillinger Hüttenwerke, Werkstraße 1, D-66763 Dillingen, Germany

Abstract. Modern dual-phase (DP) steels show favorable material properties due to their complex microstructure, which results in a wide use in industry. Hence, in the presented work a microstructure-based FEM model is developed for DP steel to achieve a deeper understanding of the underlying structure-property relation.

1 Introduction

The microstructure of DP steel consists of a relatively soft ferritic matrix and very hard martensite particles. As a result of the production process, this structure leads to favorable material properties, especially a high level of ductility combined with significant work hardening and strength [1]. These properties open a wide field of applications for DP steel in different industrial areas, e.g. energy absorbing, strength-relevant structures in automotive industry. Therefore, a transfer to heavy plate steel is desirable.

Even macroscopically simple loads lead to complex stress-strain states on the microscale due to a long-range interdependency in the deformation of the material. Simple two-dimensional FEM models are unable to correctly describe the material behavior and have to be extended to three dimensions [2, 3]. In combination with microscale experiments and data reduction methods, these three-dimensional FEM models can be used to simulate the material behavior in a reasonable amount of time even without using high-performance computing.

2 Experiments

The experimental basis of this work consists mainly of two parts, namely 3D serial section tomography and nanoindentation, which are used to characterize the microstructure in detail.

The 3D serial section tomography is used to obtain the microstructure of the investigated DP steel [4]. In a cycle of polishing and etching for microstructure contrasting an image of each layer of the material is made. After a binarization process, these images can be used to three-dimensionally reconstruct the microstructure, see Figure 1.

An important part of a realistic mechanical description is the determination of the material parameters of the ferrite and martensite phase. Hence, multiple nanoindentations of single grains of ferrite and martensite are carried out with a cube corner indenter as basis for a parameter identification with inverse methods.

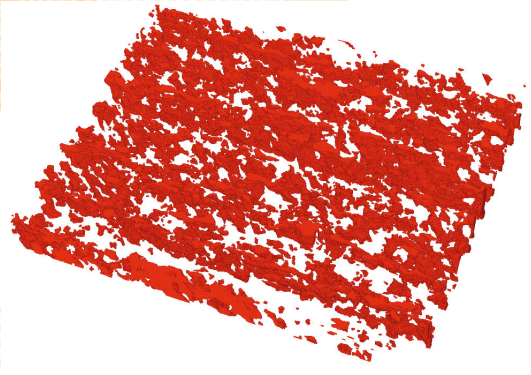

Fig. 1. DP steel microstructure (martensite in red, ferrite transparent).

3 Mechanical Model and Numerical Realization

Based on the nanoindentations, a FEM model in *Abaqus*® is set up. A homogeneous material of infinite extendis assumed in this case, since the single grains are big compared to the indent. The model is reduced to two dimensions and the tetrahedral indenter is represented by a conic section with the same penetration depth to contact surface relation as the original indenter to minimize computational effort. A Nelder-Mead-Simplex optimization process is performed to obtain the material parameters of ferrite and martensite by inverse computations using this model [5].

The voxelized microstructure tomography is then transferred into a two phase hexahedral mesh. Because of the size of the tomography, data reduction is implemented. Several voxels are summarized in one mesh element and the original phase distribution is represented by a material definition at the integration points to preserve the microstructure resolution [6]. Hanging-node-meshing is applied as a further method of data reduction. The ferritic and martensitic parts of the structure are both modeled as elasto-plastic materials with isotropic hardening using the material parameters obtained by the nanoindentation. Additionally, the hardening effects caused by the austenite martensite transformation during DP steel production are considered. Numerical tensile tests are performed to calculate the resulting flow curves. The deformation is evaluated in an iterative process using a Newton-Raphson method in combination with a numerical tangent [7]. The described model is implemented in the C++ finite element library *deal.II* [8].

4 Results and Conclusion

A material model is set up to calculate stress - strain - curves for DP steel microstructures, taking into account material parameters determined by nanoindentation simulation and a data reduction method with material definition at the integration point and hanging-node-meshing. Figure 2 shows a numerical flow curve and a curve obtained by uniaxial tensile tests performed on a sample of the same material. It can clearly be

observed that the simulation shows good accordance to the experiment, although a reduction of computation time by a factor of about 10 compared to standard FEM models is accomplished.

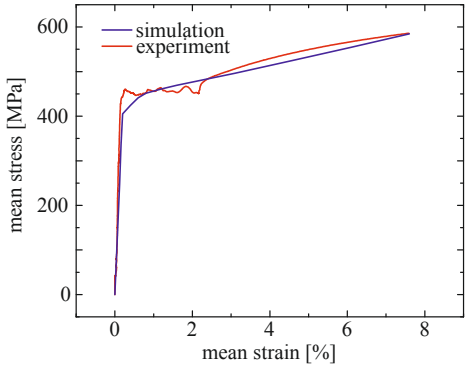

Fig. 2. Mean stress - mean strain - curves for a DP steel.

Acknowledgment: The support of AG der Dillinger Hüttenwerke is gratefully acknowledged. Many thanks to Lehrstuhl für Funktionswerkstoffe at Universität des Saarlandes for providing the 3D-tomographies and nanoindentations and to Lehrstuhl für Experimentelle Methodik der Werkstoffwissenschaften at Universität des Saarlandes for the nanoindentations.

References

1. M. Marvi-Mashhadi, A. Rezaee-Bazzaz, and M. Mazinani, Materials Science Forum **706**(1), 1503–1508 (2012).
2. M. Diehl, P. Shanthraj, P. Eisenlohr, and F. Roters, Meccanica **51**(2), 429–441 (2016).
3. A. Zeghadi, S. Forest, A. F. Gourgues, and O. Bouaziz, Philosophical Magazine **87**(8–9), 1425–1446 (2007).
4. F. Mücklich, M. Engstler, D. Britz, J. Barrirero, and P. Rossi, Practical Metallography **52**(9), 507–524 (2015).
5. Z. Chen, and S. Diebels, Archive of Applied Mechanics **82**(8), 1041–1056 (2012).
6. F. Scherff, F. Goldschmidt, S. Scholl, and S. Diebels, Proc. Appl. Math. Mech. **16**(1), 391–392 (2016).
7. F. Goldschmidt, Modellierung und Simulation von Klebeverbindungen mit gradierten mechanischen Eigenschaften, PhD thesis, Universität des Saarlandes, Saarbrücken, 2015.
8. W. Bangerth, R. Hartmann, and G. Kanschat, ACM Trans. Math. Softw. **33**(4), 24/1–24/27 (2007).

Sensitivity Analysis of VOF Simulations regarding Free Falling Metal Melt Jets

Sebastian Neumann*, Rüdiger Schwarze*

*Institut für Mechanik und Fluiddynamik, Technische Universität Bergakademie Freiberg, Lampadiusstraße 4, 09599 Freiberg, Germany, Phone: +49-(0)3731-39-3053, Email: Sebastian.Neumann@imfd.tu-freiberg.de

Extended abstract:

In the field of the metallurgy casting processes are very common. Therefore, free falling metal melt jets are present in different production steps, e.g. the tapping of the electric arc furnace or in the production process of steel powder. The main concerns in the research of free falling melt jets are the shape and behavior of the free surface of the jet. At the TU Bergakademie Freiberg different investigations focusing on this issue with explicit differing dimensions are part of the research.

In case of the tapping of the electric arc furnace, the metal melt jet falls into a ladle. During this process the metal melt can reoxidise with the oxygen of the surrounding air, which has to be avoided due to the demand of defined material properties and high qualities of the resulting product. The shape of the free falling metal melt jet is identified as an important parameter, because the dimension of the free surface correlates with the absorption of oxygen in the metal melt. Furthermore, research shows that the input of alloying agents, which are added to the liquid metal to avoid reoxidation, needs the knowledge about the melt jet surface for an effective wettability of the desoxidiser.

Another research topic is part of the Collaborative Research Center specific CRC 799 (TRIP- Matrix-Composite), which investigates metal matrix composites (MMCs), based on a TRIP-steel

and a matrix-embedded partially stabilized zirconia (PSZ) ceramic phase. To achieve a high green strength similar particle sizes (ceramic $d \approx 3\mu m$) are required. The production process for the steel powder is predominantly an atomization of a compact melt jet. However, in contrast to the tapping jet, the investigations of the atomization of metal melt jets show better results in case of highly disturbed and corrugated jet surfaces and the dominance of a well developed primary breakup of ligaments and droplets.

The main differences between the considered processes are the dimensions and the jet properties, like previously discussed. The geometry for the tapping of the electric arc furnace has a diameter of the nozzle exit D with $D_{tapping} \sim 40 \cdot D_{atomization}$ and a length of the free falling metal melt jet L with $L_{tapping} \sim 300 \cdot L_{atomization}$. The fluid flow velocity at the nozzle exit U is $U_{tapping} \sim 2.6 \cdot U_{atomization}$. However, there are similarities between the cases. Both processes have a predomination by gravitation and the fluid column above the nozzle exit, which are influencing the free falling metal melt jet. Furthermore, the temperature of the hot metal melt is very high (~ 1800 K), which do not allow precise experiments. Therefore, a numerical investigation of the free falling liquid steel jets using implicit large eddy simulations (ILES) combined with the Volume Of Fluid (VOF) approach is done to consider the jet properties, e.g. the jet shape and surface, as well as the primary breakup with ligaments and droplets. The standard interFoam solver of the open-source computational fluid dynamics library OpenFOAM is employed.

A sensitivity analysis of VOF simulations regarding free falling metal melt jets was investigated observing different influencing parameter. Therefore, the free falling melt jet of the atomization process is researched for different operation conditions with different mesh resolutions in the area of the melt jet and the near gas flow. In figure 1 (left), a free falling melt jet is shown for the

operation point including the circumferential velocity of the melt at the nozzle exit $U_{rot,exit} = 1.26\,ms^{-1}$ and an axial flow velocity of $U_{ax} = 1.55\,ms^{-1}$ after 0.20s inflow. The results of the simulations depend strongly on the mesh resolution. It can be observed, that the behavior and the shape of the metal melt jet strongly changes with rising quality of the mesh. The influence of the rotation and the surface disturbances can only be observed in the finest mesh, there a helix shaped jet develops, which has the largest jet surface.

Further, the time step underlies restrictions based on the stability of the numerical model. For resolving the propagation of capillary waves, the explicit discretization of the surface tension term is highly influencing. Therefore, a constraint on the time step is used to contain the amplification of interface capillary waves. This criterion is significantly solver dependent. In figure 1 (right) the results for the simulations with different time steps are shown. The free falling melt jet is defined for the operation point like discussed before. The results show explicit differences for the jet surface, where the stimulation of the surface waves increase with reducing time step. The overall jet behavior is comparable, but marginal differences for the helix structure can be observed reducing the time step.

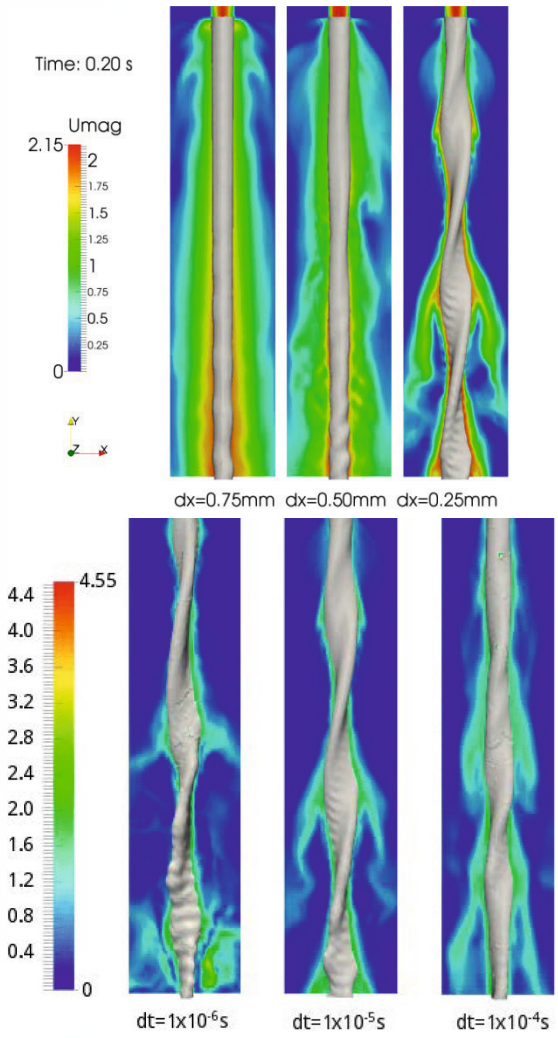

Figure1: Free falling melt jet of the atomization process for different meshes (left) and different time steps (right)

Quantification of relationships between structural characteristics and mechanical properties of agglomerates

M. Weber, A. Spettl, M. Dosta, S. Heinrich and V. Schmidt

Keywords: structure-property relationship, agglomerate breakage, DEM simulation, stochastic microstructure model, breakage probability, breakage function, copula

The internal microstructure of agglomerates has a great influence on their stability and breakage behavior. Therefore, to optimize production processes and to improve characteristics of the final product, it is very important to understand the relationship between structural and mechanical properties of agglomerates. We discuss usage of the discrete element method (DEM), implemented in the software system MUSEN [1], for understanding the breakage behavior of spherical agglomerates under uniaxial compression depending on their microstructure. This knowledge is important because it can be used as part of the modeling of particle breakage on the macro-scale, which has practical applications in industrial processes [2].

A flexible stochastic model has been developed to generate agglomerates with various types of microstructures [3]. This model is based on random placing of particles inside a given sampling window. At the beginning they are allowed to overlap. These overlaps are removed by applying a modified version of the so-called force-biased algorithm [4] to the system of particles. Then, a network of bonds is generated by an optimization algorithm using the relative neighborhood graph, the minimum-spanning tree thereof and a particle-particle distance criterion in order to fit a predefined relative bond volume (compared to the volume of the particles).

As an example, we investigate the effect of the primary particle size distribution on agglomerate strength and breakage behavior. In particular, the size distribution of primary particles is specified by a mixing of two fixed particle sizes. The model construction ensures that the size and mass of agglomerates as well as primary particles and binder content remain constant in all experiments. From the obtained results it can be seen that the breakage behavior of agglomerates is influenced in different ways by their internal microstructure. Breakage energy and the maximum force applied before the primary break depend on the mixing ratio and the variability inside the microstructure. On the other hand, the size of fragments is very similar for all mixing ratios.

The stability and breakage behavior of agglomerates is of interest in many applications. Since the internal microstructure is of great influence, it is very important to understand and quantify the relationship of structural properties and mechanical behavior further. Therefore, our stochastic microstructure model has been extended to generate spherical agglomerates consisting of spherical primary particles, arranged as core and shell [5]. Structural properties can be varied in core and shell independently. Applying DEM simulations, we again investigate the influence of the primary particle size distributions in core and shell on the breakage behavior under uniaxial compressive load. Moreover we perform compression experiments of the same agglomerate with different direc-

tions of force and investigate the variation in breakage behavior.
DEM simulations are an effective computational technique that is used to investigate the mechanical behavior of various particle systems like, for example, agglomerates. However, for systems of perfectly spherical and non-overlapping particles, the structural input is almost always based only qualitatively on experimentally observed structures. In order to get quantitative information about the internal structure of agglomerates, we consider highly resolved image data of agglomerates, obtained from micro tomographic measurements, where particles are nearly spherical and connected by bonds. A novel bonded-particle extraction (BPE) method is proposed for the automated generation of such agglomerate structures from tomographic data sets [6]. By BPE, sphere-like primary particles are represented each by exactly one (perfect) sphere, and the final set of spheres is non-overlapping. Furthermore, the solid bridge bonds between primary particles are retained. Having derived such a simple description of complex tomographic data sets, one can perform DEM simulations with well-established models like our bonded-particle model. Moreover, it is shown that a larger data base of statistically equivalent microstructures can be generated by our stochastic modeling approach. This approach reduces the need for (time-consuming) experimental agglomerate production and characterization.
In process engineering, the breakage behavior of particles is needed for the modeling and optimization of comminution processes. A popular tool to describe (dynamic) processes is population balance modeling, which captures the statistical distribution of particle properties and their evolution over time [7]. It has been suggested previously to split up the description of breakage into a machine function (modeling of loading conditions) and a material function (modeling of particle response to mechanical stress). Based on this idea, we present a mathematical formulation of machine and material functions and a general approach to compute them. Both functions are modeled using multivariate probability distributions, where in particular so-called copulas [8] are helpful. These can be fitted to data obtained from our stochastic microstructure model and from DEM simulations. We describe the proposed copula-based breakage model, and we construct such a model for a sample dataset that allows to evaluate the prediction quality [9].
Caking or sintering of various materials from food products up to ceramics plays an important role in different industries. During a heat treatment, the diffusion of material leads to a growth of solid bonds and a formation of an aggregate. Despite large amount of research work in this area, it has not yet been quantified and there has not been a microstructure model describing this effect. It is important that this phenomenon gets quantified because growing bonds have a major influence on the mechanical stability of the agglomerate. Therefore, we propose a new dynamic model describing this effect [10] based on a slightly modified version of the previously developed stochastic microstructure model for agglomerates and additionally involving Markov chains [11] in order to describe the dynamics of the agglomerate microstructure. The modifications relate to the so far not yet considered gravity which has an impact on the surface roughness and the solid bonds network which are important characteristics regarding the mechanical properties of agglomerates. For the development of the model we took three Maltodextrin agglomerate datasets regarding three timesteps (with respect to the time they spend in a climate chamber) into account. The model is able to generate agglomerate microstructures at different stages of the cak-

ing process. Therefore, it also allows to forecast material structures for time points at which no measurements took place yet. With the help of this model and using DEM simulations, we are also able to analyze the strength of an agglomerate at different time points for many different initial particle packings, which is obviously not possible in real experiments. The developed model will be validated structurally but also mechanically regarding simulated and real compression experiments.

References

[1] M. Dosta, S. Antonyuk, S. Heinrich *Multiscale simulation of agglomerate breakage in fluidized beds*, Industrial & Engineering Chemistry Research 52 (33) (2013) 11275 – 11281.

[2] V. Skorych, M. Dosta, E.-U. Hartge, S. Heinrich *Novel system for dynamic flowsheet simulation of solids processes*, Powder Technology (2017).

[3] A. Spettl, M. Dosta, S. Antonyuk, S. Heinrich, V. Schmidt *Statistical investigation of agglomerate breakage based on combined stochastic microstructure modeling and DEM simulations*, Advanced Powder Technology 26 (2015), 1021 – 1030.

[4] J. Mościński, M. Bargie l, Z. A. Rycerz, P.W. M. Jacobs *The force-biased algorithm for the irregular close packing of equal hard spheres*, Molecular Simulation 3 (4) (1989) 201 – 212.

[5] M. Weber, A. Spettl, M. Dosta, S. Heinrich, V. Schmidt *Simulation-based investigation of core-shell agglomerates: influence of spatial heterogeneity in particle sizes on breakage characteristics*, Computational Materials Science (submitted).

[6] A. Spettl, M. Dosta, S. Bachstein, S. Heinrich, V. Schmidt *Bonded-particle extraction and stochastic modeling of internal agglomerate structures*, Advanced Powder Technology 27 (2016), 1761 – 1774.

[7] D. Ramkrishna *Population Balances: Theory and Applications to Particulate Systems in Engineering*, Academic Press, San Diego, 2000.

[8] J.-F. Mai, M. Scherer *Simulating Copulas: Stochastic Models, Sampling Algorithms, and Applications*, Imperial College Press, Singapur, 2012.

[9] A. Spettl, M. Dosta, F. Klingner, S. Heinrich and V. Schmidt *Copula-based approximation of particle breakage as link between DEM and PBM*, Computers & Chemical Engineering 99 (2017), 158 – 170.

[10] F. Klingner, M. Dosta, M. Goslinska, A. Spettl, S. Heinrich and V. Schmidt *Solid bridge evolution during heat treatments of agglomerates and its effect on mechanical behavior: experiment, modeling and simulation*, Working paper (under preparation).

[11] S. Meyn, R. L. Tweedie *Markov Chains and Stochastic Stability, 2nd Edition*, Cambridge University Press, Cambridge, 2009.

Modelling and simulation of polycrystalline microstructures by tessellations

Ondřej Šedivý[1], Daniel Westhoff[1], Carl E. Krill III[2], and Volker Schmidt[1]

[1] Institute of Stochastics, Ulm University, Ulm, Germany
[2] Institute of Micro and Nanomaterials, Ulm University, Ulm, Germany

For the description of the highly complex geometries of grain boundaries observed in polycrystalline microstructures, there is a need for developing appropriate mathematical models and their implementation for practical use. Parametric tessellation models, investigated in the field of stochastic geometry, have proven to be a suitable concept. Here, each grain is represented by a small number of parameters that — through their interaction with parameters of other grains — determine its size and shape. An immediate advantage of this representation is significant data reduction, as a large voxel-based dataset can be reduced to a much smaller set of parameters, the size of which grows linearly with the number of grains.

Tessellation models and related simulation tools are being developed hand in hand with the continuous enhancement of experimental methods for 3D image data acquisition at various length scales. Tomographic images result in a realistic impression of the spatial arrangement of grain boundary networks. Among various tessellation models used for the description of such networks, great interest has been devoted to Laguerre tessellations, being comprehensive descriptors of structures with convex grains. In [3], planes are fitted to the boundaries between neighbouring grains using orthogonal regression. This method allows for the fast and accurate extraction of parametric cells from 3D image data. Note that, as output information, we obtain not the tessellation parameters themselves but rather the positions of the planar faces between cells. An approximate method for solving the inverse problem, i.e. estimating the tessellation parameters from the knowledge of its faces, was proposed in [1].

The Laguerre model is often preferred due to its simplicity. However, it is not able to capture finer microstructural features and curvatures of the grain boundaries. Thus, we have focused on tessellation models based on an initial approximation of the grains by ellipsoids. These represent the most accurate tessellation models used so far for the approximation of grain boundaries in polycrystalline materials. In [7] we show that the ellipsoid-based tessellations are able to fit the curvatures of individual grain boundaries with high accuracy; datasets subjected to our analysis are depicted in Figure 1. However, the number of parameters in this model is much higher than, e.g., for Laguerre tessellation. Thus, a natural question arises in regard to the determination of models offering sufficient accuracy while relying on a reasonably small number of parameters. Certain model selection criteria are the subject of a forthcoming paper [8] that is currently under preparation.

Methods for fitting tessellation models to empirical data can be divided roughly into two groups: heuristic methods and iterative procedures. Heuristic approaches allow to estimate the model parameters instantaneously, using certain characteristics extracted from empirical data. However, these methods often are not sufficiently accurate; rather, they serve as a starting point for further iterative improvement. Using iterative procedures, the model parameters are changed in each step either in a deterministic or in a random fashion, such that the quality of fit is improved iteratively. Recently, we developed two advanced iterative methods based on stochastic optimization. The first method deals with approximating the microstructure by Laguerre tessellations [2]. For minimization of a certain discrepancy measure, a cross-entropy approach is used. The second method has been applied in the fitting of a so-called generalized balanced power diagram, which is an ellipsoid-based tessellation with additive weights. For this more complex model, an algorithm based on simulated annealing was developed [6]. Both methods are able to fit the model to empirical data with very good accuracy, and they can deal with large sample sizes while maintaining a reasonable computation time.

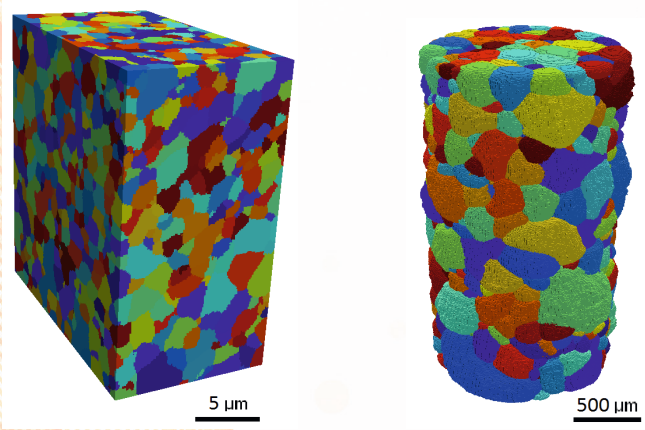

a) b)

Fig. 1. Grain microstructure of the samples analyzed in [7]. a) Sample of Al-3 wt% Mg-0.2 wt% Sc acquired by 3D electron backscatter diffraction; b) sample of Al-1 wt% Mg acquired by 3D X-ray diffraction microscopy.

For the explanation of many physical phenomena, it is of great help to have a tool for generating virtual materials. These virtual data possess, from the statistical point of view, the same microstuctural characteristics as observed in the experimental data. Such a simulation tool is provided by stochastic models based on random tessellations. Recently, we have focused on the phenomenon of Ostwald ripening at ultra-high volume fractions of the coarsening phase. This effort

resulted in a stochastic model that utilizes Laguerre tessellations for the approximation of grains in the solid phase [5]. Dynamics are added to the model through a continuous change in its parameter values over time. Parameters are modified in such a way that the structure possesses self-similarity and the development of grain sizes satisfies the power law predicted by the classical Lifshitz-Slyozov-Wagner (LSW) theory. In [4], this stochastic model served as a basis for tracking the behaviour of individual grains during Ostwald ripening; see Figure 2. In the individual grain tracking model, an advanced statistical method was employed in which multivariate probability distributions are represented by copulas.

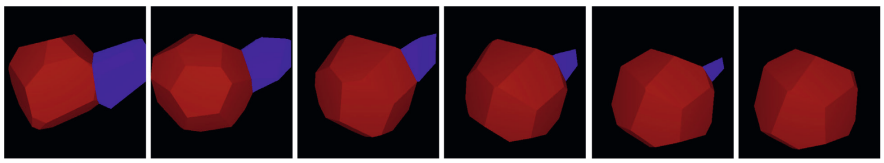

Fig. 2. Evolution of the morphology of two adjacent grains from a realization of the stochastic microstructure model proposed in [4].

References

1. Duan, Q., Kroese, D., Brereton, T., Spettl, A., Schmidt, V.: Inverting Laguerre tessellations. The Computer Journal 57(9), 1431 (2014)
2. Spettl, A., Brereton, T., Duan, Q., Werz, T., Krill III, C.E., Kroese, D.P., Schmidt, V.: Fitting Laguerre tessellation approximations to tomographic image data. Philosophical Magazine 96(2), 166–189 (2016)
3. Spettl, A., Werz, T., Krill III, C.E., Schmidt, V.: Parametric representation of 3D grain ensembles in polycrystalline microstructures. Journal of Statistical Physics 154(4), 913–928 (2014)
4. Spettl, A., Werz, T., Krill III, C.E., Schmidt, V.: Stochastic modeling of individual grain behavior during Ostwald ripening at ultra-high volume fractions of the coarsening phase. Computational Materials Science 124, 290–303 (2016)
5. Spettl, A., Wimmer, R., Werz, T., Heinze, M., Odenbach, S., Krill III, C.E., Schmidt, V.: Stochastic 3D modeling of Ostwald ripening at ultra-high volume fractions of the coarsening phase. Modelling and Simulation in Materials Science and Engineering 23(6), 065001 (2015)
6. Šedivý, O., Brereton, T., Westhoff, D., Polívka, L., Beneš, V. Schmidt, V., Jäger, A.: 3D reconstruction of grains in polycrystalline materials using a tessellation model with curved grain boundaries. Philosophical Magazine 96(18), 1926–1949 (2016)
7. Šedivý, O., Dake, J., Krill III, C.E., Schmidt, V., Jäger, A.: Description of the 3D morphology of grain boundaries in aluminum alloys using tessellation models generated by ellipsoids. Image Analysis and Stereology (2017), under revision
8. Šedivý, O., Westhoff, D., Polívka, L., Krill III, C.E., Schmidt, V.: Data-driven selection of tessellation models describing polycrystalline microstructures (2017), in preparation

Time-adaptive finite element computations in Solid Mechanics of inelastic materials

Stefan Hartmann[1] and Matthias Grafenhorst

Institute of Applied Mechanics, Clausthal University of Technology,
38678 Clausthal-Zellerfeld, Germany,
{stefan.hartmann,matthias.grafenhorst}@tu-clausthal.de,
WWW home page: http://www.itm.tu-clausthal.de/en/

Abstract. Transient boundary-value problems in solid mechanics are commonly solved by a space-time discretization using the method of vertical lines, where, for the spatial discretization, finite elements and, for the time discretization, low order methods are chosen. In this presentation, an overview of the application of higher-order diagonally-implicit Runge-Kutta methods with step-size control is given, which are applied to material non-linearities, thermo-mechanically coupled simulations and dynamics. A comparison to further methods (Rosenbrock-type methods, half-explicit Runge-Kutta methods) and some drawbacks are presented as well. Finally, the challenging problem of 3D-contact problems is addressed in view of time-integration.

Keywords: finite element method, diagonally-implicit Runge-Kutta methods, thermo-mechanically coupling

1 Basic Problem

In quasi-static problems of solid mechanics the balance of linear momentum in combination with material non-linearities on the basis of evolution equations for internal variables yield after the spatial discretization using finite elements a system of differential-algebraic equations (DAE-system)

$$\begin{aligned} \boldsymbol{g}_{\mathrm{u}}(t, \boldsymbol{u}, \boldsymbol{q}) &= \boldsymbol{0}, \\ \dot{\boldsymbol{q}}(t) &= \boldsymbol{r}_{\mathrm{Q}}(t, \boldsymbol{u}, \boldsymbol{q}), \end{aligned} \tag{1}$$

where $\boldsymbol{u}$ are the unknown nodal displacements and $\boldsymbol{q}$ all internal variables related to all spatial integration points of the structure. Large deformations and models of viscoelasticity, rate-independent plasticity or viscoplasticity are embedded as well. In [1] time-adaptive, high order, diagonally-implicit Runge-Kutta methods were applied showing that order reduction can be observed for models (plasticity) with case distinctions. Since that time the concept has been extended to

- displacement-controlled processes to incorporate reaction force computation [3],

– temperature-dependent problems, where, apart from the balance of linear momentum, the heat equation couples the material properties to the temperature [8],
– high-order schemes in space and time [5],
– electro-thermomechanically coupled situations, where the electrical potential generates heat, which influences again the material properties [4],
– dynamical systems, where the entire problem is a coupling of second-order and first-order ordinary differential equations requiring a scheme that each variable achieves its convergence order [2].

The advantage of the entire time-discretization scheme lies in the high-order schemes – at least second-order – providing for the same computational time as in first-order approaches more accurate results, and the possibility of a step-size controlled scheme so that the solver adapts to the problem itself.

In this presentation we extend our investigations to much more challenging harder problems, namely contact of two deformable bodies. For isothermal, 3D-contact problems in the large deformation regime, which are much harder than the previous investigations caused by non-smooth kinematical discontinuities, we combine the mortar element formulation proposed by [6, 7] with the time-integration mentioned before. We study some examples in view of the convergence order and in view of step-size control. Depending on the problem under consideration, the convergence order can be achieved.

References

1. Ellsiepen, P., Hartmann, S.: Remarks on the interpretation of current non-linear finite-element-analyses as differential-algebraic equations. International Journal for Numerical Methods in Engineering 51, 679–707 (2001)
2. Grafenhorst, M., Rang, J., Hartmann, S.: Time-adaptive finite element simulations of dynamical problems for temperature-dependent materials. Journal of Mechanics of Materials and Structures 12(1), 57–91 (2017)
3. Hartmann, S., Quint, K.J., Hamkar, A.W.: Displacement control in time-adaptive non-linear finite-element analysis. ZAMM Journal of Applied Mathematics and Mechanics 88(5), 342–364 (2008)
4. Hartmann, S., Rothe, S., Frage, N.: Electro-thermo-elastic simulation of graphite tools used in SPS processes. In: Altenbach, H., Forest, S., Krivtsov, A. (eds.) Generalized Continua as Models of Materials, Advanced Structured Materials, vol. 22, pp. 143 – 161. Springer, Berlin (2013)
5. Netz, T., Hartmann, S.: A monolithic finite element approach using high-order schemes in time and space applied to finite strain thermo-viscoelasticity. Computers and Mathematics with Applications 70, 1457–1480 (2015)
6. Popp, A., Gitterle, M., Gee, M.W., Wall, W.A.: A dual mortar approach for 3d finite deformation contact with consistent linearization. International Journal for Numerical Methods in Engineering 83(11), 1428–1465 (2010)
7. Popp, A., Seitz, A., Gee, M.W., Wall, W.A.: Improved robustness and consistency of 3d contact algorithms based on a dual mortar approach. Computer Methods in Applied Mechanics and Engineering 264, 67 – 80 (2013)

8. Rothe, S., Erbts, P., Düster, A., Hartmann, S.: Monolithic and partitioned coupling schemes for thermo-viscoplasticity. Computer Methods in Applied Mechanics and Engineering 293, 375 – 410 (2015)

Numerical Investigation of Inclusions Filtration in an Induction Crucible Furnace

Amjad Asad[1], Rüdiger Schwarze[1]

[1] Institute of Mechanic and Fluid Dynamics, Technische Universität Bergakademie Freiberg, Lampadiusstr. 4, 09599 Freiberg, Germany

Email: Amjad.Asad@imfd.tu-freiberg.de

During casting operations, non-metallic inclusions arise in the steel melt. This can decrease the strength and the machinability of the casting. Thus, inclusion removal can play an important role gaining high quality of steel. Using ceramic foam filters (CFF) to remove non-metallic inclusions is an innovative way to capture the inclusions before they are trapped by the solidifying shell in the casting mold. CFFs are state of the art in batch casting, but little information is only available about the performance of CFFs in continuous casting.

The performance and the efficiency of such CFFs are investigated at the Technische Universität Bergakademie Freiberg in frame of the Collaborative Research Centre (CRC 920) by operating the steel casting simulator facility. Here, the CFF is immersed in the melt in the induction crucible furnace (ICF) of this steel casting simulator to estimate its efficiency.

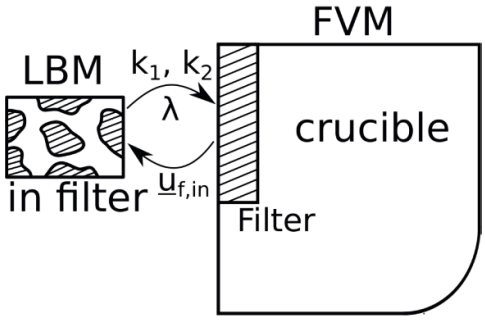

Figure 1: Schematic sketch of the coupling between the macro-scale and pore-scale simulations

In order to determine the filter efficiency of ceramic filters in the ICF, pore-scale and macro-scale simulations are performed. Here, the discrete phase model is adopted to track the inclusions, moving inside the induction furnace and in the filter. In the macro-scale simulation, the used filter is considered here as a homogenous porous body and the Darcy-Forchheimer's law is adopted to compute the pressure drop in the filter. The required permeability k_1, Forchheimer coefficient k_2, and the filtration coefficient λ of the filter are obtained from the pore-scale simulation of the melt and particle transport inside the detailed filter structure, gained by computed tomography scanning. The finite volume method (FVM) is used in the macro-scale simulation, while the pore-scale simulation has been carried out using the lattice-Boltzmann method (LBM). The coupling between the macro-scale and pore-scale simulations is sketched in Figure 1.

Using the filtration coefficient λ obtained from the pore-scale simulation, the filtration probability χ of an inclusion, moving through the filter can be determined. χ decreases exponentially with the increased path length l that the inclusion travels in the filter. In order to model the stochastic deposition at the filter walls, a random number z is defined for each particle travelling through the filter. If $z < \chi$, the particle is assumed to be captured by the filter. Then it is removed from the simulation.

The melt flow in the ICF is driven by the Lorentz force. From Figure 2a, it is obvious that the flow is dominated by two toroidal vortices in the upper part and in the lower part of the crucible for both considered pore densities of the filter. Inspite of the axisymmetrical distribution of

Lorenz force, the melt flow has a slight deviation from axisymmetry. The overall flow structure is dominated by radial-directed streamlines. Furthermore, it is observed that the immersion of the filter in the melt causes a reduction in the melt velocity in the central region of the crucible because of the high flow resistance caused by the filter.

Figure 3 indicates the effect of pore density of the filter on the filter efficiency η. As it can be seen, reducing the pore density of the filter results in increasing the filter efficiency. This finding is attributed to the fact that the mass flow rate through the filter is higher in the case of the filter with a lower pore density (10 ppi). In the case of the higher pore density, the filter causes higher flow resistance in the region where it is located. This means that fewer particles can pass through the filter and then be captured by the filter.

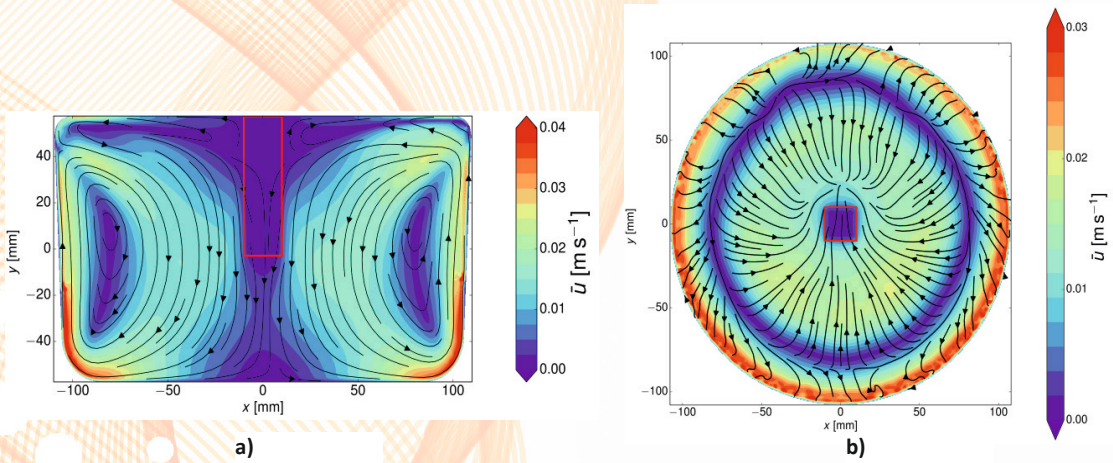

Figure 3: Time averaged flow field in the case of an immersed ceramic filter with pore density of 30 ppi; a) vertical midplane, b) horizontal plane. The ceramic filter is located at the central axis of the crucible.

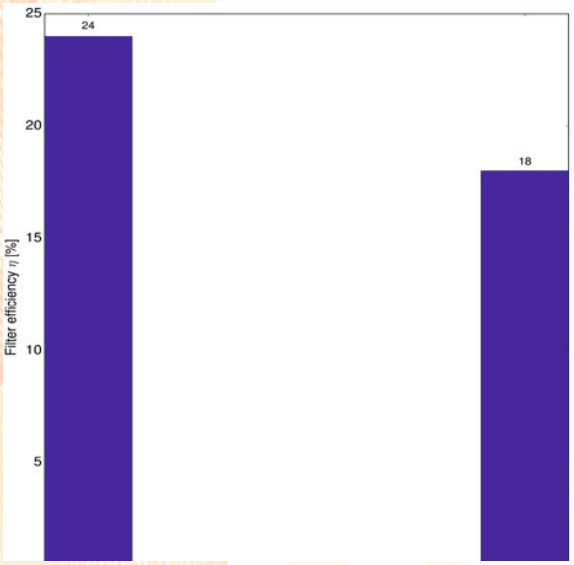

Quantification of the microstructure influence on effective conductivity by virtual materials testing

Matthias Neumann[1], Lorenz Holzer[2], and Volker Schmidt[1]

[1] Institute of Stochastics, Ulm University, D-89069 Ulm, Germany
[2] Institute of Computational Physics, ZHAW Winterthur, CH-8400 Winterthur, Switzerland

In many applications the functionality of materials strongly depends on their microstructure. This is the case for, e.g. electrodes in solid oxide fuel cells or lithium-ion batteries, which are future technologies with small environmental impact. In order to optimize microstructures in functional materials, the relationship between microstructure characteristics and functional properties has to be understood quantitatively, which is often not the case or just for some special types of simple microstructures [8].

The progress of 3D imaging during the last decades enables the computation of well-defined microstructure characteristics from real data, which can be compared to effective properties that are either measured experimentally or simulated with numerical models. Although this approach allows a direct investigation of the relationship between microstructure and effective properties, it is limited due to the high costs of 3D imaging.

Thus, we present an alternative approach, called virtual materials testing. Stochastic microstructure modeling is combined with numerical simulations of physical processes to investigate the quantitative relationship between microstructure characteristics and functional properties. Here we consider effective conductivity σ_{eff} in porous materials as the functional property. The use of stochastic microstructure models allows us to generate virtual, but realistic, microstructures in short time, where certain microstructure characteristics can be varied systematically. The virtual microstructures are used as an input for finite element modeling (FEM) where the corresponding effective conductivities are simulated. Then, a sufficiently large data set is available to study the relationship between microstructure and σ_{eff}.

In this talk, we give an overview of the results regarding the microstructure influence on effective conductivity which have been achieved in [3,6,7] by virtual materials testing. Here it is assumed that the essential microstructure characteristics for σ_{eff} are the volume fraction ε of the conducting phase, its tortuosity τ and its constrictivity β. Tortuosity τ measures the windedness of transportation paths, where two concepts of tortuosity are considered, i.e. geometric tortuosity τ_{geom} and geodesic tortuosity τ_{geod}. Constrictivity β is a value between 0 and 1, which quantifies the strength of bottleneck effects based on the concept of continuous phase size distributions [4]. If β is close to 0 the bottleneck effect is strong and if $\beta = 1$ there are no bottlenecks at all.

In order to investigate the influence of these microstructure characteristics on σ_{eff} a stochastic microstructure model has been introduced in [3], which gener-

ates realistic virtual 3D microstructures, where the three microstructure characteristics mentioned above can be varied systematically. Based on methods from stochastic geometry [1] the conducting phase is modeled as a dilated random network with local variations of the dilations radii. For 45 virtual microstructures the effective conductivities have been obtained by FEM. Regression analysis has then led to the prediction formula

$$\sigma_{\text{eff}} = \sigma_0 \, \min\{1, \max\{0, 2.03\, \varepsilon^{1.57}\, \beta^{0.72}\, \tau_{\text{geom}}^{-2}\}\}, \tag{1}$$

where σ_0 denotes the intrinsic conductivity of the conducting material.

The same set of virtual microstructures has been used in [7] for further investigations of the microstructure influence on effective conductivity. A comparison between τ_{geom} and τ_{geod} has indicated that geometric tortuosity has a tendency to overestimate the length of transport paths. Additionally, the prediction formula given in Equation (1) could be improved by using the geodesic instead of the geometric tortuosity, i.e.

$$\sigma_{\text{eff}} = \sigma_0\, \varepsilon^{1.15}\, \beta^{0.37}\, \tau_{\text{geod}}^{-4.39}. \tag{2}$$

Note that Equation (1) remains valid, when σ_{eff} is predicted by $\varepsilon, \tau_{\text{geom}}$ and β.

While the investigations in [3] and [7] are based on 45 virtual microstructures, a much larger set of more than 8000 virtual microstructures has been generated in an extensive simulation study [6]. This is – to the best of our knowledge – by far the largest set of microstructures that has ever been analyzed. For this purpose, virtual microstructures have not only been generated by the model developed in [3], but also the model introduced in [5] has been used. The interpretable formula given in Equation (2) has led to good predictions regarding all the more than 8000 virtual microstructures, although it was just fitted to 45 of them. Using non-parametric regression methods from statistical learning [2], namely neural networks and random forests, an even more accurate prediction of σ_{eff} by $\varepsilon, \tau_{\text{geod}}$ and β has been achieved.

Validation with experimental microstructures has shown that the generated virtual microstructures are sufficiently realistic to derive prediction models for effective conductivity. Overall, virtual materials testing is a powerful tool to establish quantitative relationships between microstructure characteristics and functional properties. The presented relationships enable the identification of improved microstructures with respect to effective conductivity. The method itself is not restricted to conduction processes in two-phase materials. In future work, we will investigate conduction processes through multi-phase materials, where the different phases vary in their intrinsic conductivities. Here we expect that additional microstructure characteristics have to be taken into account, like e.g. the areas of the interphase boundaries. Moreover, virtual materials testing can be used to investigate relationships between microstructure characteristics and other functional properties, like e.g effective permeability or mechanical stress-strain curves.

References

1. Chiu, S.N., Stoyan, D., Kendall, W.S., Mecke, J.: Stochastic Geometry and its Applications. J. Wiley & Sons, Chichester, 3rd edn. (2013)
2. Friedman, J., Hastie, T., Tibshirani, R.: The Elements of Statistical Learning. Springer, New York, 2nd edn. (2008)
3. Gaiselmann, G., Neumann, M., Pecho, O.M., Hocker, T., Schmidt, V., Holzer, L.: Quantitative relationships between microstructure and effective transport properties based on virtual materials testing. AIChE Journal 60(6), 1983–1999 (2014)
4. Holzer, L., Wiedenmann, D., Münch, B., Keller, L., Prestat, M., Gasser, P., Robertson, I., Grobéty, B.: The influence of constrictivity on the effective transport properties of porous layers in electrolysis and fuel cells. Journal of Materials Science 48, 2934–2952 (2013)
5. Stenzel, O., Hassfeld, H., Thiedmann, R., Koster, L.J.A., Oosterhout, S.D., van Bavel, S.S., Wienk, M.M., Loos, J., Janssen, R.A.J., Schmidt, V.: Spatial modeling of the 3D morphology of hybrid polymer-ZnO solar cells, based on electron tomography data. The Annals of Applied Statistics 5, 1920–1947 (2011)
6. Stenzel, O., Neumann, M., Pecho, O.M., Holzer, L., Schmidt, V.: Big data for microstructure-property relationships: A case study of predicting effective conductivities. Submitted (2017)
7. Stenzel, O., Pecho, O.M., Holzer, L., Neumann, M., Schmidt, V.: Predicting effective conductivities based on geometric microstructure characteristics. AIChE Journal 62, 1834–1843 (2016)
8. Torquato, S.: Random Heterogeneous Materials: Microstructure and Macroscopic Properties. Springer, New York (2013)

Parallel hybrid Molecular Statics / Monte Carlo for Segregation of Interstitials in Solids

Godehard Sutmann[1,2], Hariprasath Ganesan[2], and Christoph Begau[2]

[1] Jülich Supercomputing Centre, Forschungszentrum Jülich, D-52425 Jülich
[2] Interdisciplinary Centre for Advanced Materials Simulation (ICAMS), Ruhr-University Bochum, D-44801 Bochum
g.sutmann@fz-juelich.de

1 Introduction

Macroscopic quantities like yield strength in crystalline metallic materials are driven by atomic length scale mechanisms like solute segregation. Modelling such rare event processes by atomistic molecular dynamics (MD) in large systems is particularly challenging due to small time steps and a large number of particle oscillations in a local environment until an energy barrier crossing takes place. Considering the complexity of a system including its chemical environment and strain field due to crystal defects these processes cannot be explored with traditional deterministic methods. In principle the same applies to local Monte Carlo trial moves, which might be also trapped in a local energy basin. As a solution, we propose a coupled framework of MD and Monte Carlo using virtual atoms to model interstitial solute segregation for single crystal with arbitrary defects. Nonlocal trial moves are performed which sample configuration space more efficiently and are able to overcome local energy barriers. The approach is valid for interstitial atoms in solids and it is demonstrated to work for carbon segregation in ferritic iron including screw dislocations. Upon randomly sampling the simulation domain without introducing any bias, the results for 0 K simulations show a high carbon concentration near the dislocation core, which is in qualitative agreement with previous works.

2 Method

We apply a hybrid formulation between Molecular Dynamics and Monte Carlo simulation protocols. The basic procedure consists of changing the position of one interstitial particle in the system via stochastic selection rules, i.e. one has to consider the coupled events in two sub-volumes. In general this exchange results in a non-equilibrium configuration which, for 0 K simulations, is relaxed in a sub-sequent step via molecular statics. After having relaxed the structure, the new configuration is accepted, if the energy difference between the two states is negative, i.e.

$$\delta E = E\{\Omega_1, 1 \to 2\} + E\{\Omega_2, 2 \to 1\} - E\{\Omega_1, 1\} - E\{\Omega_2, 2\} < 0 \qquad (1)$$

Here, Ω_i, Ω_j are sub-volumes in the system, which are chosen randomly for a trial exchange of a particle with a void location, i, j. This trial exchange can be considered as a 1-step limiting case of a switching process, which is performed in discrete steps [1–3]. According to a $T = 0\,K$ energy minimization, the trial state is accepted if the energy in the new combined state is lower than in the old state. Accordingly, the configuration is explored towards the minimum energetical state of the system, although it is quite probable that the absolute minimum is not reached and the system is confined in a local minimum. This behavior is quite tolerable as a physical system will most probably also not reach the absolute minimum, due to the diffusive process of atoms which will also be captured in local minima. Therefore the method is able to reproduce real trends of system behaviour and to compute statistically significant density distributions of diffusive particles.

Since local trial moves of atoms will most probable lead to high rejection rates due to large energy barriers between neighboured energy basins, the idea is to propagate the system via non-local moves, which explores configuration space more efficiently. However, since completely random trial moves of particles will most likely result in unfavourable locations and therefore are most likely to be rejected, the present approach relies on so called virtual particles. These are placeholders, which are located at interstitial positions in the lattice and which have an asymmetric interaction, i.e. they are influenced by the interaction with the material atoms, e.g. Fe particles, but in turn they do not influence the material atoms, i.e. there is no force from the virtual particles to the material. Therefore, they follow any lattice configuration changes, e.g. deformation, in a consistent way, but do not affect the configuration by their presence. In this way, when interstitial atoms are exchanged with a virtual atom, they are placed in a position, which is already near to local equilibrium and the number of relaxation steps after a particle swap gets minimal.

3 Parallelization

For the parallelization a manager-worker approach is chosen. A work queue is created by the manager and each item in the queue is related to a processor, associated with a pair of particles, i.e. a virtual particle V and an interstitial particle I. The master owns a copy of all the coordinates of the system and sends appropriate information to the processors, i.e. which atoms I, V to exchange and all coordinates $\{\mathbf{x}(\Omega_I)\}$ and $\{\mathbf{x}(\Omega_V)\}$ of particles which belong to a spherical environment of radius R_c with a total volume $\Omega_{I,V}(p) = \Omega_I \cup \Omega_V$ on a processor p. The particle swap together with the molecular statics calculation is performed on a given processor p and the evaluation of the energy difference, Eq.1, is sent back to the master. In case that $\delta E < 0$, also the coordinates are sent back to the master. Since many processors are working asynchronously in parallel and independently from each other, false overlap between interaction ranges can occur, i.e. $\Omega_{I,V}(p_i) \cup \Omega_{I,V}(p_j) \neq \emptyset$, which risks that the outcome of the processor which is at a later position in the work queue would depend on the

outcome of the other processor. Therefore, the master has to analyse this possible overlap between regions and discards those results from processors j, which have accepted configurations and overlap with processors i which come earlier in the queue and have also accepted configurations. It is obvious that the higher I-concentration or the larger the processor count, the more likely false overlap takes place [4]. This situation has been analysed experimentally and analytically and it was found that for homogeneous distributions of carbon interstitials with a concentration of $n_C = 0.01wt\%$ in a system of $N_{Fe} = 10^6$ iron particles, the scalability gets up to ≈ 60 processors. The realisation of larger processor counts will be realised when introducing hybrid schemes, where the relaxation for each Ω is done on sub-partitions of the compute system.

4 Results and Conclusions

To demonstrate the applicability of the method, a hybrid MD-MC scheme has been applied to a C-Fe system, consisting of $N_{Fe} = 10^6$, $N_V = 3 \times 10^6$ virtual atoms and $N_C = 500$ carbon atoms and including a screw dislocation (cf. Fig. 1). Starting from a homogeneous distribution of C-atoms, it could be shown that the segregation process in the presence of the dislocation can be simulated very efficiently, although the parallel scalability of the scheme is reduced due to false overlap when the concentration of C-atoms increases around the dislocation core during segregation. This efficiency degradation will be compensated by an additional parallel-replica approach in near future. For a homogeneous defect free Fe-C-system with $N_{Fe} \approx 10^6$ particles, scalability could be obtained up to 32-64 processors. Work is in progress towards an efficiency control scheme which decides on-the-fly for a given number of processors upon an extension towards a replica system method.

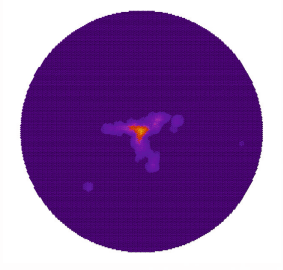

Fig. 1. Density distribution of segregated C atoms in Fe in the presence of a screw dislocation in the centre of the system.

References

1. D. Frenkel. Lecture notes on: free energy calculations. In M. Meyer and V. Pontikis, editors, *Computer simulation in materials science*, page 85, Amsterdam, 1991. Kluwer Academic Publishers.
2. C. Jarzynski. Nonequilibrium Equality for Free Energy Differences. *Phys. Rev. Lett.*, 78:2690, 1997.
3. G.E. Crooks. Nonequilibrium measurements of free energy differences for microscopically reversible Markovian systems. *J. Stat. Phys.*, 90:1481, 1998.
4. G. Sutmann, H. Ganesan, and C. Begau. Cluster Formation in Overlapping Disk Systems. Proc. Int. Conf. Num. Anal. Appl. Math. 2016 (ICNAAM), AIP Conference Proceedings (in press).

3D microstructure modelling und simulation of materials in lithium-ion battery cells

J. Feinauer, D. Westhoff and V. Schmidt

Institute of Stochastics, Ulm University, D-89069 Ulm, Germany

The usage of lithium-ion battery cells is steadily growing in various fields of daily life. This implies the necessity for further improvement of battery materials. As laboratory experiments are expensive in time and costs, model-based simulations of electrochemical processes in battery cells have become an important part of battery research. Simulations are also necessary for the optimization of charging strategies and control systems [13].
Electrochemical simulation models go back to the famous work of Newman and co-workers [10]. However, these models neglect the geometry of the cell and their 3D microstructure by using averaged characteristics. Recently, spatially resolved transport models have been developed to simulate the transport of the charges in lithium-ion battery cells [8, 9].
In this talk we focus on stochastic 3D microstructure models which are the basis of spatially resolved transport models, where highly resolved image data of 3D microstructures of battery materials are necessary for model calibration. The major advantage of the combination of stochastic microstructure models with spatially resolved transport models is that this approach can be used for realistic simulations of local effects like lithium-plating and other aging mechanisms which are influenced by local potentials. Furthermore, the computational complexity of this approach can be reduced for specific applications like cycle-life simulations by reduced basis methods [2].

General approach. Methods of stochastic geometry and and spatial statistics have been proven to be a viable tool for the simulation of the 3D microstructure of energy materials like those used in fuel cells or solar cells [4, 5, 14]. The general idea of these methods is to provide microstructure models based on a few parameters that are able to generate 3D microstructures which are similar in a statistical sense to those observed in experimental data. This means that averaged characteristics like volume fractions or specific surface areas but also more refined descriptors of microstructures like the geometric tortuosity of transportation paths or the pore size distribution are in good agreement.
Furthermore, most of these models and the corresponding simulation algorithms are off-grid meaning that they can be used to generate structures on arbitrary length scales. The computer time it takes to generate a realization of such a microstructure model is usually very small. Thus, the usual problems of tomographic imaging related with the generation of a sufficiently large amount of highly resolved 3D images in suffiently large regions of interest can be solved once such a model is developed and fitted to experimental data.

Simulation of invidividual particles. Lithium-ion battery electrodes consist of systems of connected particles that can have complex shapes. For the

electrode models it is very important to fit fundamental microstructure characteristics like porosity and specific surface area exactly [12]. Another important characteristic of the electrodes is the high connectivity of particles. This means that each particle is connected to many neighbouring particles. Thus, the model of individual particle sizes and shapes has to be flexible enough to meet all these conditions. We developed a stochastic particle model which possesses this property. Is is based on the representation of particles as linear combinations of spherical harmonics. Particles with random sizes and shapes can then be simulated using Gaussian random fields on the sphere whose parameters are fitted to the coefficients of the spherical harmonics expansions of particles from experimental data [3].

Simulation of particulate materials. With the method for modeling and simulation of individual particles described above, we are able to build models for different kinds of negative electrode materials. Electrodes in so-called energy cells like the ones used in electric vehicles have high particle densities and relatively small porosities such that tessellations from stochastic geometry can be used as a basic modeling tool. Note that a tessellation divides the space into disjoint convex polyhedra. Together with a connectivity graph, boundary conditions can be calculated for each polyhedron and a particle can be sampled and placed inside [1]. The simulated 3D microstructures are then used for spatially resolved transport simulations [6] where the focus is put on the electrochemical validation of the simulated microstructures. Moreover, in [2], the electrochemical simulations performed on simulated 3D microstructures are combined with model order reduction methods to accelerate the whole procedure.
In lithium-ion cells designed for power application like the ones used in plugin hybrid vehicles, the volume fraction of active material is lower but the specific surface area is higher to allow for higher charge and discharge currents. Such 3D microstructures have been generated with an extended version of the modeling approach described above for energy cells, where a refined tessellation model is used and some polyhedra are left empty when placing the particles [15].

Related work & Outlook. Currently we are working on a further extension of the stochastic microstructure model to simulate the 3D microstructures of positive electrode materials [7]. Furthermore, we are extending our modeling tools for particulate materials to incorporate cracked particles. In [11] we propose an application of machine learning for the detection of cracked particles in tomographic images from negative electrode materials of lithium-ion batteries. The automated detection of cracked particles combined with the parametric representation of individual particles described above enables statistical investigations of the relationship between the morphology of particles and their cracking behavior.

References

1. Feinauer, J., Brereton, T., Spettl, A., Weber, M., Manke, I., Schmidt, V.: Stochastic 3D modeling of the microstructure of lithium-ion battery anodes via Gaussian random fields on the sphere. Computational Materials Science 109, 137–146 (2015)

2. Feinauer, J., Hein, S., Rave, S., Schmidt, S., Westhoff, D., Zausch, J., Iliev, O., Latz, A., Ohlberger, M., Schmidt, V.: Multibat: Unified workfow for fast electrochemical 3D simulations of lithium-ion cells combining virtual stochastic microstructures, electrochemical degradation models and model order reduction. Journal of Power Sources (submitted)
3. Feinauer, J., Spettl, A., Manke, I., Strege, S., Kwade, A., Pott, A., Schmidt, V.: Structural characterization of particle systems using spherical harmonics. Materials Characterization 106, 123–133 (2015)
4. Gaiselmann, G., Neumann, M., Holzer, L., Hocker, T., Prestat, M., Schmidt, V.: Stochastic 3D modeling of LSC cathodes based on structural segmentation of FIB-SEM images. Computational Materials Science 67, 48–62 (2013)
5. Gaiselmann, G., Thiedmann, R., Manke, I., Lehnert, W., Schmidt, V.: Stochastic 3D modeling of fiber-based materials. Computational Materials Science 59, 75–86 (2012)
6. Hein, S., Feinauer, J., Westhoff, D., Manke, I., Schmidt, V., Latz, A.: Stochastic microstructure modeling and electrochemical simulation of lithium-ion cell anodes in 3D. Journal of Power Sources 336, 161–171 (2016)
7. Kuchler, K., Westhoff, D., Feinauer, J., Mitsch, T., Manke, I., Schmidt, V.: Stochastic model of the 3D microstructure of Li-ion battery cathodes under various cyclical aging secenarios. (under preparation)
8. Latz, A., Zausch, J.: Thermodynamic consistent transport theory of Li-ion batteries. Journal of Power Sources 196, 3296–3302 (2011)
9. Latz, A., Zausch, J.: Thermodynamic derivation of a ButlerVolmer model for intercalation in Li-ion batteries. Electrochimica Acta 110, 358–362 (2013)
10. Newman, J., Thomas, K., Hafezi, H., Wheeler, D.: Modeling of lithium-ion batteries. Journal of Power Sources 119, 838–843 (2003)
11. Petrich, L., Westhoff, D., Feinauer, J., Finegan, D., Daemi, S., Shearing, P., Schmidt, V.: Crack detection in lithium-ion cells using machine learning. Computational Materials Science (submitted)
12. Pfaffmann, L., Birkenmaier, C., Müller, M., Bauer, W., Mitsch, T., Feinauer, J., Scheiba, F., Hintennach, A., Schleid, T., Schmidt, V., Ehrenberg, H.: Investigation of the electrochemical active surface area and lithium diffusion in graphite anodes by a novel OsO4 staining method. Journal of Power Sources 307, 762–771 (2016)
13. Remmlinger, J., Tippmann, S., Buchholz, M., Dietmayer, K.: Low-temperature charging of lithium-ion cells Part II: Model reduction and application. Journal of Power Sources 254, 268–276 (2014)
14. Stenzel, O., Koster, L., Thiedmann, R., Oosterhout, S., Janssen, R., Schmidt, V.: A new approach to model-based simulation of disordered polymer blend solar cells. Advanced Functional Materials 22, 1236–1244 (2012)
15. Westhoff, D., Feinauer, J., Kuchler, K., Mitsch, T., Manke, I., Hein, S., Latz, A., Schmidt, V.: Parametric stochastic 3D model for the microstructure of anodes in lithium-ion power cells. Computational Materials Science 126, 453–467 (2017)

Transparent Model-Driven Provisioning of Computing Resources for Numerically Intensive Simulations

Fabian Glaser[1], Alexander Bufe[2], Christian Köhler[3], Gunther Brenner[2], Jens Grabowski[1], and Philipp Wieder[3]

[1] Institute of Computer Science, University of Göttingen
37077 Göttingen, Germany
[2] Institute of Applied Mechanics, Clausthal University of Technology
38678 Clausthal-Zellerfeld, Germany
[3] Gesellschaft für wissenschaftliche Datenverarbeitung mbH Göttingen (GWDG)
37077 Göttingen, Germany

1 Introduction

Scientific simulations are often computation intensive and time consuming and can highly profit from choosing a suitable computing resource type and scale. However, choosing the right computing resource and an appropriate scale is not a trivial task, especially in modern computing centers that offer access to a heterogeneous infrastructure including cloud services, high performance computing clusters and clusters with specialized accelerators (e.g., GPU cards). All of these different resource types have their own technical peculiarities and require the simulation scientist to invest time to learn when and how to use them. It might even be necessary to switch the resource type and scale during the lifetime of a simulation, e.g., when transitioning from testing simulation code to running parameter studies, or when the problem size increases and suddenly requires more computing resources. To overcome this burden, we develop a transparent integration mechanism for heterogeneous computing resources. The goal is to semi-automatically deploy and execute simulation applications on the most suitable resource type. To achieve this goal, we model the simulation application structure and behaviour in a resource-agnostic way and provide model transformators that automatically transform the abstract simulation application model into resource-specific models. In this paper, we introduce a conceptual framework that implements the concept of model-driven provisioning of computing resources for simulation application and provide an initial evaluation with help of a numerical intensive simulation from fluid mechanics.

2 Use Case

As an exemplary use case, the simulation of the flow in porous media with the lattice-Boltzmann method was chosen. The *Lattice-Boltzmann method* (LBM)

originates from Boltzmann's kinetic molecular dynamics and may be understood as a discretization in space and time of the velocity-discrete Boltzmann equation. Its main advantages are the inherent parallelism which leads to great performance on many architectures and easy handling of complex geometries.

Particle filled beds are of great technical importance e.g. in catalysator packings. Thus, the knowledge of the pressure drops in such packings is crucial. Confining walls can have a significant influence on the pressure drop and therefore the pressure drop as function of the sphere diameter to wall distance ratio is systematically studied. A high number of packings is created using an algorithm and a scale-resolving simulation of the flow in the packing with LBM is performed (figure 1). In previous work, measured and simulated pressure drops in slit-type milli-channels with different packings were compared. Very good agreement between measured and simulated pressure drops was achieved. [2]

This use case can be seen as a typical parameter study which are common in engineering. The same program is plurally started with different parameters (in this case sphere diameter to wall distance ratio). The computational cost of a single program run is relatively low and the high effort is mainly caused by the multiple execution. The demands on the infrastructure are therefore different from a single large simulation like an aerodynamic simulation with a great number of mesh cells and more complex domain boundaries, where the simulation is distributed over many nodes which must be synchronized after every time step and thus has higher demands on the network connection. A more involved simulation may therefore necessitate the switch to a different infrastructure.

To shield the simulator from the manual adaptation of the provided resources to the different simulation types, we build an infrastructure that helps to provision resources of the correct type and scale transparently.

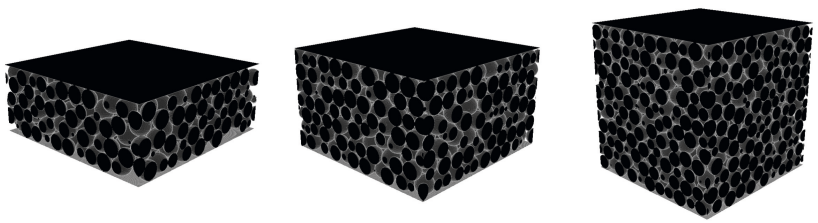

Fig. 1: Exemplary packings of spheres between to plates with a sphere diameter to wall distance ratio of 4, 6 and 10.

3 Model-Driven Resource Provisioning

In our work, we use a formal model of the simulation application topology and its behaviour to automatically provision suitable computing resources. The overall

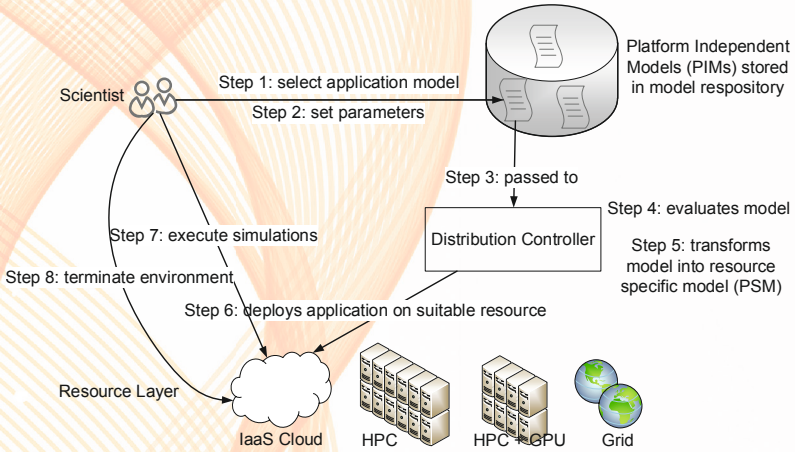

Fig. 2: Workflow for model-driven resource provisioning for simulation applications.

workflow that is implemented by our infrastructure is depicted in Figure 2. To distinguish the models used on the different layers we orientate on the notations introduced with the *Model Driven Architecture* (MDA)[5], developed by the *Object Management Group* (OMG).

A *Platform Independent Model* (PIM) encodes the structure and behaviour of the simulation application in a target resource independent way and is stored in a model repository. The simulator is then able to select (Step 1) and adapt (Step 2) the existing models from the repository. The selected and instantiated model is then passed to a *Distribution Controller* (Step 3) that evaluates the parameters of the model (Step 4), selects the suitable target infrastructure accordingly and transforms the selected model into a *Platform Specific Model* (PSM) that matches the requirements of the targeted infrastructure (Step 5). In the next step, the resource provisioning and the automated deployment of the simulation application on the targeted resource is triggered (Step 6). After that, the simulator is given access to the provided resource via a *Command Line Interface* (CLI) and can execute his simulations accordingly (Step 7). When all simulation runs are done, the simulator can collect the output data and triggers the cleanup and termination of the provided infrastructure (Step 8).

Different resource-specific formats for defining the simulation application for the different target infrastructures exist. For *Infrastructure as a Service* (IaaS), we adopt the *Topology and Orchestration Specification for Cloud Applications* (TOSCA) [4] which is currently developed by a large technical consortiuum and allows to define the topology and the behaviour of cloud applications in a provider-agnostic way. To build a format for describing the PIM, we extend TOSCA to not only be able to capture cloud-specific information, but also the information that is necessary to deploy the application on the other targeted resources, like classical HPC or HPC+GPU setups. We first concentrate on uti-

lizing the *IBM Load Sharing Facility* (LSF)[3], i.e. generating jobscripts ready for submission. For a given simulation application, this entails taking into account parameters that are fixed upon deployment, for instance the infrastructure model for the compute cluster, as well as parameters that may vary between execution steps like differing mesh resolutions or choices of which data to operate on.

The model-driven approach is also employed to describe the infrastructure on which the simulation application will be deployed and executed. Keeping the application and infrastructure models up to date regarding evolving software versions, for example of the Load Scheduler, is as important as making them available to the simulation user in the first place. We therefore intend the repository to be maintained independently for the application and infrastructure models. This way, a PIM of the Load Scheduler is combined with information about a specific cluster setup by its administrator to yield a PSM for the users. The result is combined with the PIM for the simulation application, which can in turn be maintained by its developers. Our approach exemplifies a separation of concerns of the knowledge about the specific compute cluster and about the simulation application from the technical details regarding the transformation of their respective models in the *Distribution Controller*. Consequently, each type of model can developed by the group of people best equipped to do so, which is a core tenet of MDA.

4 Current state

Outcome of the simulations that provide the use case have been partially published elsewhere [2]. Cloud-specific PIMs and PSMs have already been developed and evaluated [1]. They serve as the basis for the recourse-agnostic simulation application metamodel. We created a model for a generic LSF-based compute cluster, which abstracts the compute resources as well as the queues used to organize them, and one for the jobs that are submitted to the cluster. These are intended to constitute the PIM, which is to be combined with a concrete cluster setup and subsequently the application model for our use case's workflow. The whole workflow for the use case will be shown at the workshop.

5 Conclusions and Outlook

We develop an architecture which provides a transparent resource provisioning mechanism for simulation applications for heterogeneous compute infrastructures, which are todays reality and many scientific computing centers. The goal is to shield the simulator from complicated infrastructure internals. In this paper, we present the initial architecture, which orientates on the MDA and demonstrate its usefulness with help of a LBM simulation from fluid mechanics.

Acknowledgements

We thank the Simulationswissenschaftliches Zentrum Clausthal-Göttingen (SWZ) for financial support.

References

1. F. Glaser. Domain Model Optimized Deployment and Execution of Cloud Applications with TOSCA. In Jens Grabowski and Steffen Herbold, editors, *System Analysis and Modeling. Technology-Specific Aspects of Models*, LNCS, Cham, October 2016. Springer International Publishing.
2. S. Hofmann, A. Bufe, G. Brenner, and T. Turek. Pressure drop study on packings of differently shaped particles in milli-structured channels. *Chemical Engineering Science*, 155:376–385, 2016.
3. IBM Corporation. Introduction to IBM Platform LSF. Available Online: https://www.ibm.com/support/knowledgecenter/SSETD4_9.1.2/lsf_foundations/lsf_introduction_to.html, Last Retrieved: 05.01.2017.
4. OASIS. Topology and Orchestration Specification for Cloud Applications (TOSCA) 1.0, November 2013. Available online: http://docs.oasis-open.org/tosca/TOSCA/v1.0/os/TOSCA-v1.0-os.html, Last Retrieved: 05.01.2017.
5. Object Management Group. Model Driven Architecture. Available Online: http://www.omg.org/cgi-bin/doc?ormsc/14-06-01.pdf, Last Retrieved: 05.01.2017.

Performance of Big Data versus High-Performance Computing: Some Observations

Helmut Neukirchen

School of Engineering and Natural Sciences, University of Iceland, Reykjavík, Iceland
Email: helmut@hi.is

Abstract. The two prevalent paradigms for parallel processing are HPC and the newer big data platforms. In addition to comparing their general properties, a survey and run-time comparison of implementations of the DBSCAN clustering algorithm for these two paradigms are provided.

Keywords: Big Data, High-Performance Computing, Benchmarking

1 Introduction

Computationally intensive simulations require parallel processing. The standard technology for huge non-embarrassingly parallel, but rather tightly-coupled computational problems is *High-Performance Computing* (HPC). Highly praised contenders for huge parallel processing problems are big data processing frameworks such as Apache Hadoop or Apache Spark. Hence, they might be considered an alternative to HPC for distributed simulations. To be able to decide whether HPC or big data platforms are better suited for computationally intensive problems, this paper gives a brief overview on these two paradigms and their platforms and compares as main contribution their run-time performance and scalability using as examples different implementations of the *Density-Based Spatial Clustering of Applications with Noise* (DBSCAN) clustering algorithm.

2 Paradigm shift: HPC versus Big Data

HPC is tailored to typically CPU-bound computationally expensive jobs. Hence, rather expensive hardware is used, e.g. compute nodes containing fast CPUs including many cores, very fast interconnects (e.g. InfiniBand) for communication between nodes, and centralized *Storage-Area Network* (SAN) storage. To make use of the many cores per CPU, shared-memory multi-threading based on *Open Multi-Processing* (OpenMP) is applied. To make use of the many nodes connected via the interconnects, an implementation of the *Message Passing Interface* (MPI) is used. The underlying programming model is low-level, but allows tightly-coupled parallel processing. Low-level, but fast programming languages such as C, C++ and Fortran are used.

The big data paradigm is tailored to process huge amounts of data, however the actual computations to be performed on this data are often not that computationally intensive. To achieve high-throughput, locality of data storage is exploited by using distributed file systems storing locally on each node a part of the data. The big data approach aims at doing computations on those

Table 1. Run-time (in Seconds) vs. Number of Cores for 3 704 351 points

Number of cores	1	2	4	8	16	32
HPDBSCAN	114	59	30	16	8	6
PDSDBSCAN	288	162	106	90	85	88
ELKI	997	–	–	–	–	–
RDD-DBSCAN	7 311	3 521	1 994	1 219	889	832

nodes where the data is locally available. An example is Apache Hadoop which, however, has the disadvantage that only the MapReduce paradigm is supported which restricts the possible class of parallel algorithms and in particular may lead to unnecessarily storing intermediate data on disk instead of allowing to keep it in fast RAM. This weakness is overcome by Apache Spark [2] which is based on *Resilient Distributed Datasets* (RDDs) which are able to store a whole data set in RAM, distributed in partitions over the nodes of a cluster. While RDDs may be kept in RAM, required data may not be available in the local RDD partition of a node. In this case, it is necessary to re-distribute data between nodes. Such shuffle operations are expensive, because slow network transfers are needed for them. High-level programming languages such as Java, Scala or Python are used.

3 Run-time/Scalability of DBSCAN Implementations

To investigate the run-time performance and scalability of existing scientific libraries (needed to ease building parallel applications, such as simulations) and their underlying HPC or Spark platform, we surveyed and benchmarked parallel open-source implementations of the the clustering algorithm DBSCAN [4]. The underlying idea of DBSCAN is that for each data point, the neighbourhood within a given *eps* radius has to contain at least a *minpts* points to form a cluster, otherwise it is considered as noise. Depending on the implementation and the size of *eps* in comparison to the size of the whole data, the time complexity is $O(n \log n)$ to $O(n^2)$ with the latter leading to scalability problems for big data.

We found two open-source parallel DBSCAN implementations for HPC using C++: PDSDBSCAN. [7] and HPDBSCAN [5]). The highly-optimized serial Java implementation ELKI [9] was used as reference for the four parallel Scala/*Java Virtual Machine* (JVM)-based open-source implementations we found for Spark: Spark DBSCAN [6], RDD-DBSCAN [3], Spark_DBSCAN [1], and DBSCAN On Spark [8]. Results from running the first four implementations[1] are shown in Table 1. All measurements were performed on the same, identical cluster for HPC and Spark using 3 704 351 2D geo-tagged tweets: except HPDBSCAN, none of the implementations scaled well beyond 16 cores and in particular the RDD-DBSCAN implementation for Spark was significantly slower.

To investigate performance on a bigger dataset using more cores, we clustered 16 602 137 geo-tagged tweets on several hundred cores (Table 2). Again, the HPC implementation performed significantly better than the ones for Spark. As these were already with a high number of cores very slow (RDD-DBSCAN with

[1] For the latter three, no detailed experiments were made due to $O(n^2)$ complexity (RDD-DBSCAN), being already extremely slow with 928 cores (Spark_DBSCAN) and providing in fact only an approximation of DBSCAN (DBSCAN on Spark).

Table 2. Run-time (in Seconds) vs. Number of Cores for 16 602 137 points

Number of cores	1	384	768	928
HPBDBSCAN	2 079	10	8	–
ELKI	15 362	–	–	–
Spark_DBSCAN	–	–	–	Exception
RDD-DBSCAN	–	–	–	5 335

928 cores was only three times faster than ELKI using one core) or threw an exception, we did not perform measurements with a lower number of cores.

4 Conclusions

In summary, none of the DBSCAN implementations for Apache Spark is anywhere near to the HPC implementations. It can be speculated that this is because in HPC, parallelization needs to manually implemented and thus gets more attention in contrast to the high-level big data approaches where the developer gets not in touch with parallelization. Another reason to prefer HPC for compute-intensive simulations is that already based on the used programming languages, run-time performance of the JVM-based Spark platform can be expected to be one order of magnitude slower than C/C++ (compare ELKI vs. HPDBSCAN). While RDDs support a bigger class of non-embarrassingly parallel problems than MapReduce, Spark still does not support as tight-coupling as OpenMP and MPI used in HPC – which might however be required for simulations. On the other hand, due to the high-level programming languages such as Scala and the fact that Spark code can be written like serial code without having to care about parallelization, considerably less implementation efforts can be expected when using Spark. Also, in contrast to HPC where no fault tolerance is included (a single failure on one of the many cores will cause the whole HPC job to fail), the big data platforms have the advantage of being are fault-tolerant. Finally, the commodity hardware typically used as big data platform is cheaper.

References

1. aizook: Spark_DBSCAN source code. GitHub repository (2014), `https://github.com/aizook/SparkAI`
2. Apache Software Foundation: Apache Spark (2016), `http://spark.apache.org/`
3. Cordova, I., Moh, T.S.: DBSCAN on Resilient Distributed Datasets. In: 2015 Int. Conf. on High Performance Computing & Simulation (HPCS). IEEE (2015)
4. Ester, M., et al.: Density-based spatial clustering of applications with noise. In: Proc. of the 2nd Int. Conf. on Knowl. Discovery and Data Mining. AAAI (1996)
5. Götz, M., et al.: HPDBSCAN: highly parallel DBSCAN. In: Proc. of the Workshop on Machine Learning in High-Performance Computing Environments. ACM (2015)
6. Litouka, A.: Spark DBSCAN source code. GitHub repository (2014), `https://github.com/alitouka/spark_dbscan`
7. Patwary, M.M.A., et al.: A new scalable parallel DBSCAN algorithm using the disjoint-set data structure. In: Supercomputing (SC2012). IEEE (2012)
8. Raad, M.: DBSCAN On Spark source code. GitHub repository (2016), `https://github.com/mraad/dbscan-spark`
9. Schubert, E., et al.: A framework for clustering uncertain data. PVLDB 8(12), 1976–1979 (2015)

Assessing Simulated Software Graphs using Conditional Random Fields

Marlon Welter, Daniel Honsel Verena Herbold, Andre Staedtler, Jens Grabowski, and Stephan Waack

Institue of Computer Science, Georg-August-Universität Göttingen
Goldschmidtstrasse 7, D-37077 Göttingen

Abstract. In the field of software evolution, simulating the software development process is an important tool to understand the reasons why some projects fail, yet others prosper. For each simulation however, there is a need to have an assessment of the simulation results. We use Conditional Random Fields, specifically a variant based on the Ising model from theoretical physics, to assess software graph quality. The determination of the required parameters of our model is done using a training that we call the parsimonious community homogeneity training.

Keywords: simulating software graphs, conditional random fields, parsimonious homogeneity training

1 Introduction

We propose a method to assess software graphs of simulated software projects that can also be used to assess the current state of a real software project and predict its likely progression in the future. The focus of our method is on providing a high level quality assessment on the one hand and the modelling of dependencies between software entities on the other hand.
We address the problem of evaluating quality of software systems as a node classification problem for undirected graphs using the model class of conditional random fields (CRFs), in particular a form derived from the Ising model as described in Section 2.
CRFs are commonly used in Bioinformatics to predict protein-protein-interaction sites ([1], [2]). To our best knowledge, we are the first who apply CRFs in the context of software system quality assurance. We use a heuristic described in Dong et al. [3] to approximate a classification of maximum posterior probability. In Section 3 we show some graphical output using our method.

2 Theory

The Software project is modelled as a graph, where each node represents a software entity (e.g. class or file). Two nodes are connected by an edge if they have been changed in a small changeset together at least twice (change coupling graph

as described in [5]). We assume that joint appearance in small changesets is a good indicator for dependencies between software entities.
Our classification method has two main goals: 1) Provide an easy to understand quality assessment on a high level and 2) model the influences between software entities regarding their quality assessment. The idea behind 1) is that e.g. a manager who wants to assess the state of a software project needs a comprehensible level of abstraction, which is not given by simple classification of software entities, since those can be in the thousands in bigger software projects. The reasoning for 2) is that a file can be acceptable in all metrics, but can yet be problematic because it depends on other files that are flawed or bugged.
All software graphs occurring in this paper have several highly connected parts which we denote as communities. In our model these communities represent logical parts of the software project (e.g. database connection or user management). Homogenization of the entity classifications in communities is our strategy to achieve a high level assessment of the quality of the software graph.
We use a model similar to the Ising Model from theoretical physics (see [4]). The Ising model is used in ferro magnetics. We chose it because this model has the potential to homogenise the classifications of connected regions in the graph, which helps us reach our goal 1).
Each node has a local quality label (acceptable/problematic) that is assigned to it by the simulation process. Once a certain threshold of bugs on an entity is reached, its local label is set to problematic (see [5]). Our method then uses these local quality labels and the information about the entity dependencies from the software graph to produce a new final classification for each entity.
The Ising model has the two parameters correlation and conformity that determine the final classification. Conformity determines the pressure to classify an entity in the final classification equal to its local quality label, whereas correlation determines the pressure that is exerted through edges to classify neighbouring entities with the same label. Determining these parameters, however, has a particular intrinsic difficulty, since there does not exist labelled training data for supervised learning.

Parsimonious Community Homogeneity (PCH) Training: We solved this issue by developing and implementing a training paradigm which we refer to as PCH training. This training determines the Ising parameters considering the following goals: a) community homogeneity: communities are broadly classified homogeneously and b) parsimonious homogeneity: the classifications of one community have little impact on the classifications of another community. The reasoning for a) is that this enables us to reach our training goal 1) mentioned earlier. Once we have broadly homogeneous classifications of communities, a comprehensible visualisation of the state of the software can be reached. The second goal is the counterpart to a), since we would end up in complete homogenisation of the graph if we only had a) as a goal. The parsimonious homogeneity reflects our intuition that we want to homogenise parts of the graph for clarity, but not homogenise the classification of the entire graph, as in that case we would lose too many information. We assume that problems in some part of the software (e.g.

in data visualisation) do only have a small impact on other parts of the software (e.g. database connection).
The target function of our training is defined as the sum of two values: average community homogeneity and average community independence. The average community homogeneity is the ratio of the prevalent classification (+1 (acceptable) or -1 (problematic) in a community, whereas the average independence of communities is defined as the ratio of unchanged classifications if we disconnect the communities (i.e. cut all inter-community-edges) and then classify each community separately.

3 Experiments and Results

Data Creation: In our training, we used a 10×10 -grid with values ranging from 0 to 1 in 0.1 steps, where the first dimension represents the conformity value and the second dimension represents the correlation value. For each of these parameter combinations we created 1000 random graphs, that approximate the structure of real software graphs regarding size, number of communities and connectivity degree. The analysis of the real software graphs is described in [5] and [6]. Details about the graph creation method will be described in the full paper. For each node, the local quality label (acceptable or problematic) was assigned using the following method: For each community, we draw a random number p between 0 and 1. For each node n in that community, we then draw another random number p_n between 0 and 1 and assign +1 (acceptable) as observation to n if $p_n < p$ and -1 (problematic) otherwise. This method ensures that we create a broad spectrum of communities regarding their local quality.
We then computed the average homogeneity and the average community independence as described in the theory section. In the last step, we chose the set of parameters that had the maximum sum of average homogeneity and average community independence as the output of our training.

The obtained parameters have been used to create classifications of software graphs. Examples can be found in Figure 1.

4 Discussion

With the parameters achieved in Section 3, our method provides on average a broadly homogeneous classification inside communities. This is a helpful tool in judging the overall quality state of the software, since e.g. a manager, who wants to assess the state of some software project, does not need to know about the quality of every individual file. Broadly homogeneous communities provide a solid basis for such an assessment, because trends become obvious on a larger scale.

Why was the development of a new training paradigm (PCH) necessary? It was not possible to use a standard approach from machine learning, since there was no reference data for software graph quality. This implies that we could not use standard evaluation methods for parameter sets of our model,

Fig. 1. Example of classifications of software graphs, where each node represents a software entity and each edge represents a dependency between two entities. The colour light green represents the label acceptable, the colour dark red represents the label problematic. The two graphs on the left side are coloured according to their local quality label. On the right side, the same two graphs are coloured according to their final classification using the PCH training and the inference heuristic described in Dong et al. [3].

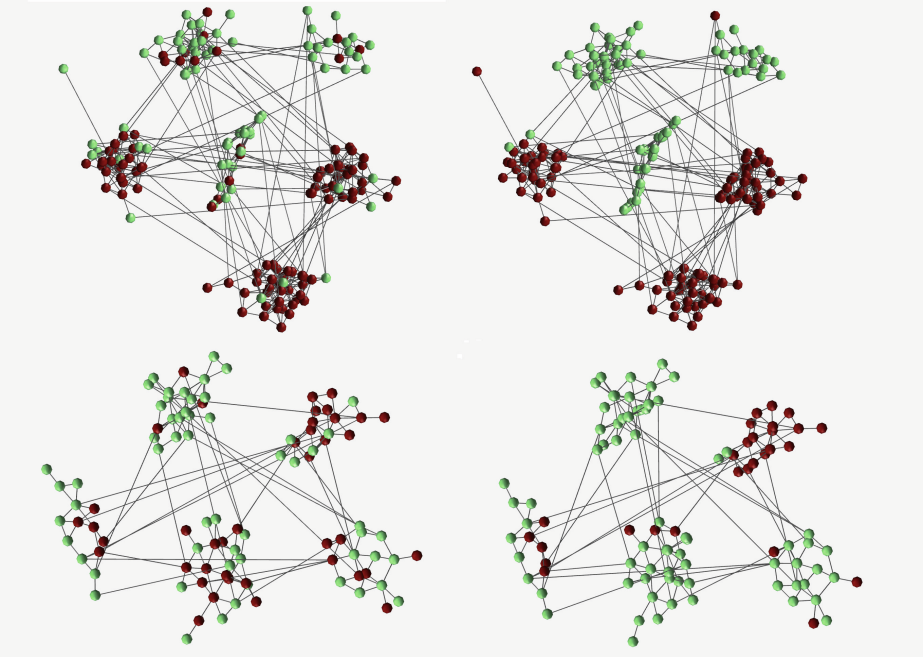

i.e. evaluation on the reference data. so we developed a new target function that would result in classifications that are easier to comprehend for human observers (community homogeneity), but not overly simplistic by homogenising the entire graph to acceptable or problematic (community independence). An advantage of this approach is in our opinion that the fine tuning (at what point will a community switch from a broadly acceptable to a broadly problematic state?) is determined by the definition of the local quality labels and therefore up to the user and her specific problem.

References

1. John Lafferty, Andrew McCallum, and Fernando Pereira. Conditional Random Fields: Probabilistic Models for Segmenting and Labeling Sequence Data. In: Proc. 18th International Conf. on Machine Learning. 2001, pp. 282289. url: citeseer.ist.psu.edu/lafferty01conditional.html.

2. Ming-Hui Li, Lei Lin, Xiao-Long Wang, and Tao Liu. Protein-protein interaction site prediction based on conditional random fields. In: Bioinformatics 23.5 (2007), pp. 597604.
3. Zhijie Dong, Keyu Wang, Truong Khanh Linh Dang, Mehmet G ultas, Marlon Welter, Torsten Wierschin, Mario Stanke, and Stephan Waack. CRF-based models of protein surfaces improve protein-protein interaction site predictions. In: BMC Bioinformatics 15 (2014), p. 277. doi: 10.1186/1471-2105-15-277. url: http://dx.doi.org/10.1186/1471-2105-15-277.
4. Ernst Ising. Beitrag zur Theorie des Ferromagnetismus. In: Z. Phys. 31.1 (1925), pp. 253258.
5. Daniel Honsel, Verena Honsel, Marlon Welter, Stephan Waack, and Jens Grabowski. 2016. Monitoring Software Quality by Means of Simulation Methods. In Proceedings of the 10th ACM/IEEE International Symposium on Empirical Software Engineering and Measurement (ESEM '16). ACM, New York, NY, USA, , Article 11 , 6 pages. DOI: https://doi.org/10.1145/2961111.2962617
6. Verena Honsel, Daniel Honsel, Steffen Herbold, Jens Grabowski, and Stephan Waack. Mining software dependency networks for agent-based simulation of software evolution. In ASE Workshop, 2015.

Parallel Radio Channel Emulation and Protocol Simulation for Wireless Sensor Networks with Hardware-in-the-Loop

Sebastian Boehm and Michael Kirsche

Computer Networks and Communication Systems Group
Brandenburg University of Technology Cottbus-Senftenberg, Germany
eMail: {sebastian.boehm, michael.kirsche}@b-tu.de

Abstract. This work-in-progress report introduces our Hardware-in-the-Loop (HIL)-based approach to combine an emulation of the radio channel of Wireless Sensor Networks (WSNs) with a discrete event-based protocol simulation. We aim to bridge the gap between abstract simulation environments and realistic sensor network testbeds.

1 Introduction

Practical applications of Wireless Sensor Networks (WSNs) require extensive testing on all layers: from application and protocol data flows to Radio Frequency (RF) channel effects and influences. Pre-deployment tests can be performed through either simulation, emulation or real-life testbeds. While a simulation of networked systems requires (abstract) models and representations of the systems under test, emulation uses components from the original systems and tries to emulate the usage scenario. Real-life testbeds, in turn, try to replicate the exact same application conditions. All three methods have their advantages and drawbacks (cp. [4] and [7] for further discussion). Simulation allows for a repetition of tests under non-deviating conditions (including the RF channel), while it lacks accuracy due to the abstractness of models. Real-life testbeds are cost-intensive and hard to scale, whereas emulation only covers system parts.

2 Methodology

We introduce a HIL architecture for WSN research and testing. To mitigate most of the flaws of the three listed methods, we use a combination of simulation, emulation and real hardware, working together on different layers of the complete system. Figure 1 depicts a sensor node's protocol stack and the three levels (numbered 1 to 3) of collaboration. Time-discrete event simulations (① in Fig. 1) of the higher layers of the protocol stack (e.g., application, transport and network layer) allow us to easily construct different architectures, device topologies, and application models with the help of simulation environments like OMNeT++[1] and accompanied frameworks like INET[2].

[1] OMNeT++ discrete event simulator: `https://omnetpp.org/`
[2] INET framework `https://inet.omnetpp.org/`

Using real hardware (② in Fig. 1) for an accurate representation of parts of the Medium Access Control (MAC) layer and the complete Physical (PHY) layer mitigates a major drawback of typical simulations. MAC and especially PHY simulation models are often abstracted in simulation frameworks that provide accurate models for higher layer protocols. WSN-specific simulation environments like Cooja [6] can provide more accurate representations of real WSN hardware due to real-life code execution, but their PHY and wireless propagation models are similar to those of generic simulators like OMNeT++. Even more problematic is the restriction of low-level simulators like Cooja to specific operating systems (i.e., Contiki [3] for Cooja).

While testbeds can also provide these advantages, they lack scalability and unvarying reproducibility of tests. We use RF channel emulation (③ in Fig. 1) to bypass these drawbacks. By emulating the wireless channel in a controlled environment, we can provide adjustable PHY conditions comparable to simulation environments, while refraining from using abstracted wireless propagation and PHY models. This combination of real WSN hardware with higher layer network simulations through a Hardware-in-the-Loop (HIL) approach leverages their strengths to enable an accurate representation of the lower layers combined with the protocol and model variety of OMNeT++ / INET.

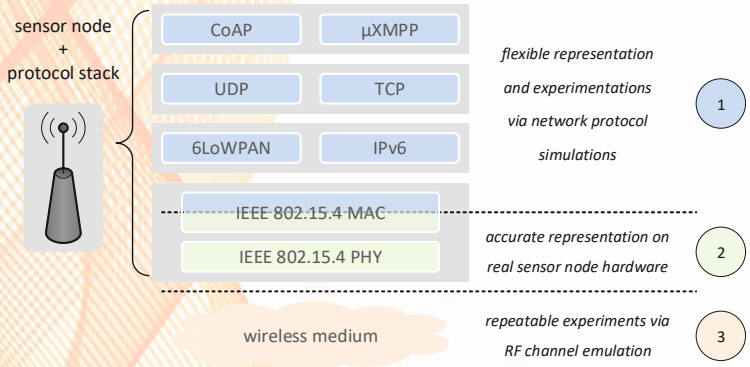

Fig. 1. Combined protocol simulation, real hardware, and RF channel emulation

3 Background and Current Work

In previous work [5], we introduced a new simulation model for IEEE 802.15.4 Wireless Personal Area Networks (WPANs), which was built to simulate the complex behavior of the 802.15.4 MAC layer in a detailed fashion via OMNeT++.

Furthermore, we work with RoSeNet[3] [2], a network emulation platform for wireless technologies, which focuses on hardware-based channel emulation via a controllable coaxial cable radio environment (③ in Fig. 1).

[3] RoSeNet project: `https://www.dresden-elektronik.de/funktechnik/knowhow/research-projects/rosenet/?L=1`

We focus on unifying real hardware transceivers with simulated MAC Protocol Data Units (MPDUs) from precise link layer simulation models, where the simulator acts as a HIL execution system and custom schedulers and interfaces are used to receive and transmit packets to and from the simulation model.

A transparent forwarder application between the simulator and the target emulation system interchanges data in the Packet Capture (PCAP) format. PCAP protocol data packets that arrive at the node's hardware level (e.g., sensor node platforms or transceivers) are decapsulated by custom emulation firmwares and transmitted through the RF interface (as depicted by ② in Fig. 1).

Our current prototype includes extensions for OMNeT++ / INET and the IEEE 802.15.4 MAC simulation model. An `IEEE802154ExtInterface` operates with a `IEEE802154Serializer` and a `PCAPScheduler` to convert between raw PCAP packet data bytes and OMNeT++ MAC packet objects. We extended Contiki [3] to enable the reception of PCAP protocol frames via a serial interface, to create the according MAC events, and to transmit real radio frames between sensor nodes on the introduced RoSeNet emulation platform.

4 Conclusion and Future Work

In addition to plain MPDU transmissions, we plan to support determination and exchange of radio transmission parameters (e.g., data rate, modulation, transmission power, transmission channel) by using optional extension headers from the PCAP(NG) file format and custom link layer types with so-called *Radiotap* headers [1], combined with IEEE 802.15.4 PHY data structures and service primitives which are already implemented within our simulation model. Currently, we port the simulation model to the latest OMNeT++ version and continue with the full integration of the prototype. Our approach will eventually introduce a new tool chain for performance evaluation and cross-layer optimization in WSNs.

References

1. Berg, J.: Radiotap: De facto Standard for 802.11 Frame Injection and Reception, `http://www.radiotap.org/`
2. Böhm, S., Kirsche, M.: Looking into Hardware-in-the-Loop Coupling of OMNeT++ and RoSeNet. In: Proc. of the 2nd OMNeT++ Community Summit (09 2015)
3. Dunkels, A., Gronvall, B., Voigt, T.: Contiki - A Lightweight and Flexible Operating System for Tiny Networked Sensors. In: Proc. of the 29th Annual IEEE Conference on Local Computer Networks (LCN). pp. 455–462. IEEE Computer Society (2004)
4. Imran, M., Said, A., Hasbullah, H.: A Survey of Simulators, Emulators and Testbeds for Wireless Sensor Networks. In: International Symposium in Information Technology (ITSim). IEEE (2010)
5. Kirsche, M., Schnurbusch, M.: A New IEEE 802.15.4 Simulation Model for OMNeT++ / INET. In: Proc. of the 1st OMNeT++ Community Summit (09 2014)
6. Osterlind, F., Dunkels, A., Eriksson, J., Finne, N., Voigt, T.: Cross-Level Sensor Network Simulation with COOJA. In: Proc. of the 31th IEEE Conference on Local Computer Networks (LCN). pp. 641–648. IEEE Computer Society (2006)
7. Wehrle, K., Güneş, M., Gross, J.: Modeling and Tools for Network Simulation. Springer, 1. edn. (2010)

Simulation-based Technician Field Service Management

Michael Voessing[1], Clemens Wolff[2] and Jannis Walk[3]

[1] Karlsruhe Service Research Institute (KSRI), Karlsruhe Institute of Technology (KIT), Kaiserstraße 89, 76133 Karlsruhe, Germany, michael.voessing@kit.edu
[2] Karlsruhe Service Research Institute (KSRI), Karlsruhe Institute of Technology (KIT), Kaiserstraße 89, 76133 Karlsruhe, Germany, clemens.wolff@kit.edu
[3] Karlsruhe Service Research Institute (KSRI), Karlsruhe Institute of Technology (KIT), Kaiserstraße 89, 76133 Karlsruhe, Germany, jannis.walk@kit.edu

Keywords: Field Service Management, Discrete-Event Simulation, Industry 4.0, Industrial Maintenance, Decision Support System

1 Motivation

Due to growing servitization in the industrial sector – the process of supplementing products with services – today machinery is sold alongside maintenance, repair and overhaul (MRO) contracts (Baines et al. 2009). In many industries, these services have become main competitive differentiators and important income sources for traditional manufacturers (Finke and Hertz 2011). To deliver MRO field services, many industrial machine manufactures have assembled extensive field service workforces that need to be managed efficiently. In addition, connected machinery – powered by the Industrial Internet of Things – allows dispatching decision making to be supplemented with real-time information and derived knowledge. So far, little research has been conducted on how Industry 4.0 and predictive maintenance techniques will affect downstream service processes. The following research examines how current industry best practices for dispatching decisions can be evaluated, and how emerging technologies will affect the field service delivery process.

2 Fundamentals and Research Objectives

The complex process of field service delivery can be divided into three steps: service preparation, service dispatching, and service delivery (see figure 1).

Given this simplified process, three main areas of interest have been identified for the research at hand: First, the efficiency of currently used dispatching strategies has to be evaluated individually. In addition, the influence of system changes (e.g. technical developments such as predictive maintenance) on the technician field service delivery process has to be analyzed. Lastly, the implications of offering new business models that include customer objectives on the service system (e.g. provider and customer) has to be evaluated. Those three research objectives will now be presented in detail:

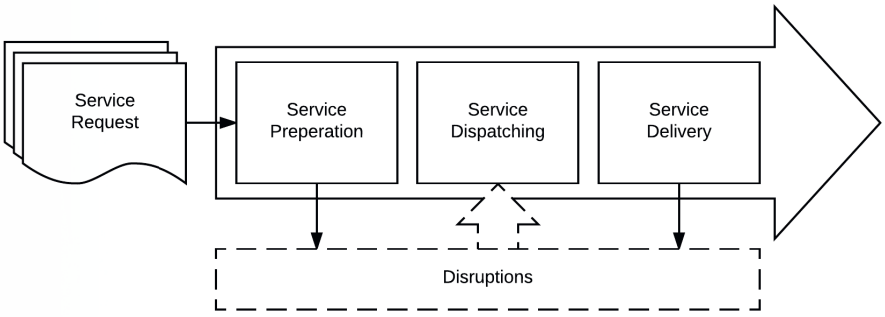

Fig. 1. Simplified Field Service Delivery Process

(a) *Strategies*: Interviews conducted with dispatchers have highlighted that the process of assigning service tickets to individual field technicians is usually performed manually by dispatchers with little technical support. Dispatching strategies often vary significantly between dispatchers. Some dispatchers plan weeks ahead and perform major rescheduling when needed, while others only assign essential jobs in advance in order to avoid rescheduling. These established strategies generally have developed over several years, but are rarely formally defined through company-wide policies. To support field service management new tools to evaluate the efficiency of individual dispatching strategies, identify optimal sets of strategies or deduct new strategies will be developed.

(b) *System Changes*: With current trends – like increasing computing power, the wide-spread adoption of sensors and smart devices in industrial machinery and emerging technologies (e.g. analytics and data mining) – a shift towards condition-based maintenance policies can be observed. In theory, maintenance policies built on these new technologies allow service providers to maintain high service levels (e.g. a low number of machine breakdowns) while reducing overhead (e.g. avoiding unnecessary maintenance calls). Unfortunately, these advantages are not realized since traditional dispatching strategies do not yet leverage predictive maintenance technology. The current field service delivery process is designed for short-term repairs and time-based maintenance schedules. To prepare the service process for these emerging technologies, the implications of predictive signals on the service process will be analyzed and evaluated.

(c) *Business Models*: Currently, MRO contracts favor cost optimization for service providers. Interviews conducted with service managers have suggested that business models that incentivize the reduction of overall costs (including service provider costs as well as downtime costs) promise benefits for both service providers and customers. The research at hand evaluates the feasibility and requirements of new collaborative business models which anticipate customer's individual willingness to pay and risk aversion. The impact of these business models on the system can be evaluated from different perspectives (e.g. the customers or service providers point of view). Based on the analysis, new business models will be developed.

3 Methodology

As the field service delivery process is deeply embedded in day-to-day MRO operations, it is difficult to evaluate how strategies, system changes, and business models affect the process without disrupting ongoing operations. Simulation modeling provides an risk-free environment to identify improvement potentials in complex systems – as it enables experiments not possible in the real world due to process and cost constraints. Discrete event simulation – a subset of simulation modeling – is well suited for the analysis, as the field service delivery process can be modeled as a discrete sequence of events. Each event depends on the sum of previous events (e.g. previous scheduling decision, disruptions, ...), but no changes are assumed to occur in-between events. Therefore, the simulation can directly proceed from one event to the next. Further no continuous observation of system parameters is required, as the aspects of interest (e.g. technician utilization, time of road, costs of service, ...) can be quantified after running the simulation.

The simulation model is based on the idea of matching service demand and service supply. Service demand is generated as service request – sampled from historic service incidents – based on stochastic distributed failure rates of the assets owned by customers. Service supply is represented through technicians and their individual availability. Further two concepts are introduced that differentiate the approach from previous simulation models (Dear and Sherif 2000; Hill 1992; Homer 1999; Rapaccini et al. 2008; Watson et al. 1998):

(a) *Complex Dispatching Function*: So far, academic research has largely focused on evaluating field service delivery from a strategical perspective. One of the main limitations has been the complex and computing-intensive tasks of modeling the multitude of individual dispatching decision during each simulation run. The proposed simulation model focuses on operational aspects. The manual dispatching process is modeled by combining rule-based approaches – based on best-practise of dispatchers obtained through interviews – with state-of-the-art, cost-based, heuristic optimization.

(b) *Disruptions*: Interviews conducted with industry partners have revealed that managing disruptions is one of the main challenges in field service delivery. As the simulation model at hand represents the process on an operational level, now disruptions (e.g. high priority tasks that lead to the rescheduling of lower priority tasks, traffic jams, customer that are not available at the agreed appointment, as well as appointments that are longer or shorter than anticipated) can be included in the analysis.

4 Outlook

The simulation model is currently being developed in close cooperation with an international manufacturer of industrial machines. The current service process of the company has been recorded, relevant entities of the simulation have been identified and relevant data source have been selected. First results will be available at the Simulation Science Workshop in May 2017.

Simulation-based Multi-Object Tracking using the Ensemble Kalman Filter

Fabian Sigges and Marcus Baum

Institute of Computer Science, University of Göttingen, Germany
{fabian.sigges, marcus.baum}@cs.uni-goettingen.de

Abstract. In this work, we develop a novel method based on the Ensemble Kalman Filter (EnKF) for multi-object tracking based on noisy unlabeled measurements. The method is evaluated in a scenario with three moving objects in close proximity and it is shown that the EnKF outperforms a Nearest-Neighbor Kalman Filter (NNKF).

Keywords: Ensemble Kalman Filter, Multi-Object Tracking

1 Introduction

The Ensemble Kalman Filter (EnKF) is a simulation-based technique for dynamic estimation that is tailored to high-dimensional state spaces. It was first published by Evensen [3] in 1994 in the context of oceanography and meteorology. The new approach was necessary due to the high dimension of the state space in these areas, which usually arises from the discretization of Partial Differential Equations (PDEs). For a state vector with a dimension in the order of millions, storage of the covariance matrix becomes infeasible. The key idea of the EnKF is to represent the first two moments of the posterior density of the state by means of an ensemble of states (i.e., simulations). Today, it is known that the EnKF converges to the Kalman Filter for growing ensemble sizes in case of linear, Gaussian systems [4]. Since the development of the EnKF mostly took place in the meteorology community, it is widely unnoticed in the signal processing and tracking areas. Only recently, multiple papers, e.g. [5], picked up the EnKF and applied it in tracking scenarios.

2 Ensemble Kalman Filter

We consider a linear process and measurement model with Gaussian noise

$$\boldsymbol{x}_{k+1} = A\boldsymbol{x}_k + \boldsymbol{w}_k, \qquad \boldsymbol{w}_k \sim \mathcal{N}_n(0, R), \tag{1}$$

$$\boldsymbol{z}_k = H\boldsymbol{x}_k + \boldsymbol{v}_k, \qquad \boldsymbol{v}_k \sim \mathcal{N}_m(0, Q), \tag{2}$$

where $\boldsymbol{x}_k$ denotes the n-dimensional state of the system and $\boldsymbol{z}_k$ is the m-dimensional measurement. The objective is to recursively estimate the state $\boldsymbol{x}_k$ by means of the observations z_k. For this purpose, the standard Kalman Filter

formulas provide the optimal solution by means of alternating prediction and update steps. Both steps involve the calculation of a $n \times n$ covariance matrix, which is not an option if n is of the order of millions or higher. The EnKF [2, 1] circumvents this problem by representing the state with a number N of ensemble members. The ensemble $\widehat{\boldsymbol{x}}_k^1, \ldots, \widehat{\boldsymbol{x}}_k^N$ is supposed to represent the posterior distribution of the state. The prediction, or forecast in geophysical terms, is similar to the Kalman Filter. The process model is simply applied to every ensemble member individually

$$\widetilde{\boldsymbol{x}}_{k+1}^i = A\widehat{\boldsymbol{x}}_k^i + \boldsymbol{w}_k^i, \quad i = 1, \ldots, N. \tag{3}$$

Assuming the ensemble represented the correct posterior, it can be shown that the new ensemble will be a draw from the correct prior distribution. Updating the forecast ensemble is almost similar to the Kalman Filter

$$\widehat{\boldsymbol{x}}_{k+1}^i = \widetilde{\boldsymbol{x}}_{k+1}^i + K_{k+1}(\widetilde{\boldsymbol{z}}_{k+1}^i - H\widetilde{\boldsymbol{x}}_{k+1}^i), \tag{4}$$

where K_{k+1} is the Kalman gain matrix. One difference is the use of perturbed measurements

$$\widetilde{\boldsymbol{z}}_{k+1}^i = \boldsymbol{z}_{k+1} + \boldsymbol{v}_{k+1}^i, \quad i = 1, \ldots, N. \tag{5}$$

The other difference concerns the computation of the Kalman gain matrix K_{k+1}. Instead of storing and updating the state covariance matrix, we simply use the unbiased sample covariance of the ensemble as an approximation to the true covariance matrix. The sample mean and the sample covariance now provide an estimate of the state.

3 Multi-Object Tracking

With the ever increasing interest in autonomous systems, the reliable tracking of targets becomes more and more important. One major issue that makes tracking of multiple objects a lot harder than tracking a single target is the problem of associating the measurements to the correct tracks. Especially when tracks of targets are close together or cross paths the association is usually unclear. In our first investigation to use the EnKF for tracking we decided to use a linear assignment algorithm, which minimizes the sum of the distances from predicted tracks to measurements. The full algorithm then looks as follows:

1. Create forecast ensemble from old state using the process model
2. Run linear assignment algorithm for each ensemble member
3. Update each ensemble member with the correct track - measurement association

The test scenario for the EnKF is displayed in Fig. 1 on the left hand side. All objects move with the same velocity from the left to right side, such that difficult situations, where multiple objects are in close proximity, arise. For reasons of clarity, the ensemble size is chosen to be only $N = 10$. In the right image of Fig.

1, we can see a comparison between the EnKF with $N = 50$ and the Nearest-Neighbor Kalman Filter (NNKF) averaged over 50 runs. The EnKF performs better throughout the whole scenario. This situation does not change for smaller ensembles such as $N = 10$ or larger ones like $N = 500$.

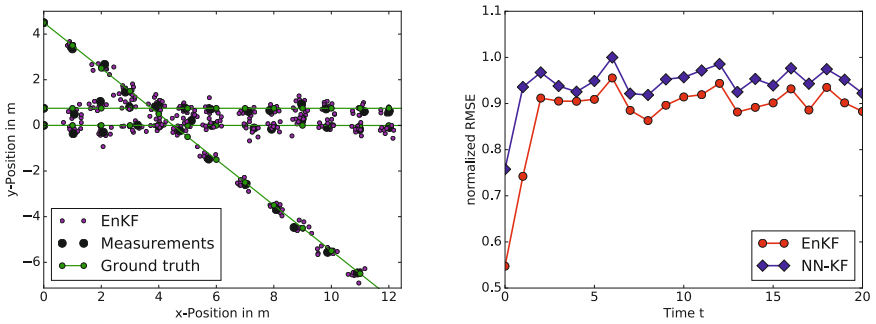

Fig. 1. Left: The chosen scenario with ensemble size $N = 10$. Objects move from left to right. Right: Normalized error of Nearest-Neighbor Kalman Filter and EnKF.

4 Conclusion

We proposed a possible way to apply the EnKF in a multi-object tracking scenario. Here, the EnKF was compared to the NNKF and it shows promising results, that encourage further investigation, especially in cluttered environments with more objects.

References

1. Anderson, J.L.: Ensemble Kalman filters for large geophysical applications. IEEE Control Systems Magazine 29(3), 66–82 (June 2009)
2. Burgers, G., van Leeuwen, P.J., Evensen, G.: Analysis scheme in the ensemble Kalman filter. Monthly Weather Review 126(6), 1719–1724 (June 1998)
3. Evensen, G.: Sequential data assimilation with a nonlinear quasi-geostrophic model using Monte Carlo methods to forecast error statistics. Journal of Geophysical Research 99, 10143–10162 (1994)
4. Mandel, J., Cobb, L., Beezley, J.D.: On the Convergence of the Ensemble Kalman Filter. Applications of Mathematics 56(6), 533–541 (Januar 2011)
5. Roth, M., Fritsche, C., Hendeby, G., Gustafsson, F.: The Ensemble Kalman Filter and its Relations to Other Nonlinear Filters. In: Proceedings of the 2015 European Signal Processing Conference (EUSIPCO 2015). pp. 1236–1240. European Signal Processing Conference, Institute of Electrical and Electronics Engineers (IEEE) (2015)

Using Monte Carlo Simulation for Reliability Assessment of Cloud Applications

Xiaowei Wang, Fabian Glaser, Steffen Herbold, and Jens Grabowski

Institute of Computer Science, University of Göttingen, Göttingen, Germany

1 Introduction

Monte Carlo Simulation (MCS) is often utilized to assess the reliability of complex systems due to its applicability regardless of the dimension of the system. The component-based structure of cloud applications makes it possible to simulate the application state by simulating the state of its components. However, regarding the reliability assessment of cloud services or applications, only few works consider MCS [1]. To compare the reliability of different structures for deploying an application, we can use MCS to derive the reliability of each structure with required accuracies within a relatively short time, especially for highly reliable applications who suffer failures with long intervals. There are mainly two challenges for applying MCS. On one hand, we need a model of cloud applications to determine the application state based on component states. On the other hand, we need to define appropriate input and stopping rules for MCS. To tackle the first challenge, we model a cloud application considering relatively comprehensive components and their dependencies. To address the second challenge, we design the input according to the failure distribution of components and the stopping rule according to flexible accuracy requirements.

2 Application Model

When deploying applications on clouds, consumers usually divide an application into services. For fault tolerance, a service is normally deployed with several Service Instances (SIs), which are hosted by Virtual Machines (VMs) that are hosted by Physical Servers (PSs). Services, SIs, VMs, and PSs are the main components to comprise the layered deployment stack of an application.

We model deployment stacks with Layered Dependency Graphs (LDGs) [2]. An LDG consists of four layers from top to bottom, a service layer, an SI layer, a VM layer, and a PS layer. An LDG is formally defined as a Directed Acyclic Graph (DAG) $G(V, E)$, where V is the set of components and E represents the set of dependencies between them. A component is defined as $v(t, m, k, n)$, where t is the type of the component, which can be one of *PS*, *VM*, *SI* and *service*, m is the name of the component, and k and n are for services which have n SIs and need at least k of them to succeed. A dependency is defined as an edge $e(p, s, d, w)$, where p and s are the *head* and *tail*, respectively, d is the type and w is the weight of the dependency. The type d can be a dependency between services or others.

3 Monte Carlo Simulation

To design an MCS, we must consider two main aspects: input and stopping rule.

Input. We assume that the failure rate λ of a non-service component, i.e., PSs, VMs, and SIs, is constant, therefore, the reliability r of a component can be calculated with the exponential reliability model:

$$r = e^{-\lambda t} \tag{1}$$

where t is time. If we consider a time unit, i.e., $t = 1$, the component reliability is $e^{-\lambda}$. When the failure rate is given, we can determine the component state after a time unit according to (1). We assume that the component state during a time unit is either *success*, denoted by 1, or *failure*, denoted by 0, and the probability of each state equals r and $1 - r$, respectively. Therefore, for each time unit, we can sample a float d from a uniform distribution $U[0, 1)$ and determine the component state ST with:

$$ST = \begin{cases} 0 \text{ if } d \leq 1 - e^{-\lambda} \\ 1 \text{ if } d > 1 - e^{-\lambda} \end{cases} \tag{2}$$

Stopping Rule. Taking a time unit as a round, for an n-round MCS, the simulated reliability $\overline{R_{\text{sim}}}$ of the application equals the mean ($\bar{\mu}_n$) of all rounds' simulated reliability:

$$\overline{R_{\text{sim}}} = \bar{\mu}_{\text{n}} = \frac{1}{n} \sum_{i=1}^{n} R_{\text{sim}_i} \tag{3}$$

where R_{sim_i} is the application state of the ith round and can only be 0 or 1.

The number of rounds is determined by the stopping rule of the MCS. In this paper, we define two conditions for stopping an MCS: confidence interval and number of significant figures after the decimal point. As discussed by Owen [4], the confidence interval of $\overline{R_{\text{sim}}}$ for a significance level α is of the form:

$$|R_{\text{rea}} - \overline{R_{\text{sim}}}| \leq \Phi^{-1}(1 - \alpha/2)s/\sqrt{n} \tag{4}$$

where $s = \sqrt{\frac{1}{n-1} \sum_{i=1}^{n} (R_{\text{sim}_i} - \overline{R_{\text{sim}}})^2}$ is the Standard Deviation (SD) of the simulation results, R_{rea} is the real reliability of the application, and Φ^{-1} is the inverse function of the Cumulative Distribution Function (CDF) of the standard normal distribution.

Regarding the number of significant figures, a $\overline{R_{\text{sim}}}$ with b significant figures after the decimal point should meet [3]:

$$|R_{\text{rea}} - \overline{R_{\text{sim}}}| < 5 \times 10^{-(b+1)} \tag{5}$$

Combining (4) and (5), the MCS will stop when the $\overline{R_{\text{sim}}}$ meet:

$$\Phi^{-1}(1 - \alpha/2)s/\sqrt{n} < 5 \times 10^{-(b+1)} \tag{6}$$

where α and b can be adjusted according to specific accuracy requirements.

Based on the input and stopping rule, we propose an MCS algorithm, as shown in Algorithm 1.1, for simulating the application reliability within a time unit. The simulation of the application state involves two steps. First, the states of non-service components are determined according to their reliability and dependencies, e.g., when a PS fails, all VMs on this PS also fail. Secondly, service states are determined according to the number of successful SIs and the application state is determined according to the service states.

Algorithm 1.1: MCS algorithm

Input: LDG *ldg*, λs of non-service components, α and b for stopping rule
Output: reliability of the application deployed with *ldg*

do
  foreach *non-service component in ldg* **do**
    sample a float d from $U[0, 1)$
    determine the component state according to (2) and *ldg*
  end
  determine the states of services and the application according to *ldg*
  calculate $\overline{R_{\text{sim}}}$ with (3)
  calculate s
  $round \leftarrow round + 1$
while (6) *does not hold*
return $\overline{R_{\text{sim}}}$

4 Conclusion

We presented an MCS algorithm for assessing the reliability of cloud applications. We model cloud applications with LDGs based on the components in the deployment stack and dependencies. Based on the LDG model, we design an MCS algorithm including the input and stopping rule. With the algorithm, we can get the application reliability for different deployment structures with certain accuracies for comparison.

References

[1] Snyder B., Ringenberg J., Green R., Devabhaktuni V., Alam M.: Evaluation and design of highly reliable and highly utilized cloud computing systems. Journal of Cloud Computing. 28;4(1):11 (2015)
[2] Wang, X., Grabowski, J.: A reliability assessment framework for cloud applications. CLOUD COMPUTING 2015, pp. 127–130 (2015)
[3] Higham, N.: Accuracy and stability of numerical algorithms. Society for industrial and applied mathematics (2002)
[4] Owen, A.: Monte Carlo theory, methods and examples. (2013)

High-Performance Computing and Simulation in Clouds

Pavle Ivanovic and Harald Richter

Clausthal University of Technology

Abstract. High-Performance-Computing (HPC) and simulation is traditionally performed on a supercomputer or on a parallel computer. The main reason for the employment of such powerful machines lies in the significant reduction of processing time for simulations of complex models and systems. Additionally, very short-running simulations can also be executed on a multi-core PC in the own office within minutes or hours. However, the prevalent computing paradigm, which is nowadays cloud computing, is not used for both, neither HPC nor simulation, because it is the common experience of the respective user community that clouds are not efficient for codes which are based on the Message Passing Interface (MPI). This is the case, although MPI is the standard library for HPC, together with OpenMP. OpenMP, however, is normally not applicable for clouds, because Cloud service providers do not allow a shared memory between separate virtual machines (VMs) on the same server, as this could create cyber security problems between tenants. Furthermore, since shared-memory does not exist between servers either, the usage of OpenMP is very limited and thus excluded in most cloud installations. On the other hand, MPI libraries have adaptive algorithms for the automatic recognition and selection of the shortest communication paths, which makes MPI a good candidate for both, intra and inter server communication. In addition it is a fact that cloud resources can be obtained in the Teraflops and Terabytes range for a few dozen Euros only, for example from auctions in the Amazon Web Service (AWS), which makes cloud computing, in principle at least, very appealing for HPC. With such cost and performance offers, scientists could use their computational models and simulation tools more often and visit their laboratories for tedious lab work less frequently than today. Finally, the performance problems, which MPI-based codes in clouds have, result from the underlying TCP/IP communication, and in case of private clouds also from an insufficient integration of Infiniband into the cloud. Even with the employment of the latest hardware accelerators, such as SR-IOV and VT-d, the integration of an Infiniband network in a cloud has many hurdles. For instance, the most common open-source cloud-operating system, which is OpenStack, does not support Infiniband at all, thus making it very difficult to use it. On top of that, OpenStack shows high inefficiency with respect to inter-VM communication, which is as a consequence of the huge software overhead necessary for a network based on virtual devices and VM isolation. In standard clouds, regardless whether private or public, all traffic between VMs on different servers has to be routed through the TCP/IP protocol via Ethernet, which allows smaller bandwidth and higher latency only, compared to Infiniband. Furthermore, the VMs on the same server and even the virtual cores (vCPUs) inside of the same VM are using TCP/IP for their inter-VM and inter-vCPU communication, which is not needed at all and very ineffi-

cient as well. This is the consequence of the Linux KVM/QEMU hypervisor, which only knows virtual Ethernet devices (vNICs) but not virtual Infiniband. Because of KVM/QEMU, any other communication means beside Ethernet requires third-party devices and own driver development, in addition to significant kernel modifications, which is all bad. On the other hand, it is well-known from supercomputing and parallel computing that HPC efficiency is determined by the bandwidth and latency that can be achieved by the communicating parts of a parallel code. Therefore, one of the main objectives in cloud-based HPC is the mitigation of overhead for data exchange between logical processing elements (or vCPUs), and between VMs that contain these vCPUs.

In this paper, it is shown how standard private clouds can be augmented to be HPC-efficient. We achieve this without modifying the Linux kernel or the cloud's hypervisor or cloud OS, which was KVM/QEMU and OpenStack, respectively, in our cloud. Furthermore, OpenStack was fully excluded by us from HPC communication, which is an advantage when it comes to efficiency. For that purpose, we used a virtual PCI device called "ivshmem", which establishes a real shared memory between the vCPUs of a VM, and as an option also between VMs on the same server. This ivshmem device is provided by the widespread libvirt library and emulated by KVM/QEMU. Ivshmem enables a VM to access in the host a region of POSIX shared memory called SHM, which acts in turn as a guest/host bridge, thus making the vSwitch component of OpenStack obsolete for MPI communications. Additionally, POSIX SHM is newer, better and has a simpler application programming interface (API) than the old SystemV shared memory. Additionally, for SHM, a POSIX semaphore is available for the mutual exclusion of memory-accessing processes, in order to synchronize them. The guest/host bridge is accomplished via the SHM shared-memory object by mapping I/O address space from the Guest OS into the Host OS. This enables a zero-copy VM-to-Host communication, which is very efficient with respect to bandwidth and latency, because no internal data buffer exists. Furthermore, ivshmem is compatible to remote direct-memory access (RDMA), which is the fastest way to communicate via Infiniband, and it is even compatible with OpenStack and its way to create VMs. Consequently, our main focus in the integration and application of ivshmem for HPC was to modify an existing user-level application library in the Guest OS only. This approach enables efficient inter-process communication (IPC) between user applications in the guest OS, because a device driver is used as shared-memory, and it avoids modifications of the Guest OS as well and removes overhead. The new approach is implemented by the creation of a new MPI communication channel, which directly connects user-level libraries via ivshmem. Thus it enables the usage of shared-memory in the VM's Guest OS for IPC. Because of that, we can eliminate inefficient TCP/IP socket IPC for both, intra and inter-VM communication on a single server. We will show in the paper that significant improvements in bandwidth and latency can be thus achieved. Finally, with additional code from us, it is even possible to efficiently emulate a shared memory between VMs that are residing on different servers. This is accomplished by inserting a code layer from us between communicating MPI libraries on different machines. As a consequence, we could efficiently integrate Infiniband into our private cloud, which was not possible so far.

The Virtual Microscope - Simulation and Visualization of Particle Mixtures on Parallel Hardware

Feng Gu[⋆], Zhixing Yang[⋆⋆], Thorsten Grosch[⋆⋆⋆], and Michael Kolonko[†]

Institute of Computer Science, Technical University of Clausthal and Institute of Applied Stochastics and Operations Research, Technical University of Clausthal

1 Introduction

Dry particle mixtures are the basis of many materials like traditional concrete, casting moulds in foundries, pills and tablets in the pharmaceutical industry or powders for 3D printing. Properties of the particles like shape and size distributions are often crucial for properties of the final material. Therefore material scientists are highly interested in means to simulate random close particle packings on a computer and to inspect the result before costly laboratory experiments are started.

In the first step, we restrict particle shapes to spheres. Then, a mixture is completely characterized by its *particle size distribution* (PSD) $p(r)$, giving the relative frequency of particles of radius r within the mixture. We want to determine properties of a random close packing of p and we want to study and optimize its properties as e.g. its *space filling* $\Phi(p)$. At the same time we want to enable the visual study of the simulated packing as it would be possible under a microscope. Our virtual microscope will allow us to check e.g. the distribution and size of the empty spaces or a possible disintegration of the mixture under pressure.

Even with spherical particles, the simulation of 50 000 particles takes about 20 minute on traditional sequential hardware and about 30 hours for 1 million spheres. Therefore, the crucial part of this project is the use of parallel hardware (GPGPU) which allows a tremendous speed-up in the simulation and a direct integration of simulation and visualization.

2 Simulation

In order to obtain a packing as dense as a real dry mixture, the *initial placement* locates the spheres of the sample at random positions in a container that is so

⋆ feng.gu@tu-clausthal.de
⋆⋆ Zhixing.Yang@tu-clausthal.de
⋆⋆⋆ Thorsten.Grosch@tu-clausthal.de
† kolonko@math.tu-clausthal.de

small that spheres must overlap. In the second phase, the so-called *collective rearrangement* (CR), a repulsion force between overlapping spheres is applied that distributes the overlap evenly over the sample. Then the container is slightly enlarged and CR takes place again. This is repeated several times until all overlaps have vanished and the spheres form a dense packing.

In the existing sequential version, sophisticated data structures, in particular for the detection of overlapping spheres, have to be used (see [1], [2]) resulting in an overall complexity of $O(n \log n)$ in the number of spheres.

Using a GPGPU for this task requires new data structures and a revised collective rearrangement to allow the parallel processing of a large number of spheres. All single processes should have a similar workload and should work on contiguous parts of the memory. Though the single process may not be as efficient as in the sequential case, the overall acceleration is enormous due to the high parallelism. First results indicate that we are now able to simulate the packing of 1 million spheres in a few minutes, an acceleration by a factor larger than 200. Empirically, the time complexity of this approach seems to be almost linear.

This speed-up will also allow to include non-spherical particles, each of which is formed by a group of (overlapping) spheres that are treated as a fixed ensemble during CR.

3 Visualization

As the simulation runs on the GPGPU, the visualization may use the same memory locations without the need of intermediate storage or copying of the results. This allows to picture the initial placement of the particles as well as the steps of the CR process almost without delaying the simulation. Besides, we can also track a single particle and its interaction with other particles during the CR process. In this way, we are able to detect flaws of the simulation algorithm or to study the impact certain parameters have on the process.

As the number of spheres shown on the screen increases, it becomes more important to visually mark certain situations, e.g. the overlap of two spheres or the empty space between the spheres, by so-called voxels (see, e.g. [3]). Here, it is necessary to develop new hierarchical systems of voxelization in order to obtain a fine-grained, meaningful picture. Based on these pictures, a material expert will then be able to decide whether this mixture is worth checking in the laboratory or not.

As the interplay between simulation and visualization is so close and fast, we plan to introduce additional interaction into the simulation process, a kind of 'virtual stirring'. The effect of the stirring could be seen in the visualization in real time, which will allow to better understand the process of rearrangement.

4 Acknowledgements

Zhixing Yang is supported by Dyckerhoff Stiftung, grant number T218/26441 /2015. Feng Gu receives a scholarship of the Simulation Science Center Clausthal-Göttingen within the project 'Virtual Microscope'.

References

1. M. Kolonko, S. Raschdorf, D. Wäsch, A hierarchical approach to simulate the packing density of particle mixtures on a computer, Granular Matter 12 (6) (2010) 629–643.
2. S. Raschdorf, M. Kolonko, A comparison of data structures for the simulation of polydisperse particle packings, International journal for numerical methods in engineering 85 (5) (2011) 625–639.
3. S. Thiedemann, N. Henrich, T. Grosch and S. Mueller, Voxel-based Global Illumination. ACM Symposium on Interactive 3D Graphics and Games (i3D) 2011.

Two-layered Cyber-Physical System Simulation

Tobias Koch[1], Dietmar P. F. Möller[2], and Andreas Deutschmann[1]

[1] German Aerospace Center, Lilienthalplatz 7, 38108 Braunschweig
[2] TU Clausthal, Institute of Applied Stochastics and Operations Research, Erzstraße 1, 38678 Clausthal-Zellerfeld, Germany

Abstract. With the increasing exposure of critical infrastructures to external factors, critical infrastructure protection gained attention within security research. To develop protection methods the effect of external factors on critical infrastructures has to be known. In this paper we present an event-based, dynamic modeling approach using power flow analysis and network flow analysis to simulate the effect on the critical infrastructure with object-based programming. The highly interconnected cyber-physical system is defined as a two-layered system with separated cyber and physical properties. Network stability and cyber infection status is checked with two control feedback loops to maintain grid stability and to observe infection status. Therefore with given object load powers and network interconnections the working capability of infrastructure parts can be predicted for various scenarios.

1 Introduction

Due to an increasing number of cyber-attacks and damage related to them [1], cyber-security gained a lot of attention not only in the media, but also from governmental side. The main interest from governmental side is critical infrastructure protection (CIP) [2,3]. Nowadays critical infrastructures (CIs) have to be considered as cyber-physical-systems (CPS) i. e. their operability depends on information and communication technology (ICT) and physical properties such as power supplies. Control systems build the interface between the physical and cyber level and are therefore an excellent point to attack a CPS. Cyber attacks on these control systems occurred in many different types of CIs e.g. water services [4], nuclear power plants [5], or electricity distribution stations [6]. Incidents are not always caused by human attacks. Especially the CI power supply is vulnerable to environmental hazard (falling trees, geomagnetic storms etc.) or even human failures [7]. To improve the resilience and preparedness of CIs we have to understand the impact of external factors on the system. Modeling and simulation approaches are powerful tools to gain knowledge about complex systems and help to identify vulnerable points within the system. This is one of the most important parts within risk management and a necessary step to develop emergency plans in case of successful cyber attacks. Therefore, a time dependent operability check for network components is needed from the physical as well as the ICT side.

2 Cyber-Physical System Simulation

We use a two-level network system for our description of the cyber-physical system. The first one describes physical and the second one ICT properties. In addition lists with all directly connected objects are assigned to each single object for both levels. Due to power line communication physically connected objects are also considered to be connected on ICT level. To check operability at each timesteps we use two control feedback loops. The first one checks wether voltage and frequency are within a tolerance interval that enables operability and the second one is the status of software infection of the object. The input for this feedback loops is calculated via a dynamical load flow analysis and network infection flow.

2.1 Load Flow Dynamics

The principle of static load flow analysis is a commonly used method to determine the voltages and phases within power distribution systems at given load powers [8] via solving a system of non-linear equations with iterative methods. As load power conditions at object i vary over time we introduce time dependent apparent power $S_i(t_j)$ as a dynamic boundary condition. Repeating the load flow analysis at several time steps leads to a time-series for voltage magnitude $U_i(t_j)$ and phase $\phi_i(t_i)$. The frequency can be obtained by the change of phase with time (1). The timestep Δt to resolve f_{max} is limited by the Nyquist-Shannon sampling theorem via $\Delta t_{max} = \frac{1}{2f\,\max}$.

$$f(t) = \frac{1}{2\pi}\frac{d\phi}{dt} \approx \frac{1}{2\pi}\frac{\Delta\phi}{\Delta t} = \frac{1}{2\pi}\frac{\phi_{n+1} - \phi_n}{t_{n+1} - t_n} \tag{1}$$

Under the constraints that the voltage magnitudes $U_i(t_j)$ and frequency $f_i(t_j)$ determined for object i at time t_j is within an a priori defined tolerance interval and that the source is able to deliver the demanded power, the operability of object i on physical side is guaranteed. If the grid is not stable, load shedding schemes are used to balance demanded and supplied power.. In addition blackouts can be simulated by directly setting object working status to false.

2.2 Network Infection Flow

We represent the ICT network level as an undirected, weighted graph. This weights are introduced to combine all factors affecting propagation time like the operating system, computer architecture, data transfer rate, type of connection, used protocols and encryptions or security precautions into one macroscopic measure (in seconds) being a weighting parameter w_{ij} for the edge between objects i and j. If objects i and j are not connected w_{ij} is set to infinity. From there on Dijkstra algorithm is applied to determine the shortest path from the intrusion point of the network, which is defined within the cyber attack event. This pathlength sets the time $t_{i,inf}$ for an infection of object i. The second control

loop checks whether the for the object indispensable applications are affected or not. This is done via a simple comparison of listed properties of the object and the defined event. If the software is afflicted, the objects functionability is set to false.

3 Conclusions

A new simulation approach for CPS was presented that is based on a two-layered network approach, dividing physical from software properties. The static load flow analysis, know from electrical engineering, was enhanced to a time-dependent network stability control method driven by dynamic boundary conditions. Occuring events may trigger (partial-)blackouts or the intrusion of malicious software. The propagation time of the infection within the network is calculated via solving the shortest graph problem in an undirected graph with weighted edges.

Though, this approach needs a lot of information about the network structure, the consideration of expert knowledge is possible. Moreover, even in more modern CIs the data needed for data-driven machine learning approaches [9] is not available. As the simulation approach can be adapted to other CIs, the application within the field of CIP might be very diverse. However, a lot of work has to be done, while connecting the operability of single objects or object groups with CI specific processes.

References

1. "Managing cyber risks in an interconnected world - Key findings from The Global State of Information Security Survey 2015," PricewaterhouseCoopers International, Tech. Rep., 2014.
2. "Critical Infrastructure Protection - Challenges and Efforts to Secure Control Systems," U.S. Government Accountability Office, Tech. Rep., 2004.
3. "On a new approach to the European Programme for Critical Infrastructure Protection Making European Critical Infrastructures more secure," 2013.
4. M. Abrams and J. Weiss, "Malicious Control System Cyber Security Attack Case Study - Maroochy Water Services, Australia," The MITRE Corporation Applied Control Solutions, Tech. Rep., 2008.
5. B. Kesler, "The Vulnerability of Nuclear Facilities to Cyber Attack," Strategic Insights, Tech. Rep., 2011.
6. "Analysis of the Cyber Attack on the Ukrainian Power Grid," Electricity Information Sharing and Analysis Center, Tech. Rep., 2016.
7. "Report by the Federal Network Agency for Electricity, Gas, Telecommunications, Post and Railways on the disturbance in the German and European power system on the 4th of November 2006," Bundesnetzagentur, Tech. Rep., 2007.
8. J. J. Grainger and W. D. Stevenson Jr., *Power System Analysis*, 1st ed., ser. Electrical and Computer Engineering. McGraw-Hill Education, 1994.
9. O. Niggemann, G. Biswas, K. J. S., H. Khorasgani, S. Volgmann, and A. Bunte, "Data-Driven Monitoring of Cyber-Physical Systems Leveraging on Big Data and the Internet-of-Things for Diagnosis and Control," in *International Workshop on Principles of Diagnosis*, 2016.

A simulation-based genetic algorithm approach for competitive analysis of online scheduling problems

Martin Dahmen
Institute of Applied Stochastics and Operations Research, TU Clausthal
Erzstr. 1, 38678 Clausthal-Zellerfeld, Germany
{martin.dahmen@tu-clausthal.de}

Scheduling is one of the most investigated research areas in operations research and mathematical optimization, as it is a critical issue in planning and managing of manufacturing processes in almost all modern industries. A common scheduling problem is given by a set of jobs that must be assigned to a set of machines and different timeslots, under the restriction of various constraints. In the case of practical scheduling problems this often leads to a highly dimensional and complex combinatorial optimization problem, which is too large to be solved efficiently by traditional methods of linear and integer programming. In our case, we add an additional online characteristic to our scheduling problems. This means that jobs will appear subsequently and as soon as a job appears an online algorithm has to decide which machine it will be assigned to, without knowledge of what the rest of the sequence looks like. The objective of online optimization is to find an online strategy, or in most cases an algorithm that best solves the online problem in the worst-case scenario. This makes online optimization a two-player game, consisting of an online player and the offline adversary, who sets up the sequence for the online player and returns the optimal solution himself. The ratio between the computed online solution and the optimal solution is called competitiveness and is to be minimized ([1],[2]).

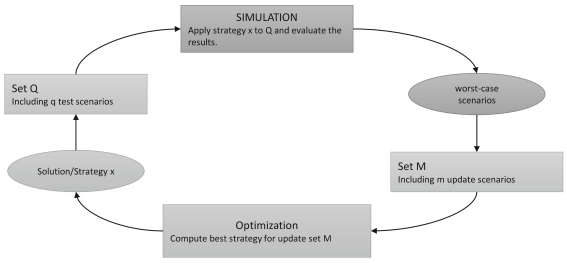

Figure 1: The concept of the simulation-based optimization approach. Simulation and optimization alternate within one iteration of the cycle.

The challenge of worst-case and competitive analysis is to deal with a large number of possible strategies and scenarios that have to be examined. Often the worst-case scenarios depend on the strategies and change with the choice of a different algorithm. As part of this project, we present an approach that combines theoretical principles of mathematical optimization with practice-oriented analytic methods of simulation to solve worst-case problems in terms of online optimization. The alternating interaction of an optimization and a simulation step is the fundamental concept of the simulation-based optimization approach so that output data of the optimization forms the input for the simulation and vice versa (Figure 1). The goal of the study is to show that even in the case of complex optimization problems a small fraction of the scenarios is sufficient to evaluate algorithms and strategies since in many cases, the scenarios with the greatest impact on the objective value have a very particular structure. With respect to online optimization, the optimization process con-

sists of the choice of an online strategy by the online player. In the simulation process, the offline adversary chooses his sequence that best counters the online strategy. In an ideal case, the alternating optimization and evaluation of an online strategy and its worst-case sequence converge in the iteration process. Some references for solving the minimax problem we encounter during the optimization step with a genetic algorithm approach can be found in [4]. But there are still no efficient approaches to find worst-case sequences of online optimization problems by algorithmic means. For this reason, we use methods of genetic algorithms to create a population of test sequences as part of the simulation-based optimization process.

A worst-case sequence, in general, has a very specific structure according to the given problem. In online scheduling on m identical machines, for example, it can be shown that the worst-case sequence of the graham's greedy heuristic consists of exactly $m \cdot (m-1)$ short jobs of length 1 and one long job of length m ([5]). Like in most scheduling problems, a good online strategy cannot handle the large job at the end of the sequence well, as it must balance out the previous jobs among all machines to be competitive.

This observation motivates the idea that testing an online strategy in the simulation step of our simulation-based optimization approach should not be based on totally randomized test sequences, but rather on a good genetic approach for creating the population of our scenarios. The application of genetic algorithms to solve complex optimization problems has been a common approach in research for a long time and they have become a sophisticated method to solve significant problems in the fields of operations research ([3]) and scheduling ([6],[7]). A genetic approach is an efficient search heuristic that operates on a population of solutions to find an optimal solution or an approximate value sufficiently close to the optimum.

Chromosomes of our population are represented by online sequences of varying length and consist of single requests called genes. In each iteration of our simulation-based optimization approach, some evolutionary process takes place with effect on our population. Selection, mutation and crossover operations are applied to find new sequences to solve the maximization problem for the competitiveness of a given online strategy. New sequences are created by manipulation and combination of the specific structures of previous found worst-case sequences. A listed table of genetic operators applied to the sequences is given in Figure 2. In the simulation process, we evaluate the fitness of our online algorithm, depending on the population Q. Since these operators are independent of the optimization problem, they can be applied to almost any kind of online optimization problem including most scheduling problems.

Genetic Operators

Random	Create a set of (uniformly distributed) random sequences
Crossover	Create a new sequence as a combination of several previous sequences *e.g.* $\sigma_1 = [B, A, D, F, A, B, D, E, D]$, $\sigma_2 = [A, F, E, D, E, F, F, B, A]$ $\rightarrow$ $\sigma = [A, A, E, F, A, B, F, B, A]$
Mutation	Exchange some genes of a sequence with random elements *e.g.* $\sigma_1 = [B, D, F, D, A, A, E, C, C]$ $\rightarrow$ $\sigma = [B, D, C, D, A, A, B, C, C]$.
Double	Create a new sequence by duplication *e.g.* $\sigma_1 = [A, F, D, E, C]$ $\rightarrow$ $\sigma = [A, F, D, E, C, A, F, D, E, C]$
Cut	Reuse certain subsequences *e.g.* $\sigma_1 = [D, C, B, A, E, E, A, B]$ $\rightarrow$ $\sigma = [D, C, B, A, C, B, F, A]$
Invert	Create the inverse of a sequence *e.g.* $\sigma_1 = [A, A, B, A, B, B, A, A, B]$ $\rightarrow$ $\sigma = [B, B, A, B, A, A, B, B, A]$
Boundary	Create extreme sequences *e.g.* $\sigma_1 = [A]$, $\sigma_2 = [C, C, C, C, C, C, C, C]$

Figure 2: A selection of genetic operators to define a new population Q.

So far we implemented the genetic operators within a generic framework that allows us to manage the creation and manipulation of test scenarios. The evaluation of the sequences by an online strategy depends on the given problem or mostly on the objective function and has to be implemented independently. We used a weighting system to manage the selection and prioritization of the set of genetic operators based on the underlying optimization problem. Each weight is given as a parameter which can be adjusted either manually by the optimizer or automatically by the framework, based on different learning approaches. All the implemented methods within our framework operate in polynomial time.

Experimental results show that genetic operators are an efficient and effective approach to improve any convergence behavior of the simulation-based optimization approach for minor problems and those that have been solved by theoretical worst-case analysis so far. In almost all cases the framework converged to the best known online strategy as expected. In each iteration, we experienced a significant improvement of the online strategy compared to a set of totally randomized test sequences.
As a next step of our research, we are planning to expand the simulation-based optimization approach and the genetic framework to more complex scheduling tasks and real data scenarios derived from practical problems. The aim is to find new theoretical results for the worst-case analysis of open scheduling problems and to tighten bounds for the competitiveness of online algorithms by tuning parameters.

References

[1] A. Borodin and R. El-Yaniv. Online Computation and Competitive Analysis . Cambridge University Press, 1998.

[2] D. D. Sleator and R. E. Tarjan, Amortized efficiency of list update and paging rules, Communications of the ACM 28 (1985), no. 2, 202-208

[3] Goldberg, D.E. Genetic Algorithms in Search, Optimization, and Machine Learning. Addison-Wesley, Reading, Massachusetts, 1989.

[4] W. Jeffrey, Herrmann. A Genetic Algorithm for Minimax Optimization Problem. Evolutionary Computation, 1999. CEC 99. Proceedings of the 1999 Congress onVol.2, 1999.

[5] Pinedo, Michael. Scheduling: theory, algorithms and systems. Englewood Cliffs, N.J.: Prentice Hall, 1995

[6] F. Oliveira, S. Hamacher, M. R. Almeida. Process industry scheduling optimization using genetic algorithm and mathematical programming. Journal of Intelligent Manufacturing In Journal of Intelligent Manufacturing, Vol. 22, No. 5, 2011

[7] A. Sadegheih. Scheduling problem using genetic algorithm, simulated annealing and the effects of parameter values on GA performance. Appl Math Model, 2006

[8] Irene Fink, Sven O. Krumke, Stephan Westphal. New lower bounds for online k-server routing problems, Information Processing Letters, v.109 n.11, p.563-567. May, 2009

Simulating Software Refactorings based on Graph Transformations

Daniel Honsel[1], Niklas Fiekas[2], Verena Herbold[1], Marlon Welter[1], Tobias Ahlbrecht[2], Stephan Waack[1], Jürgen Dix[2], and Jens Grabowski[1]

[1] Institue of Computer Science, Georg-August-Universität Göttingen
Goldschmidtstrasse 7, D-37077 Göttingen
[2] Department of Informatics, Clausthal University of Technology
Julius-Albert-Str. 4, D-38678 Clausthal

Abstract. We deal with the *simulation* of software processes in order to assure higher *software quality*. In this paper, we consider the specific problem of how to define a *suitable* structure of software graphs. Based on the traditional idea of describing software with syntax trees, we put forward the idea of using a simulation model for *refactorings*, where we view the latter as transformations of software graphs.

1 Introduction

In previous work [see Honsel et al., 2016, 2015] we presented agent-based simulation models for software processes. In these models developers act on software entities, the behavior of which makes the software evolve over time. One identified challenge is to improve the structure of the simulated software graph. In order to do so, we require a more detailed description of exactly which files are selected for a commit and how these files change. A common approach to describe well defined code structure changes are *software refactorings*. Therefore, we propose a particular but general model for refactorings which can be easily integrated in our agent-based model developed earlier.

This work is based on well known theoretical foundations of software refactorings [see Fowler, 2009] and graph transformations [see Ehrig et al., 1999]. The background is briefly explained in the beginning of Section 2, followed by a detailed description of our approach. The idea to use graph transformations for the description of refactorings is based on the work of [Mens et al., 2005], where the authors proved that refactorings can be formalized with graph transformations. Unfortunately their proposed model is too detailed for simulation purposes. We therefore define a suitable abstraction of it.

We present our experiments and results in Section 3. We conclude with a discussion of our results and a short outlook in Section 4.

2 Background and Methodology

After a brief introduction of the required theory of software refactorings and graph transformations, we illustrate our approach, using the refactorings *Extract Method* and *Move Method*.

Refactorings. The application of a refactoring restructures the software without changing its behavior. The aim is to make the software more readable to developers and/or to increase the maintainability. Fowler [2009] contains a catalog with more than 70 different refactorings.

Graph Transformations. A graph transformation system is used to transform a given graph G according to defined rules. A rule has a left-hand side L and a right-hand side R. To apply a rule one has to execute three steps, which finally lead to the derived graph H. Firstly, one has to find a matching of L in G. Secondly, all vertices and edges that are matched by $L \setminus R$ are deleted from G. Finally, the graph H is created by pasting a copy of $R \setminus L$ to the result.

The graph representing the simulated software can be found in Definition 1. Due to the simplicity of this graph one can easily extend it. For the modeling of inheritance, for example, one can add a further edge label representing links between classes.

Definition 1. *Let $\Sigma = \{C, M\}$ be a set of node labels and $\Delta = \{mm, mc\}$ be a set of edge labels. The node types represent software entities: classes (C) and methods (M). Edges represent relationships between nodes: method memberships (mm) and method calls (mc). A graph over Σ and Δ is a System $G = (V, E, l)$, where V is a set of nodes, $l : V \to \Sigma$ is a function that assigns a label to each node, and $E \subseteq V \times \Delta \times V$ is the set of edges.*

To restrict the allowed software graphs we use a *type graph*. It is similar to the UML class diagram and expresses which nodes can be linked with a certain edge type. For instance, member method edges can only occur between a class and a method as well as method calls link two methods.

We define transformation rules for the following refactorings. The corresponding rules are depicted and explained in Figure 1.

Extract Method: This refactoring will be applied to large methods or if code fragments can be grouped together. It creates a new method that is called from the old one and moves code from the old method to the new one. Therefore, the size, measured in lines of code (LOC), of the old method decreases. The opposite of this refactoring is a refactoring called *Inline Method*.

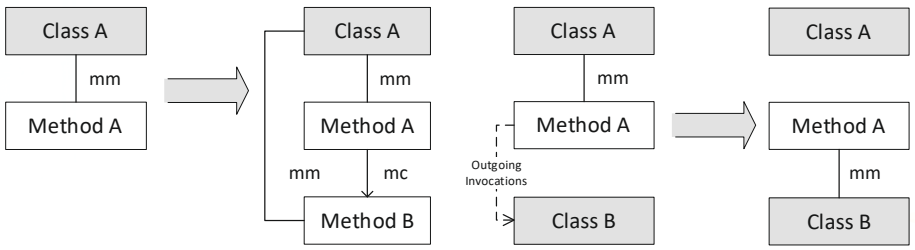

(a) Extract Method. (b) Move Method.

Fig. 1. Graph transformation rules for the selected refactorings. The left-hand side of the rule will be replaced by the right-hand side in the software graph.

Move Method: This refactoring will be applied if a method calls more methods from other classes than from its own. It moves the method to the class with the most calls and therefore, the number of outgoing invocations (NOI) of the method's old class is decreased.

To find a matching of the rules's left-hand side not only the structure of the software graph is taken into account, but also appropriate software metrics. These are, for example, LOC for extract method (Figure 1a) and NOI for move method (Figure 1b).

3 Experiments and Results

To specify which refactorings are most appropriate to model software evolution (and thus should be implemented first), we analyzed the open source project *JUnit* [JUnit, 2017]. For the basic analysis refactorings are identified by *mining the software repository* and counting their occurrences. The results are presented in Table 1.

Table 1. The three most occurring refactorings of the open source project JUnit. We analyzed in total 2069 commits in the period from March 2002 to November 2016.

Refactoring	Number of Occurrences
Move Method	171
Extract Method	164
Inline Method	136

Before including the model of refactorings in our simulation model, we test each rule separated with a initial software graph suitable for the selected rule. In order to do so, we implemented the rules described in Section 2 with Repast Simphony [see North et al., 2013] and assume that we have only one developer. This developer applies a desired refactoring to the initially generated software graph. The transformation for the refactoring move method is depicted in Figure 2.

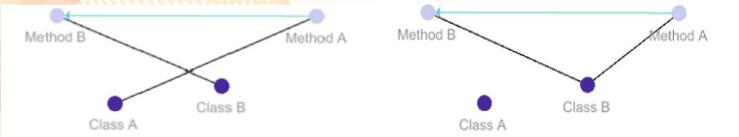

Fig. 2. Application of the refactoring move method illustrated with snapshots of the running simulation using Repast. On the left-hand side the initial software graph and on the right-hand side the graph after applying the refactoring. Initially, method A calls only method B from class B which results in $NOI_{class_A} = 1$. After applying the refactoring both methods belongs to class B which results in $NOI_{class_A} = 0$.

4 Conclusion and Outlook

In this paper, we presented an approach to model refactorings based on graph transformations: single rules are applied to initial graphs. But for integrating this model in our simulation model for software processes *we need more information* about how important software metrics behave *before and after* a refactoring. This is required for finding a matching in the graph and to give a better estimation of the overall software quality.

While such an enriched graph contains much more information and structure, it is also much larger in terms of nodes and edges. It therefore places stronger requirements on the underlying simulation platform.

We develop our own scalable agent platform, especially tailored for our purposes [see Ahlbrecht et al., 2016]. With this platform we will be able to simulate larger projects.

The full paper will contain the following additional information: (1) a description of the mining framework used for analyzing Junit, (2) the behavior of selected software metrics, and (3) first simulation results of software processes extended with refactorings.

References

Tobias Ahlbrecht, Jürgen Dix, Niklas Fiekas, Jens Grabowski, Verena Herbold, Daniel Honsel, Stephan Waack, and Marlon Welter. Agent-based simulation for software development processes. Technical Report IfI-16-02, TU Clausthal, September 2016. (to appear).

Hartmut Ehrig, Gregor Engels, Hans-Jörg Kreowski, and Grzegorz Rozenberg. *Handbook of Graph Grammars and Computing by Graph Transformation: Volume 2: Applications, Languages and Tools*. world Scientific, 1999.

Martin Fowler. *Refactoring: improving the design of existing code*. Pearson Education India, 2009.

Daniel Honsel, Verena Honsel, Marlon Welter, Stephan Waack, and Jens Grabowski. Monitoring Software Quality by Means of Simulation Methods. In *10th International Symposium on Empirical Software Engineering and Measurement (ESEM)*, 2016.

Verena Honsel, Daniel Honsel, Steffen Herbold, Jens Grabowski, and Stephan Waack. Mining software dependency networks for agent-based simulation of software evolution. In *ASE Workshop*, 2015.

JUnit. Junit, 2017. URL `http://junit.org/junit4/`. Accessed: 2017-01-20.

Tom Mens, Niels Van Eetvelde, Serge Demeyer, and Dirk Janssens. Formalizing refactorings with graph transformations. *Journal of Software Maintenance and Evolution: Research and Practice*, 17(4):247–276, 2005.

Michael J. North, Nicholson T. Collier, Jonathan Ozik, Eric R. Tatara, Charles M. Macal, Mark Bragen, and Pam Sydelko. Complex adaptive systems modeling with repast simphony. *Complex Adaptive Systems Modeling*, 2013.

Tailoring CMMI Engineering Process Areas for Simulation Systems Engineering

Somaye Mahmoodi[1], Umut Durak[1,2], Torsten Gerlach[2], Sven Hartmann[1], and Andrea D'Ambrogio[3]

[1] Clausthal University of Technology
Department of Informatics
Julius-Albert-Str. 4, 38678 Clausthal-Zellerfeld, Germany
{somaye.mahmoodi,umut.durak,sven.hartmann}@tu-clausthal.de
[2] German Aerospace Center (DLR)
Institute of Flight Systems
Lilienthalplatz 7, 38108 Braunschweig, Germany
{umut.durak,torsten.gerlach}@dlr.de
[3] University of Rome Tor Vergata
Department of Enterprise Engineering
Via del Politecnico, 1
I-00133 Roma, Italy
dambro@uniroma2.it

Abstract. Today's companies in high-tech industries develop products of high complexity which consist of complicated subsystems with many heterogeneous components integrated together. As system complexity increases, it becomes increasingly more challenging to manage the tedious development process. Capability Maturity Model Integration (CMMI) was proposed as a general framework for process management and improvement. Simulations have long been regarded as complex and integrated systems. Simulation system engineering manages the total simulation system's life-cycle process. This article investigates the possibility of tailoring CMMI engineering process area with emphasis in simulation system engineering. Having its roots from IEEE Recommended Practice for Distributed Simulation Engineering and Execution Process (DSEEP), CMMI adaptation for simulation life-cycle processes can provide a domain specific solution for simulation process management and improvement.

Keywords: Distributed Simulation Engineering and Execution Process (DSEEP), Capability Maturity Model Integration (CMMI), Simulation Process Improvement

1 Introduction

Capability Maturity Model Integration (CMMI) is a framework which provides essential practices for process improvement [1]. CMMI 'Maturity Levels' and 'Capability Levels' describe how much a product development process in one

organization is mature and capable. CMMI currently supports three areas of interest, namely development, services and acquisition. CMMI for development includes four categories: process management, project management, engineering and support. Each category contains number of process areas. As an example, the engineering category process areas are requirements development, technical solution, product integration, verification, and validation. Organizations intend to utilize CMMI for managing and improving their processes in order to come up with high quality products for the sake of achieving customer satisfaction. It was claimed by Goldenson and Gibson that companies based on CMMI process management and improvement achieve a lower cost, a better schedule, high quality products and customer satisfaction at the end [2].

In 1990, Balci defined the modeling and simulation life cycle process [3]. Later, IEEE Std 1516.3-2003, IEEE Recommended Practice for High Level Architecture (HLA) Federation Development and Execution Process (FEDEP) was developed for federation development using High Level Architecture(HLA) for distributed simulation [4]. Next, FEDEP is generalized by Simulation Interoperability Standards Organization (SISO) which lead to the IEEE Std 1730-2010 IEEE Recommended Practice for Distributed Simulation Engineering and Execution Process (DSEEP) which is engineering process for all types of distributed simulation development and execution [5]. DSEEP is a framework for simulation system engineering processes which consists of seven steps, each step having its own set of activities. Each activity has inputs, outputs and recommended tasks [6].

There have been various efforts that target adapting CMMI for particular domains. Withalm et al. proposed CMMI adaptation to support skill assessment and development in tourism [7]. Chen and colleagues proposed teaching capability maturity model for higher education [8]. In [9] Williams proposed application of CMM in medical domain. Neuhaser discussed adapting a maturity model for online course design in [10].

In 2002, Richey proposed the utilization of CMMI in modeling and simulation community [11]. While he argued that conforming such an international standard will result cost effective, easy and cohesive simulation engineering, he also remarked that it will be beneficial to have discipline specific amplifications for incorporating industry standards and best practices for building modeling and simulation products.

Fifteen years after Richey's proposal, this article investigates the feasibility of tailoring CMMI engineering process areas for simulation system engineering. The effort aims at adapting CMMI engineering process areas for simulation life-cycle processes in order to optimize its full potential in simulation domain to reach a higher level of process coverage and quality in simulation system engineering.

2 Assessment

CMMI engineering process areas assessed against the seven steps of DSEEP in order to identify the coverage of CMMI in simulation system engineering

processes. Since CMMI is a generalized framework and simulation is a specific domain with particular process requirements, CMMI fails to cover all.

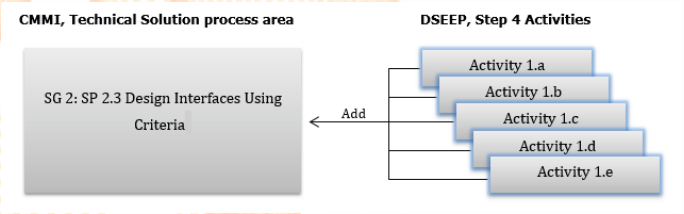

Fig. 1. *DSEEP activity 1 added in CMMI SP2.3*

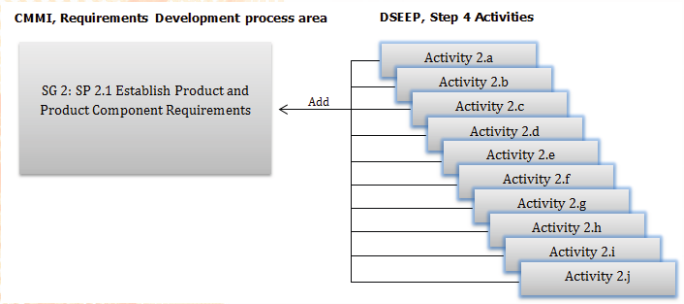

Fig. 2. *DSEEP activity 2 added in CMMI SP2.1*

In this section of the extended abstract we try to exemplify the shortcoming of CMMI against DSEEP with the following example for implementation of simulation environment. The paper will present a full coverage and a more comprehensive assessment. DSEEP [5] defines the main activities for implementation of simulation environment step as:

1. Establish data exchange model
   (a) Select an approach for Simulation Data Exchange Model (SDEM) development.
   (b) Determine appropriate SDEMs.
   (c) Looking for relevant SDEM elements in dictionaries.
   (d) Develop and document the SDEM.
   (e) Verify that the SDEM supports the conceptual model.
2. Establish simulation environment agreement
   (a) Decide the behavior of all objects.
   (b) Identify member applications software modifications were not previously identified.

(c) Decide common databases and algorithms.
(d) Diagnose reliable data sources for simulation environment databases and member application.
(e) Decide managing the time in the simulation environment.
(f) Create synchronization points for initialization of simulation environment and procedures.
(g) Decide save and restore strategy for the simulation environment.
(h) Decide data distribution across the simulation environment.
(i) Convert scenario description to an executable scenario.
(j) Establish security procedures according to security agreements.

3. Implement member applications design
   (a) Implement member application modifications.
   (b) Implement interfaces modifications or extensions of all member applications.
   (c) Develop a required new interface for member applications.
   (d) Implement design of required new member applications.
   (e) Implement supporting databases.
4. Implement simulation environment infrastructure
   (a) Confirm availability of basic facility services like electric power, air conditioning, etc.
   (b) Confirm availability of required integration/test hardware or software.
   (c) Perform required functions for system administrations for example create user accounts.
   (d) Install and configure required hardware.
   (e) Install and configure required software.
   (f) Test infrastructure.
   (g) Confirm infrastructure adherence to the security plan.

The activity 1 corresponds to interface design practices that are specific to simulation engineering. The interfaces are captured in SDEM and the execution and data exchange policy is then documented in simulation environment agreements which can be added in RD process area. Therefore CMMI SP2.3 Design Interfaces Using Criteria needs to be adapted for the activity 1 and SP 2.1 Establish Product and Product Component Requirements for activity 2. Figure 1 and 2 depict tailoring of CMMI for these activities.

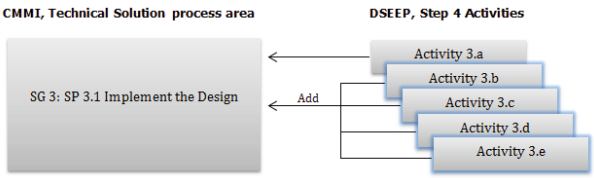

Fig. 3. *DSEEP activity 3 added in CMMI SP3.1*

Activity 3 and 4 are addressed in CMMI SP 3.1 Implement the Design. While activity 3 corresponds to software coding, activity 4 corresponds to construction of the facilities. As depicted in Figure 3 CMMI SP 3.1 can be extended with activity 3.

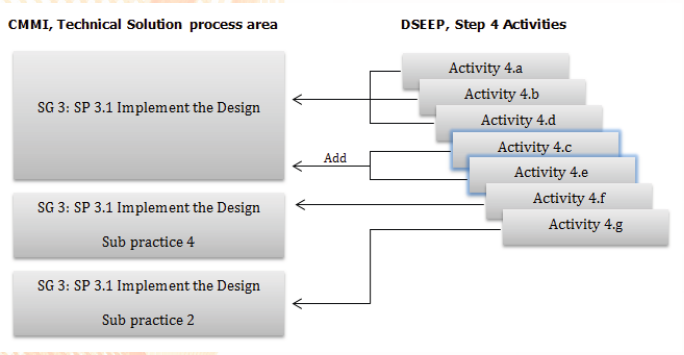

Fig. 4. *DSEEP activity 4 added in CMMI SP3.1*

There exist corresponding clauses in CMMI for all parts of activity 4 except part (c) and (e) which can be added in CMMI SP 3.1 Implement the Design. Figure 4 depicts CMMI enhancement for this activity.

CMMI-Technical Solution Process Area (Default)	CMMI-Technical Solution Process Area (Enhancement)
SG 1 Select Product Component Solutions • SP 1.1 Develop Alternative Solutions and Selection Criteria • SP 1.2 Select Product Component Solutions	**SG 1 Select Product Component Solutions** • SP 1.1 Develop Alternative Solutions and Selection Criteria • SP 1.2 Select Product Component Solutions
SG 2 Develop the Design • SP 2.1 Design the Product or Product Component • SP 2.2 Establish a Technical Data Package • SP 2.3 Design Interfaces Using Criteria • SP 2.4 Perform Make, Buy, or Reuse Analyses	**SG 2 Develop the Design** • SP 2.1 Design the Product or Product Component • SP 2.2 Establish a Technical Data Package • SP 2.3 Design Interfaces Using Criteria o Select an approach for SDEM development. o Determine appropriate SDEMs o Looking for relevant SDEM elements in dictionaries. o Develop and document the SDEM. o Verify that the SDEM supports the conceptual model. • SP 2.4 Perform Make, Buy, or Reuse Analyses
SG 3 Implement the Product Design • SP 3.1 Implement the Design • SP 3.2 Develop Product Support Documentation	**SG 3 Implement the Product Design** • SP 3.1 Implement the Design o Implement interfaces modifications or extensions of all member applications. o Develop a required new interface for member applications. o Implement design of required new member applications. o Implement supporting databases. o Install and configure required software. o Perform required functions for system administrations for example create user accounts. • SP 3.2 Develop Product Support Documentation

Fig. 5. *CMMI Technical Solution Area Enhancement*

CMMI-Requirements Development Process Area (Default)	CMMI-Requirements Development Process Area (Enhancement)
SG 1 Develop Customer Requirements • SP 1.1 Elicit Needs • SP 1.2 Develop the Customer Requirements	**SG 1 Develop Customer Requirements** • SP 1.1 Elicit Needs • SP 1.2 Develop the Customer Requirements
SG 2 Develop Product Requirements • SP 2.1 Establish Product and Product Component Requirements • SP 2.2 Allocate Product Component Requirements • SP 2.3 Identify Interface Requirements	**SG 2 Develop Product Requirements** • SP 2.1 Establish Product and Product Component Requirements o Decide the behavior of all objects. o Identify member applications software modifications were not previously identified. o Decide common databases and algorithms o Diagnose reliable data sources for simulation environment databases and member application. o Decide managing the time in the simulation environment. o Create synchronization points for initialization of simulation environment and procedures. o Decide save and restore strategy for the simulation environment. o Decide data distribution across the simulation environment. o Convert scenario description to an executable scenario. o Establish security procedures according to security agreements. • SP 2.2 Allocate Product Component Requirements • SP 2.3 Identify Interface Requirements
SG 3 Analyze and Validate Requirements • SP 3.1 Establish Operational Concepts and Scenarios • SP 3.2 Establish a Definition of Required Functionality • SP 3.3 Analyze Requirements • SP 3.4 Analyze Requirements to Achieve Balance • SP 3.5 Validate Requirements	**SG 3 Analyze and Validate Requirements** • SP 3.1 Establish Operational Concepts and Scenarios • SP 3.2 Establish a Definition of Required Functionality • SP 3.3 Analyze Requirements • SP 3.4 Analyze Requirements to Achieve Balance • SP 3.5 Validate Requirements

Fig. 6. *CMMI Requirements Development Area Enhancement*

3 Enhancement

Result of assessment leads to CMMI enhancement. Figure 5 and 6 clarify CMMI Technical Solution and Requirements Development process areas in left side and their enhancement in right side which is only for recent example in Assessment part.

4 Conclusion

The initial assessments indicated that the Capability Maturity Model Integration engineering process area is not covering completely all the requirements simulation life-cycle processes. The full paper will be presenting a comprehensive assessment of Capability Maturity Model Integration and propose enhancements.

References

1. C. P. Team, "CMMI for development, version 1.3." 2010.
2. D. Goldenson and D. L. Gibson, "Demonstrating the impact and benefits of CMMI: an update and preliminary results," 2003.
3. O. Balci, "Guidelines for successful simulation studies," in *Proceedings of the 22nd conference on Winter simulation*. IEEE Press, 1990.
4. "IEEE Recommended Practice for High Level Architecture (HLA) Federation Development and Execution Process (FEDEP)," *IEEE Std 1516.3-2003*, 2003.
5. "IEEE Recommended Practice for Distributed Simulation Engineering and Execution Process (DSEEP)," *IEEE Std 1730-2010*, 2011.
6. D. Gianni, A. D'Ambrogio, and A. Tolk, *Modeling and Simulation-Based Systems Engineering Handbook*. CRC Press, 2014.
7. J. Withalm, W. Wölfel, H. Duin, and M. Peters, "Combining CMMI with serious gaming and e-learning to support skill assessment and development in tourism," in *International Conference on Interactive Computer Aided Learning (ICL2008). University Press. Kassel*, 2008.
8. C. Chen, C. Kuo, and P. Chen, "The teaching capability maturity model for teachers in higher education: a preliminary study," in *2011 International Conference on Frontiers in Education: Computer Science and Computer Engineering*, 2011.
9. P. Williams, "A practical application of CMM to medical security capability," *Information Management & Computer Security*, vol. 16, no. 1, pp. 58–73, 2008.
10. C. Neuhauser, "A maturity model: Does it provide a path for online course design," *The Journal of Interactive Online Learning*, vol. 3, no. 1, pp. 1–17, 2004.
11. F. Richey, "Modeling and simulation CMMI: A conceptual view," *CrossTalk: The Journal of Defense Software Engineering*, vol. 15, no. 3, pp. 29–30, 2002.

Numerical Simulation of Gas-Well Casing Shoe

Jithin Mohan[1], Stefan Hartmann[1], Leonhard Ganzer[2], and Birger Hagemann[2]

[1] Institute of Applied Mechanics, Clausthal University of Technology
Adolph-Roemer-Str. 2a, 38678 Clausthal-Zellerfeld, Germany
{stefan.hartmann, jithin.mohan}@tu-clausthal.de
[2] Chair of Reservoir Engineering, Clausthal University of Technology
Agricolastr. 10, 38678 Clausthal-Zellerfeld, Germany
{leonhard.ganzer, birger.hagemann}@tu-clausthal.de

Abstract. The reduction of green house gases and a failure resistant energy supply are the major goals in energy concept. Underground energy storage has presented itself as a viable option to achieve the same. Thus, the simulation of gas-wells is one objective to be treated for identifying the integrity and efficiency of such energy storage systems. Our goal is the coupling of different simulation tools to investigate the production and injection process of a gas-well, where the final goal is a step-size controlled technique to obtain reliable results of the multi-physical problem.

1 Basic Concepts

The main goals to simulate the thermo-mechanical properties during the production and injection phase in hydrogen gas-wells is connected to the coupling of several programs. To ensure the integrity of gas-wells, the local properties in the casing shoe, i.e. the production part of the gas-well has to be investigated. Since there are changing pressure and temperature states during the injection of the gas into the cavern, and the removal of the gas from the reservoir, cyclic changes of the thermo-mechanical loads will strain the material. The material involved are the steel and the concrete of the casing, and the packer material, which frequently is a rubber-like material.

Our goals are, first, to develop a superior program for time-adaptive simulations on the basis of higher order diagonally-implicit Runge-Kutta methods (DIRK), which calls different programs: 1D pipe flow model for controlling the flux into and out of the gas-well, Openfoam [5] for the local gas flow close to the outlets in the production gas-well, Tasafem (3D inhouse finite element program for coupled problems) to determine the local thermo-mechanical behavior under cycling loading of the production well, and Dumux [4] for the hydro-mechanical flow in the surrounding porous media. Within the DIRK-method, a coupled system of non-linear equations occurs after the temporal discretization of the entire system of differential-algebraic equations. This coupled system is solved using a non-linear Gauss-Seidel scheme, which is accelerated using Aitken-relaxation methods, see [2, 3] and the literature cited therein. Regarding the overall concept of the entire approach we refer to [6].

In this poster presentation, we concentrate on the local flow field close to the outlets, which are small perforations in the casing, of the casing shoe. Initial computations are performed for the steady, incompressible laminar case in order to determine the conditions in the casing shoe and to find out whether turbulence is necessary to be determined. A simplified model with a single perforation meshed with hexahedral cells is chosen as the test case. The results are analyzed for the incompressible case. Subsequently, the influence of turbulence, compressibility and flow unsteadiness is also studied and compared to the incompressible test case. To this end the thermal and mechanical boundary conditions of a vertical test casing have to be determined. Later on this will be coupled, in a first step, with the simulation of the pipe flow to look at the production and the injection phase. The pipe flow is modeled using high order p-version finite elements to obtain accurate results in the spatial domain. In view of p-version finite elements, we refer to [1]. Later on, the coupling to the thermo-mechanical properties of the casing and the surrounding porous media is considered as well.

References

1. Babuška, I., Szabó, B.A., Katz, I.N.: The p-version of the finite element method. SIAM journal on numerical analysis 18(3), 515–545 (1981)
2. Erbts, P., Düster, A.: Accelerated staggered coupling schemes for problems of thermoelasticity at finite strains. Computers & Mathematics with Applications 64(8), 2408–2430 (2012)
3. Erbts, P., Hartmann, S., Düster, A.: A partitioned solution approach for electro-thermo-mechanical problems. Archive of Applied Mechanics 85, 1075–1101 (2015)
4. Flemisch, B., Darcis, M., Erbertseder, K., Faigle, B., Lauser, A., Mosthaf, K., Helmig, R.: Dumux: Dune for multi-phase, component, scale, physics, flow and transport in porous media. Advances in Water Resources 34(9), 1102–1112 (2011)
5. Greenshields, C.J.: The Open Source CFD Toolbox-User's Guide (2012)
6. Rothe, S., Erbts, P., Düster, A., Hartmann, S.: Monolithic and partitioned coupling schemes for thermo-viscoplasticity. Computer Methods in Applied Mechanics and Engineering 293, 375 – 410 (2015)

Learning State Mappings in Multi-Level-Simulation

Stefan H. A. Wittek

Department of Informatics, Clausthal University of Technology, Clausthal-Zellerfeld, Germany

switt@tu-clausthal.de

Keywords: co-simulation, multi-level-simulation, machine learning, regression

Abstract. Holistic simulation aids the engineering of cyber physical systems. However, its complexity makes it expensive regarding computation time and modeling effort. We introduce multi-level-simulation as a methodology to handle this complexity [1]. In this methodology, the required holistic perspective is reached on a coarse level, which is linked with multiple detailed models of small sections of the system. In order to co-simulate the levels, mappings between their states are required. This paper gives an insight into the current state of progress of using well known machine learning techniques for regression to generate these mappings using small sets of labeled training data.

1 Introduction

Cyber physical systems (CPS) are large scaled sets of hardware and software components interacting in numerous ways to realize some common behaviour. Examples of such systems are automated production facilities or networks of autonomous vehicles. Applying simulation to CPS is challenging, because it needs to provide a holistic perspective to capture the interdependencies between the components of a system, while it is limited in its complexity by computation time and modelling effort.

We propose multi-level-simulation, which aims to be efficient regarding this complexity [1]. The CPS is co-simulated on multiple levels of abstraction simultaneously. On a coarse level, a holistic perspective of the system is reached. This level is focusing on the interactions between the elements of the system. This level uses a simplified modeling technique and is less complex, resulting in a fast simulation. On a detailed level, only some relevant sections of the system are chosen to be simulated using a more complex technique. This level allows precise predictions required for specific simulation questions, but results in a slow simulation. Note that these sections are not tied to the modularity of the components, but to the purpose of the simulation. They may include several components or only fragments of them.

In order to run a co-simulation between the levels, the state of these detailed sections and the state of the corresponding sections on the coarse level have to be synchronized. Because the coarse level uses a simplified modelling technique, the states must be converted using the mappings Σ and Φ. Σ maps the detailed level state s to a coarse level state s'. Note that a set of detailed level states A is mapped to the same s' on the coarse level ($\Sigma(s) = s',\ \forall s \in A$). Σ is not surjective and thusly not reversible. Φ maps

a coarse level state s' to the detailed level state s. $\Phi(s')$ has to choose a single s among all states in A that would be mapped to s' by Σ.

How to define these mappings, is a key question towards multi-level-simulation. A variety of works focus on providing interfaces between multiple levels of abstraction using state mappings. Most approaches provide specific instances of such mappings for a given combination of modeling techniques [2,3,4]. Some provide a more general framework, but require an engineer to code the mappings [5,6]. This approaches are not optimal, because the mappings need to be defined per project and engineers typically lack the programming background to do this.

In contrast, our approach aims to uses machine learning techniques for regression to generate Σ and Φ. The engineer only has to provide small labeled training sets.

2 Learning State Mappings

In the current state of our work we focus on the mapping Σ. The state of each simulation can be formalized as a n-dimensional vector of real values. This vector captures the valuation of each variable of the simulation. We assume that each of the outputs of Σ can be predicted independently. To handle m-dimensional output, m independent regression problems have to be solved. Thus, we will consider $\Sigma: \mathbb{R}^n \rightarrow \mathbb{R}$ as a n-to-one mapping.

As described above, an engineer is supposed to provide a training set. This set consist of an observations set X that contains k observations $X = \{x_1, x_2, \dots x_k\}, x_i \in \mathbb{R}^n$ and their corresponding coarse level state set Y where $Y = \{y_1, y_2, \dots, y_k\}, y_i \in \mathbb{R}$ and x_i corresponds to y_i for $i = 1..k$.

We used the following setup to investigate the performance of three well known algorithms for regression on this problem. Four different data sets were defined. The first data set was derived from the lift example described in [1]. It was used to generate 151 9-dimentional x values. The hand coded Σ mapping of the example was utilized to generate the corresponding y values. Three additional data sets were generated using 150 random generated, normal distributed 9-dimentional real values $x \in [0,1]^9$ and the basic aggregation functions SUM, MEAN and MEDIAN to generate the corresponding y values.

The training data was sampled from each of this sets using three distinct methods. A set of 8 random drawn values (R8). A set of 20 random drawn values (R20). A set of 8 values selected manually, simulating the engineer providing 8 “useful” examples (S8).

Three techniques were used to generate predictors for y. A polynomial regression minimizing the squared error (POLY). A ε-support-vector-regression (SVR) using a radial base function. A multilayer feedforward network trained by the RProp algorithm (MLP). This setup results in 4(data sets) x 3(sampling methods) x 3(algorithms) = 36 training runs.

Figure 1 depicts the results of two of this runs. The horizontal axis rates the labelled value of y while the vertical axis rates the prediction of the trained SVR. In the left setup, the mean squared error is 0.76 while it is 0.52 in the right setup.

This example is comparable with the other runs. In all runs the results on the S8 sample were better than on the R8 sample. Over all setups neither SVR nor MLP were dominant. POLY using R20 setup was better than SVR and MLP with the SUM and MEAN data set, but worse with MEDIAN data set.

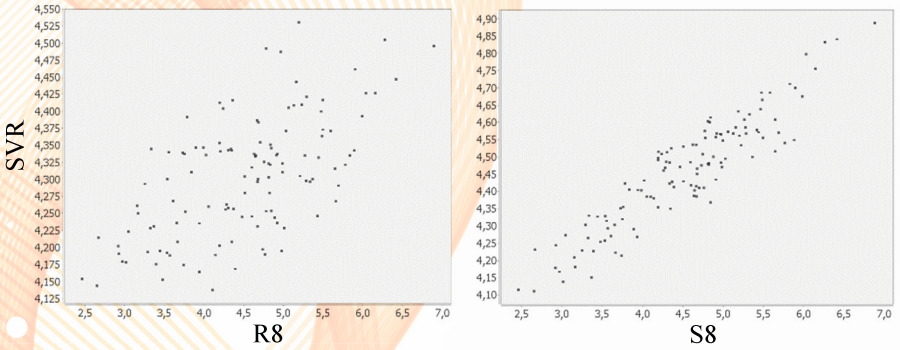

Fig. 1. Performance of SVR on the SUM data set using sampling method R8 and S8

3 Conclusion and Future Work

The presented results provide a first insight on the performance of machine learning algorithms for multi-level-simulation. Further investigations are needed to provide actual evidence for our findings. It fits the intuition, that manually selected samples perform better than randomly drawn ones. Assisting the engineer in this task could lead to even better results. The good performance of POLY with the SUM and MEAN data set is in line with our expectations since both functions can easily be expressed as a polynomial. Although the overall Performance of SVR and MPL was within our expectations, we aim to improve the predictions by providing additional guidance for the algorithms using constraints provided by the engineer. Examples of this constraints would be boundaries for the target values or structural knowledge about the states.

4 References

1. Wittek, S.H.A., Göttsche, M., Rausch, A., Grabowski, J., 2016. Towards Multi-Level-Simulation using Dynamic Cloud Environments, in: Proceedings of the 6th International Conference on Simulation and Modeling Methodologies, Technologies and Applications. pp. 297–303. doi:10.5220/0005997502970303
2. Dangelmaier, W., Mueck, B., 2004. Using Dynamic Multiresolution Modelling to Analyze Large Material Flow Systems, in: Proceedings of the 36th Conference on Winter Simulation, WSC '04. Winter Simulation Conference, Washington, D.C., pp. 1720–1727.
3. Claes, R., Holvoet, T., 2009. Multi-model Traffic Microsimulations, in: Winter Simulation Conference, WSC '09. Winter Simulation Conference, Austin, Texas, pp. 1113–1123.
4. Huber, D., Dangelmaier, W., 2011. A Method for Simulation State Mapping Between Discrete Event Material Flow Models of Different Level of Detail, in: Proceedings of the Winter Simulation Conference, WSC '11. Winter Simulation Conference, Phoenix, Arizona, pp. 2877–2886.
5. Hong, S.-Y., Kim, T.G., 2013. Specification of multi-resolution modeling space for multi-resolution system. SIMULATION 89, 28–40. doi:10.1177/0037549712450361.
6. Rao, D.M., 2003. Study of Dynamic Component Substitutions (Dissertation). University of Cincinnati.

www.simscience2017.uni-goettingen.de